

SOCIETY OF ECOLOGICAL CHEMISTRY AND ENGINEERING

**ECOLOGICAL CHEMISTRY
AND ENGINEERING A**

CHEMIA I INŻYNIERIA EKOLOGICZNA A

Vol. 23

No. 2

OPOLE 2016

EDITORIAL COMMITTEE

Witold Waclawek (Society of Ecological Chemistry and Engineering, PL) – Editor-in-Chief
Barbara Wiśniowska-Kielian (University of Agriculture, Kraków, PL) – agricultural chemistry
Marina V. Frontasyeva (Joint Institute for Nuclear Research, Dubna, RU) – heavy metals and radionuclides
Maria Waclawek (Opole University, PL) – alternative energy sources

PROGRAMMING BOARD

Witold Waclawek (Society of Ecological Chemistry and Engineering, PL) – Chairman
Jerzy Bartnicki (Meteorological Institute – DNMI, Oslo-Blindern, NO)
Mykhaylo Bratychak (National University of Technology, Lviv, UA)
Bogusław Buszewski (Nicolaus Copernicus University, Toruń, PL)
Eugenija Kupcinskiene (University of Agriculture, Kaunas, LT)
Bernd Markert (International Graduate School [IHI], Zittau, DE)
Nelson Marmiroli (University, Parma, IT)
Jacek Namieśnik (University of Technology, Gdańsk, PL)
Lucjan Pawłowski (University of Technology, Lublin, PL)
Krzysztof J. Rudziński (Institute of Physical Chemistry PAS, Warszawa, PL)
Manfred Sager (Agency for Health and Food Safety, Vienna, AT)
Mark R.D. Seaward (University of Bradford, UK)
Petr Škarpa (Mendel University of Agriculture and Forestry, Brno, CZ)
Piotr Tomasiak (University of Agriculture, Kraków, PL)
Roman Zarzycki (University of Technology, Łódź, PL)
Małgorzata Rajfur (Opole University, PL) – Secretary

STATISTICAL EDITORS

Władysław Kamiński (Technical University, Łódź, PL)
Zbigniew Ziembik (Opole University, Opole, PL)

LANGUAGE EDITOR

Ian Barnes (University of Wuppertal, Wuppertal, DE)

EDITORIAL OFFICE

Opole University
ul. kard. B. Kominka 6, 45-032 OPOLE, PL
phone: +48 77 455 91 49
email: maria.waclawek@o2.pl

SECRETARY

Małgorzata Rajfur
phone: +48 77 401 60 42
email: mrajfur@o2.pl

Copyright © by
Society of Ecological Chemistry and Engineering, Opole

Wersją pierwotną czasopisma jest wersja elektroniczna

CONTENTS

Mariusz LENART and Tomasz OLSZOWSKI – Indoor-Outdoor Relations for PM10 Mass Concentration Based on University Building	127
Anna JANICKA, Daniel MICHNIEWICZ, Maria SKRĘTOWICZ, Kamil TRZMIEL, Radosław WRÓBEL and Maciej ZAWIŚLAK – Exposure of the Driver Staying Inside the Car Cabin to Volatile Organic Compounds	139
Małgorzata KUTYŁOWSKA – Prediction of Water Conduits Failure Rate – Comparison of Support Vector Machine and Neural Network	147
Elżbieta BEZAK-MAZUR and Dagmara ADAMCZYK – Adsorption of Mixture of Two Dyes on Activated Carbon	161
Krzysztof FRĄCZEK, Dariusz ROPEK and Anna LENART-BOROŃ – The Effect of Heavy Metals on the Growth of Waterborne <i>Escherichia coli</i> of Municipal Landfill Origin	173
Gabriela KAMIŃSKA, Mariusz DUDZIAK, Jolanta BOHDZIEWICZ and Edyta KUDLEK – Effectiveness of Removal of Selected Biologically Active Micropollutants in Nanofiltration	185
Milena RUSIN, Janina GOSPODAREK and Aleksandra NADGÓRSKA-SOCHA – The Effect of Petroleum-Derived Substances on Chemical Composition of Winter Wheat	199
Karolina PETELA and Andrzej SZŁĘK – Assessment of Passive Cooling in Residential Application under Moderate Climate Conditions	211
Jakub SIKORA, Marcin NIEMIEC, Anna SZELAĞ-SIKORA, Michał CUPIAŁ and Anna KLIMAS – Utilization of Post-Ferment from Co-Fermentation Methane for Energy Purposes	227
Krzysztof SORNEK – The Impact of Micro Scale Combustion of Biomass Fuels on Environment	239
VARIA	
Invitation for ECOpole '16 Conference	251
Zaproszenie na Konferencję ECOpole '16	253
Guide for Authors	255

SPIS TREŚCI

Mariusz LENART i Tomasz OLSZOWSKI – Relacja outdoor-indoor dla stężenia masowego PM10 na przykładzie budynku uczelni	127
Anna JANICKA, Daniel MICHNIEWICZ, Maria SKRĘTOWICZ, Kamil TRZMIEL, Radosław WRÓBEL i Maciej ZAWIŚLAK – Ekspozycja kierowcy przebywającego wewnątrz kabiny nowego pojazdu na lotne związki organiczne	139
Małgorzata KUTYŁOWSKA – Przewidywanie wskaźnika awaryjności przewodów wodociągowych – wektory nośne oraz sieci neuronowe	147
Elżbieta BEZAK-MAZUR i Dagmara ADAMCZYK – Adsorpcja mieszaniny dwóch barwników na węglu aktywnym	161
Krzysztof FRĄCZEK, Dariusz ROPEK i Anna LENART-BOROŃ – Wpływ metali ciężkich na wzrost <i>Escherichia coli</i> izolowanych z wód pochodzących ze składowiska odpadów komunalnych	173
Gabriela KAMIŃSKA, Mariusz DUDZIAK, Jolanta BOHDZIEWICZ i Edyta KUDLEK – Ocena skuteczności usuwania wybranych substancji aktywnych biologicznie w procesie nanofiltracji	185
Milena RUSIN, Janina GOSPODAREK i Aleksandra NADGÓRSKA-SOCHA – Wpływ substancji ropopochodnych na skład chemiczny pszenicy ozimej	199
Karolina PETELA and Andrzej SZŁĘK – Ocena możliwości stosowania pasywnego chłodzenia do celów domowych w klimacie umiarkowanym	211
Jakub SIKORA, Marcin NIEMIEC, Anna SZELAĞ-SIKORA, Michał CUPIAŁ i Anna KLIMAS – Wykorzystanie pofermentu z kofermentacji metanowej na cele energetyczne	227
Krzysztof SORNEK – Wpływ spalania biomasy w układach mikroskalowych na środowisko	239
VARIA	
Invitation for ECOpole '16 Conference	251
Zaproszenie na Konferencję ECOpole '16	253
Guide for Authors	255

Mariusz LENART¹ and Tomasz OLSZOWSKI^{1*}

INDOOR-OUTDOOR RELATIONS FOR PM10 MASS CONCENTRATION BASED ON UNIVERSITY BUILDING

RELACJA OUTDOOR-INDOOR DLA STĘŻENIA MASOWEGO PM10 NA PRZYKŁADZIE BUDYNKU UCZELNI

Abstract: The determination of the level of pollutants and reciprocal relations “outside-inside” forms an important component in the study involving assessment and control of indoor air quality. This paper reports the results of a study with regard to the mass concentration of PM10 determined concurrently in the outdoor air surrounding a university building and inside the lecture rooms in it. The research project was undertaken in the cold season and registration included 83 independent observations with the duration of 90 minutes. The research applied a reference method involving measurements of PM10 mass concentration using gravimetric technique. The results were analyzed by application of non-parametric tests. For the purposes of classification of variables and assessment of the role of the specific variables, the analysis was based on the use of principal components. It was indicated that the mass concentration of particulate matter in the lecture rooms does not differ from the levels measured at the same time in the air surrounding the building only during the periods corresponding to periodic room ventilation. It was also found that the design and usage of the buildings, as well as the number and activity of humans determine the aerosanitary conditions in the enclosed spaces formed by the lecture rooms. It was observed that the mass concentration of particulate matter in the rooms is higher in the cold season. A statement was made that design solutions need to be implemented with the purpose of using intelligent ventilation systems.

Keywords: air contamination, aerosols, public building, PCA

Introduction

One of the most toxic pollution of the troposphere are suspended solids. This is due to their ability to absorb on the surface of many harmful substances. Worldwide epidemiological studies have shown that there is a strong correlation between the air pollutants concentration and increase the prevalence of respiratory diseases and finally mortality of people. [1, 2]. The increase in the long-term concentration of PM10

¹ Department of Thermal Engineering and Industrial Facilities, Faculty of Mechanical Engineering, Opole University of Technology (OUTech), ul. Mikołajczyka 5, 45-271 Opole, Poland, phone: +48 77 449 84 57, fax: +48 77 449 99 24, email: t.olszowski@po.opole.pl

* Corresponding author: t.olszowski@po.opole.pl

particles of 10 microns results in a several percent increase in the incidence of respiratory diseases, especially asthma [3].

Despite the fact that monitoring of the troposphere has been conducted since the middle of the last century, the issues relating to the quality of indoor air were neglected for a long period [4]. Over the years, it was taken for granted that its quality is directly relative to the parameters of the external air penetrating the buildings. Nevertheless, around the turn of last century, it was observed that the concentration of aerosols inside the buildings is often considerably higher in comparison to the quality of external air infiltrating the area [5, 6]. Simultaneously the Blacksmith Institute report stated, that *indoor air pollution and urban air quality are listed as two of the world's worst toxic pollution problems* [7].

The recent studies indicate that the air quality indoors is relative to both the factors associated with the external environment as well as endogenic factors [8]. The studies reported in [3, 9, 10] deal with the characteristics of the factors affecting the quality of air inside buildings, which were found to include air pollution, microclimate conditions, level of air ionization, exploitation conditions of the buildings as well as their design. The factors deciding about the quality of the inside environment include the ones associated with the presence as well as animal and human activity indoors [8]. The activities inside buildings can considerably affect not only on the level of the concentration of classical aerosol particles as well as the level of bioaerosols [11–13]. Air quality is also considerably influenced by the effect resulting from the existence of ventilation and air conditioning systems [14, 15]. The concentration of aerosol particles is also dependent on the season. In the moderate climate, higher aerosol concentrations are registered during winter [16].

This paper focuses on the verification of the level of mass concentration of PM₁₀ in the lecture rooms of a university during the cold season. It also aims to determine the relation between the particulate matter concentration and the parameters which characterize the quality of air outdoors. In the consideration of the fact that humans spend 85–90% of their time in enclosed spaces, including 40% in buildings with public access (work, study outside home) [17] as well as knowing that the level of probability of exposition to particulate matter is considerably higher during the heating (cold) season, the objective of the study seems to be justified.

The course of the study involves verification of two hypotheses;

- the value of the mass PM₁₀ concentration inside lecture rooms does not differ from the levels determined with regard to the outdoor air in the vicinity of the building (I),
- conditions of building exploitation do not considerably affect the value of PM₁₀ concentration (II).

Materials and methods

Measurement sites and monitoring period

Research studies on the outdoor-indoor PM₁₀ mass concentration relations were conducted at four points around and inside OUT's Mechanical Faculty building. One

point (S_{out}) was located outside, at the roof of the southern wing of Mechanical Faculty building at the height of 14 m. Three of them (points E_{in} , S_{in} and W_{in}) were located inside, in the teaching rooms, at the top floor of the eastern, southern and western wings of building (E_{in} : 50°41'00.26"N, 17°56'42.51"E; S_{in} and S_{out} : 50°40'58.79"N, 17°56'42.83"E and W_{in} : 50°41'58.50"N, 17°56'40.65"E, respectively). Buildings in the wings of the E and W form a compact blocks with a basement, while the wing S is a building on stilts. Classrooms are equipped with sealed window frames. All of classrooms are ventilated by gravity.

The measurement campaign was carried out from December 2015 to the end of March 2016.

The methodology of sampling and data analysis

Observations were carried out simultaneously in two of the four points. Each time the measurements were carried out in the selected classroom within the building (E_{in} , S_{in} , W_{in}) and outside (S_{out}). Aspirations of particulate matter were carried out with constant time of 90 minutes and always was started at noon. In spaces, dust sampler worked at the central point of the classrooms. During the indoor measurements, the number of students (S), way of conducting of classes (using chalk or without (Ch)) and the use of the premises (airing, no airing) were recorded. In addition, some parameters of internal and external air was archived. Relative humidity (RH) and temperature (T) were measured using modules embedded in dust samplers. Observations of precipitation (R) have been conducted *ad oculos*, releasing three states for measurement: 0; no precipitation, 1; immediately after rainfall, 2; >8 h after the end of rainfall. Table 1 summarizes the data on the number of observations of selected parameters of air and data on the use of classrooms. Measurements were carried out during classes for groups of students from 14 to 39 people.

Table 1

Observations data. For indoor observations data divided due to usage of the rooms

Obs. location	with airing	without airing	Total obs.	Min-Max RH _{in} [%]	Min-Max RH _{out} [%]	Min-Max T _{in} [°C]	Min-Max T _{out} [°C]	Min-Max Students (S)	Chalk use (Ch) [%]
S_{in}	7	7	14	30–57	—	18–22	—	14–27	57
E_{in}	8	6	14	28–51	—	17–22	—	19–39	54
W_{in}	6	8	14	31–62	—	19–25	—	15–28	53
S_{out}	—	—	42	—	47–93	—	(–6)–16	—	—
Σ	21	21	42 + 42	—	—	—	—	—	—

The procedure for estimating the PM10 mass concentration was conducted in accordance with guidelines of the European Standard [18]. Measurements of the PM10 airborne particulate matter, at both sampling points were carried out in the same periods using LVS 3D sets of dust collectors with control modules. The indicated flow rate was

3 m³/h. Whatman glass microfiber filters, grade GF/A with a diameter of 47 mm were used as separators for particulate matter. Filters were seasoned for 24 h in constant temperature and humidity conditions, before they were used, and then weighed on a differential dosing scales. The filters were seasoned and weighed again after aspiration. The content of PM10 [$\mu\text{g}/\text{m}^3$] fraction was measured on the basis of the following formula:

$$C = (m_1 - m_0)/V \quad (1)$$

where: C – PM10 mass concentration [$\mu\text{g}/\text{m}^3$];

m_1 – mass of the filter sputtered with dust [μg],

m_0 – the mass of the clean filter [μg],

V – volume of the air which has flow through the filter [m^3].

The expanded mass concentration measurement uncertainty (U) did not exceed 3.9%.

In the first stage of the study, it was examined whether the recorded data and the calculated results of PM10 mass concentration came from normal distribution. The Shapiro-Wilk test was used [19]. The test results allowed the choice of the methods of data analysis. For all of the cases not normal distribution of data were found, so for further analysis nonparametric tests were used. Hypotheses verification were implemented using the U-Mann-Whitney test [20]. The relationships between variables were examined using Spearman correlation [21]. Significance level of 0.05 was adopted. Finally, the study used Principal Component Analysis (PCA) [22].

Results and discussion

The results of all concurrent aspirations did not yield statistically relevant differences with regard to the indoor and outdoor mass concentration of PM10. Although the median C_{in} (52 $\mu\text{g}/\text{m}^3$) was 18% higher than C_{out} (44 $\mu\text{g}/\text{m}^3$), the comparison of 42 pairs of results conducted by the Mann-Whitney test led to the confirmation of the hypothesis (I). The value of the test probability ($p = 0.07$) was higher from the adopted critical level. The result outlined above suggests that the value of the mass concentration of PM10 inside the lecture rooms was predominantly affected by the quality of outdoor air. A similar approach is found in [3], where it was stated that air condition is affected by the operation of gravitational ventilation. Fig. 1 presents the results of the study with the breakdown relative to the individual localities (building wings). Despite the lack of statistically valid differences between the overall values of C_{in} and C_{out} , the median of PM10 concentration inside the building was higher for all localities (S, W and E). Such a condition is normal for mechanical ventilation systems [3], which was not the case in in the analyzed building. The above can indicate that for the case of micron-sized particles, the effect of endogenic sources has a more important role deciding on the level of the mass concentration. The statistical analysis of the results confirms the theory developed by the Fanger team [9], stating that the design characteristics of the buildings have a considerable impact on the value of PM10 concentration indoors. In the south building wing supported on pillars, there are statistically relevant differences

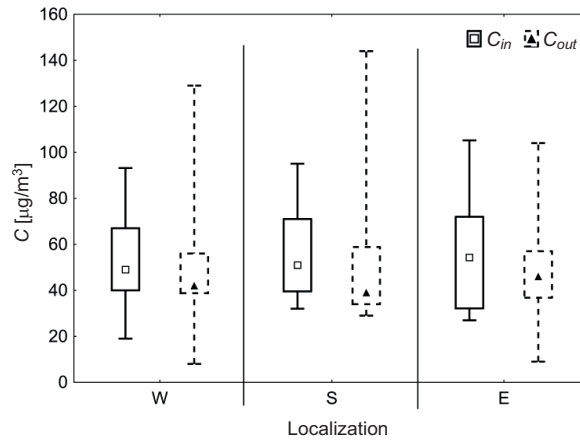


Fig. 1. PM10 concentrations inside (C_{in}) and outside (C_{out}) the building of the Mechanical Faculty with indication of lecture room locations in the examined building wings

between the in-out concentrations (p -value = 0.03), and the value of the median reaches 25%. For the case of observations performed in rooms situated in the wings of the building with a compact design and including a basement (W and E wings), the differences are statistically irrelevant ($p = 0.35$), with the in-out median difference of around 10%. The most probable reason for this can be associated with the thermal conditions in the distinct parts of the building, as the wings demonstrate different design solutions. In the winter, the rooms in the S wing are permanently cold. The lower internal temperature does not promote gravitational ventilation and seems to confirm the observation that the endogenic sources play a principal role in the formation of aerosanitary conditions indoors.

The comparison of the concurrent measurements of mass concentration of PM10 inside and outside the building is presented in Fig. 2. The triangles indicate the data for the case when additional air circulation is absent when windows and open. The circles

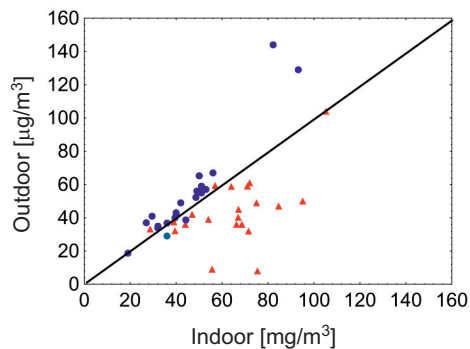


Fig. 2. Comparison of concurrently measured indoor and outdoor concentration for distinct ways of utilizing lecture rooms

denote the data gained indoors and outdoors during periods of the regular ventilation of the lecture rooms. The scatter chart uniformly indicates that for the case of poor gravitational ventilation (closed windows, lack of air diffusers), the mass concentration of PM10 is considerably higher indoors. The graphical interpretation is supported by the analysis of the results. For the case of the observation taken during the classes without possibility of keeping constant air circulation, the mass concentration of PM10 is around 34% higher indoors than outdoors, which is confirmed by the result of the Mann-Whitney test (p -value = 0.001). For the case when air circulation is boosted by the use of additional ventilation, there are no significant differences between the values of in and out concentrations (p -value = 0.33). These results indicate that the mass concentration of PM10 could depend not only on the quality of the indoor air, but also on the condition of the microclimate, the way in which the room is utilized and the number and activity of the users. For these reasons, hypothesis (II) can be rejected.

Table 2 contains the results of the Spearman correlation between the PM10 concentration inside the building and the remaining registered data.

Table 2

Spearman correlation. Results with bold fonts are statistically significant with $p < 0.05$

Variable	C_{out}	T_{out}	T_{in}	Rain	RH_{in}	RH_{out}	No. of Students	Chalk use	Room local.
Cumulative results									
C_{in}	0.59	-0.55	0.07	-0.27	-0.65	-0.05	0.84	0.28	-0.03
Results with airing									
C_{in}	0.90	-0.65	-0.06	-0.55	-0.51	-0.47	0.57	0.00	0.20
Results without airing									
C_{in}	0.44	-0.38	0.28	-0.35	-0.74	0.04	0.88	0.42	-0.29

The results of the correlation indicate that PM10 concentration inside the building (in the lecture rooms) is significantly dependent on the outside concentration only during the period when the rooms are ventilated. The important impact of endogenic factors on the indoor air quality is supported by the correlations between the concentration of PM10 and relative humidity and number of students inside the rooms. The results indicate that the increase in the number of humans in the rooms leads to the increase of PM10 concentration. The process of resuspension of surface particles from clothes, skin and hair is considered to be the principal source of enriching indoor air with particulate matter. Similar results and statistically relevant positive correlations between the number of students and particulate matter concentration were presented by Polednik [3], in which study the presence of humans was demonstrated by the considerable increase of the concentration of coarse particles (5–10 μm and $>10 \mu\text{m}$). The present results are also in conformity with the studies reported in [23, 24].

As mentioned above, the statistically relevant correlations between C_{in} and RH_{in} were also identified for the observations taken for existence and absence of ventilation.

The mass concentration of PM10 increases along with the increase of the relative humidity (dry air promotes the release of particles from the surface). In addition, similar results were found in [3]; yet, in this case the results related to the quantitative concentrations of PM10.

The results, which is surprising, do not confirm the data from the literature regarding the impact of the temperature on the particulate matter concentration in the lecture rooms. The matrix indicates the complete lack of a correlation between the location of the lecture rooms and indoor mass concentration of PM10. Concurrently, it is noteworthy that the use of chalk for writing leads to a significant improvement of the air in the aspect of its particulate matter context; however, this is only the case when there is a lack of additional ventilation in the rooms. The results gained in this way could be affected by the location of the particle aspirator.

For the subsequent verification of the obtained data Principal Component Analysis (PCA) was used. PCA is a technique used to emphasize variation and bring out strong patterns in a dataset. It's often used to make data easy to explore and visualize. A detailed description of the procedures for implementing the PCA is shown at work [22]. In the first step eigenvectors of the correlation matrix were determined (Table 3).

Table 3

Eigenvalues of the correlation matrix. Bold values indicate a realization of mixed Kaiser criterion and Cattell test

No of value	Eigenvalues	% of the total variance	Cumulated [%]
1	3.46	38.4	38.4
2	1.44	16.0	54.4
3	1.19	13.2	67.6
4	1.04	10.6	79.2
5	0.91	10.1	89.3
6	0.45	5.0	94.3
7	0.30	3.3	97.6
8	0.16	1.7	99.4
9	0.06	0.6	100.0

The results of the experiment reflect the relevance of the principal components in the explanation of the relevance of the input factors (per cent in the variability in the database). The Keiser criterion was used as the principal test of the selection of the relevance parameters, which meant that the factors investigated had an eigenvalue of >1 [25]. The selection of the factors was also supported by the Cattell scree test [26, 27] (Fig. 3). The graphical interpretation indicates that in the analyzed case, five of the principal components had a decisive role. Cumulative percentage of variation explained by five components reach almost 90%. Although factor no. 5 has the eigenvalue of <1 , its impact on the justified variability of the primary data is relevant.

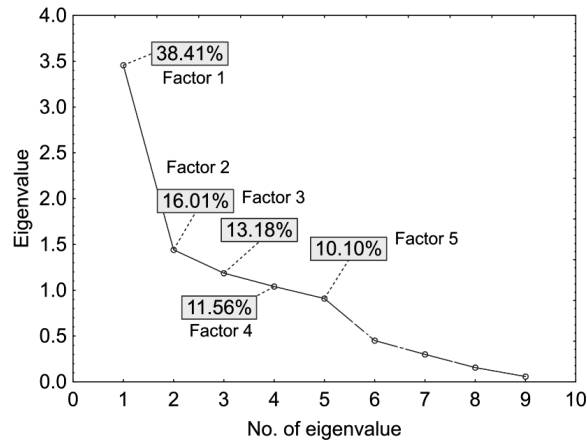


Fig. 3. Scree plot and percent of explained variability in the data

The relations between the primary and experimental principal components are presented in a graphical form in Fig. 4. Each of the variables is represented by a vector. The sense and length of the vector decides on the degree in which the particular

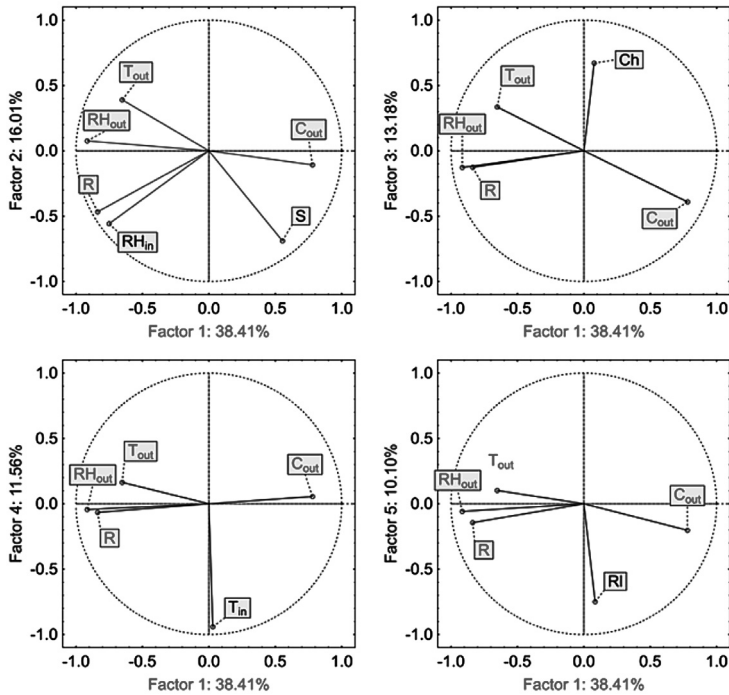


Fig. 4. Projection of variables on the factors surface on the base of eigenvector values. PCA analysis for all sites excluding C_{out}, T_{out}, T_{in}, rain (R), RH_{in}, RH_{out}, No of students (S), chalk use (Ch), classroom location (RI)

variables have an impact on the values of the principal components. In the analyzed example, nearly all of the input variables are located in the vicinity of the circle. This means that the larger part of information contained in these variables is carried by the principal components. The fact of adjacent location of two variables indicates a strongly positive correlation. The variables located on the opposite sides are negatively correlated.

The Principal Component Analysis has successfully extracted five principal components which illustrate the sources of PM10 inside considered classrooms. For the examined case, the first component is responsible for explaining 38% of information regarding the concentrations used as part of the input variables.

One can note that the principal component No.1 explains only the specific variables responsible for external parameters. It is quite clear that the concentration of PM10 outdoor is relative to the relative humidity and occurrence of precipitation. The graphical interpretation confirms this as well. The remaining principal components account for the variables which describe the external parameters; however, all of them can be considered as individual components. On the other hand, these external components account for over 50% of information regarding the mass concentration indoor. The results confirm that the value of the mass concentration of PM10 is to a large extent dependent not only on the sources of endogenic emissions, but also on the way in which the lecture rooms are utilized.

Conclusions

The conducted study confirms that several factors are responsible for the quality of indoor air. The particulate matter in the air penetrating the building is one of the sources, which is considerably dependent on way in which the rooms are utilized as well as on the efficiency of the ventilation installation. The principal internal factors include the number of people indoors and the type of their activity as well as the type of microclimate in the lecture rooms (parameters of indoor air). Hypothesis (I) was proved to be true only for the case of adequate ventilation and during the periods when adequate air circulation is maintained in the rooms. Hypothesis (II) has to be rejected as false, in particular in the conditions of limited ventilation and air infiltration. Despite the fact that PCA is a useful method in reducing the dimensionality and classification of the variables, however, the result indicates that the comprehensive description of the issue seems to be difficult. The results of the study are relevant for a particular building; however, on the other hand, they fit well in the general conclusions recognized by other authors. The higher values of PM10 mass concentration inside the lecture rooms indicate the need to use adequate ventilation in the public buildings. In this respect, the use of an intelligent system based on multi-sectoral strategy described in [3] seems to offer a feasible solution. The results indicate the need for further research in the area of the mutual relation of the sources and factors affecting the quality of indoor air.

References

- [1] ECA. Risk Assessment In Relation to Indoor Air Quality. Report. No 22, 2000. Available online at: http://www.buildingecology.com/publications/ECA_Report22.pdf
- [2] US EPA. Air Quality Criteria for Particulate Matter. EPA/600/P-99/002bF; 2004. Available online at: https://ofmpub.epa.gov/eims/eimscomm.getfile?p_download_id=435946
- [3] Polednik B. Zanieczyszczenia a jakość powietrza w wybranych pomieszczeniach [Pollution and air quality in selected rooms]. Lublin, Poland: Monografia Komitetu Inżynierii Środowiska PAN; 2013. <http://bc.pollub.pl/Content/6618/zanieczyszczenia.pdf>
- [4] Schnelle KB, Brown Ch. Clean Air Act. Air Pollution Control Technology Handbook. Boca Raton, USA: CRC Press; 2001. http://dlia.ir/Scientific/e_book/Technology/Environmental_Tech_Sanitary_Engine/TD_878_894_Special_Types_of_Environment_/020751.pdf
- [5] Fisk WJ, Faulkner D, Sullivan D, Mendell MJ. Particle Concentrations and Sizes with Normal and High Efficiency Air Filtration in a Sealed Air-Conditioned Office Building. *Aerosol Sci Tech.* 2000;32(6):527-544. DOI: 10.1080/027868200303452
- [6] Braniš M, Řezáčová P, Domasová M. The effect of outdoor air and indoor human activity on mass concentrations of PM10, PM2.5 and PM1 in a classroom. *Environ Res.* 2005;99:143-149. DOI: 10.1016/j.envres.2004.12.001
- [7] Ericson B, Hanrahan D, Kong V. The World's Worst Pollution Problems. The top ten of the toxic twenty. New York, USA: Blacksmith Institution. 2008. www.worstpolluted.org
- [8] Dudzińska MR. Aerozole w powietrzu wewnętrznym [Aerosols in indoor air]. Lublin: Monografia Komitetu Inżynierii Środowiska PAN; 2013.
- [9] Fanger PO, Popiołek Z, Wargocki P. Środowisko wewnętrzne. Wpływ na zdrowie, komfort i wydajność pracy [Indoor environment. Health, comfort and productivity impact]. Gliwice: Politechnika Śląska; 2003. http://delibra.bg.polsl.pl/Content/25398/BCPS_28971_2003_Srodowisko-wewnetrzn.pdf
- [10] Cichowicz R, Sabiniak H, Wielgosiński G. The Influence of a Ventilation on the Level of Carbon Dioxide in a Classroom at a Higher University. *Ecol Chem Eng S* 22(1);2015:61-71. DOI: 10.1515/eces-2015-0003
- [11] Fromme H, Diemer J, Dietrich S, Cyrus J, Heinrich J, Lang W, Kiranoglu M, Twardella D. Chemical and morphological properties of particulate matter (PM10, PM2.5) in school classrooms and outdoor air. *Atmos Environ.* 2008;42:6597-6605. DOI: 10.1016/j.atmosenv.2008.04.047.
- [12] Afshari A, Matson U, Ekberg LE. Characterization of indoor sources of fine and ultrafine particles: a study conducted in a full-scale chamber. *Indoor Air.* 2005;15(2):141-150. DOI: 10.1111/j.1600-0668.2005.00332.x
- [13] Hussein T, Hameri K, Heikkinen M S A, Kulmala M. Indoor and outdoor particle size characterization at a family house in Espoo/Finland. *Atmos Environ.* 2005;39: 6397-3709. DOI: 10.1016/j.atmosenv.2005.03.011
- [14] Guo H, Morawska L, He CR, Gilbert D. Impact of ventilation scenario on air exchange rates and on indoor particle number concentrations in an air-conditioned classroom. *Atmos Environ.* 2008;42:757-768. DOI:10.1016/j.atmosenv.2007.09.070
- [15] Polednik B, Dudzińska MR, Skwarczyński M. The Influence of Air-Condition System and Presence of Students on the Aerosol Concentration in the Auditorium. *Archives Environ Prot.* 2009;35(4):45-53. DOI 09.35/2083-4772
- [16] Polednik B. Particulate matter and student exposure in school classrooms in Lublin, Poland. *Environ Res.* 2012;120:134-139. DOI: 10.1016/j.envres.2012.09.006
- [17] Morawska L, He CR, Johnson G, Guo H, Uhde E, Ayoko G. Ultrafine particles in indoor air of a school: possible role of secondary organic aerosols. *Environ Sci Technol.* 2009;43:9103-9109. DOI: 10.1007/s11356-010-0306-2
- [18] EN 12341:2014. Ambient air. Standard gravimetric measurement method for the determination of the PM10 or PM2,5 mass concentration of suspended particulate matter. www.shop.bsigroup.com/ProductDetail/?pid=000000000030260964
- [19] Ruxton GD, Wilkinson DM, Neuhäuser M. Advice on testing the null hypothesis that a sample is drawn from a normal distribution. *Animal Beh.* 2015;107:249-252. DOI:10.1016/j.anbehav.2015.07.006
- [20] Siegel S, Castellan NJ. Nonparametric statistics for the behavioral sciences, New York, USA: McGraw-Hill; 1988.

- [21] John M, Priebe CE. A data-adaptive methodology for finding an optimal weighted generalized Mann–Whitney–Wilcoxon statistic. *Comput Stat Data Anal.* 2007;51(9):4337-4353. DOI: 10.1016/j.csda.2006.06.003
- [22] Jolliffe IT. *Principal Component Analysis.* New York, USA: Springer-Verlag; 1986. DOI:10.1007/b98835
- [23] Holmberg S, Chen Q. Air flow and particle control with different ventilation systems in a classroom. *Indoor Air.* 2003;13(2):200-204. DOI: 10.1034/j.1600-0668.2003.00186.x
- [24] Ferro AR, Kopperud RJ, Hildemann LM. Source strengths for indoor human activities that resuspend particulate matter. *Environ Sci Technol.* 2004;38:1759-1764. DOI: 10.1021/es0263893.
- [25] Kaiser HF. The application of electronic computers to factor analysis. *Edu Psych Meas.* 1960;20:141-151.
- [26] Cattell RB. The scree test for the number of factors. *Multivar Beh Res.* 1966;1:245-276.
- [27] Henry RC, Park ES, Spiegelman CH. Comparing a new algorithm with the classic methods for estimating the number of factors. *Chemometr Intell Lab.* 1999;48(1):91-97. DOI: 10.1016/S0169-7439(99)00015-5.

RELACJA OUTDOOR-INDOOR DLA STĘŻENIA MASOWEGO PM10 NA PRZYKŁADZIE BUDYNKU UCZELNI

Katedra Techniki Ciepłej i Aparatury Przemysłowej, Wydział Mechaniczny
Politechnika Opolska, Opole

Abstrakt: Określenie udziału źródeł zanieczyszczeń oraz wzajemnej relacji „outside-inside” jest istotnym problemem w szacowaniu i kontroli jakości powietrza wewnętrznego. Artykuł przedstawia wyniki badań nad stężeniem masowym PM10 określonym jednocześnie w okalającym budynek powietrze zewnętrzne oraz w salach dydaktycznych uczelni wyższej. Projekt badawczy przeprowadzono w sezonie chłodnym, rejestrując 84 niezależne, 90-minutowe obserwacje. W badaniach wykorzystano, opartą na grawimetrii, referencyjną metodę pomiaru stężenia masowego PM10. Rezultaty badań przeanalizowano przy użyciu testów nieparametrycznych. W badaniach, celem klasyfikacji zmiennych i oszacowania odpowiedzialności poszczególnych czynników, posłużono się analizą składowych głównych. Wykazano, że wartości stężenia masowego pyłu zmierzzonego w salach dydaktycznych nie różnią się od poziomów określonych jednocześnie w okalającym budynek powietrze zewnętrznym wyłącznie podczas okresowego wietrzenia pomieszczeń. Stwierdzono, że konstrukcja oraz sposób użytkowania budynku a także liczba i aktywność osób w znaczący sposób determinują warunki aerosanitarne w pomieszczeniach zamkniętych. Wykazano, że w sezonie chłodnym stężenie masowe pyłu zawieszony jest wyższe w pomieszczeniach. Złożono postulat przyjęcia rozwiązań polegających na implementacji inteligentnych systemów wentylacyjnych.

Słowa kluczowe: zanieczyszczenia powietrza, aerozole, budynki użyteczności publicznej, PCA

Anna JANICKA¹, Daniel MICHNIEWICZ²,
Maria SKRĘTOWICZ^{1*}, Kamil TRZMIEL¹,
Radosław WRÓBEL¹ and Maciej ZAWIŚLAK³

EXPOSURE OF THE DRIVER STAYING INSIDE THE CAR CABIN TO VOLATILE ORGANIC COMPOUNDS

EKSPOZYCJA KIEROWCY PRZEBYWAJĄCEGO WEWNĄTRZ KABINY NOWEGO POJAZDU NA LOTNE ZWIĄZKI ORGANICZNE

Abstract: Nowadays the motorization is one of the basic branch of industry. Dynamic development of the – transportation sector has very positive impact on the social and civilization benefits, but on the other side, it generates also a lot of problems, especially related to the people health and life. The road transport is one of the main air pollution source, particularly in the cities. Furthermore, the motorization development caused increased in residence time inside vehicles. In the cities the traffic intensity is significantly higher than in the rural areas. This is the reason why road congestions are created. Exhausts, including hazardous volatile organic compounds, can easily penetrate into the cabin in the road congestion situation and they are the serious danger to the drivers and passengers. In the new cars, additional sources of volatile organic compounds are elements of the cabin interior.

In this paper the results of the research on volatile organic compounds concentration inside passenger car in simulated conditions were presented. Additionally, the main sources of volatile organic compounds inside the car cabin were identify and the evaluation of driver exposure was defined.

Keywords: car vehicle interior, indoor air quality, volatile organic compounds

Introduction

Not only pedestrians or cyclists moving along the streets are exposed to the air pollution caused by exhaust emission. Obviously, in the urban conditions traffic is more

¹ Division of Automotive Engineering, Faculty of Mechanical Engineering, Wrocław University of Technology, Wyb. Wyspiańskiego 27, 50–370 Wrocław, Poland, phone: +48 71 347 79 18.

² Dr. Schneider Automotive Polska Sp.z o.o., Radomierz 1D, 58–520 Janowice Wielkie, Poland.

³ Department of Machine Design and Research, Faculty of Mechanical Engineering, Wrocław University of Technology, Wyb. Wyspiańskiego 27, 50–370 Wrocław, Poland, phone: +48 71 347 79 18.

* Corresponding author: email: maria.skretowicz@pwr.edu.pl

intensive than in rural areas. The streets are crowded, the average speed of cars is low and vehicles stop frequently at the crossroads, so the fuel consumption and consequently fumes emission increase. These are the reasons of congestion, connected with the huge amount of the vehicles moving through the city at the same time (especially in the rush hours) [1–3]. The fumes get into the vehicles staying at the congestion and pose a threat to the drivers and their passengers [4]. Exhaust gases cumulates inside the car cabin. Time of residence inside the vehicle increases with the development of motorization, hence the problem with exposure of driver at the toxic fumes components becomes more intense. Especially dangerous for people health are hydrocarbons of the volatile organic compounds (VOCs) groups' as well as polycyclic aromatic hydrocarbons (PAHs) [5]. It is therefore important to engage research on the exposure of the driver to that pollutants.

Research concept

Research consisted on evaluation of the amount of the volatile organic compounds (VOCs) getting into the passenger car cabin during simulated driving condition. The VOCs emitted from elements of vehicle equipment were ignored by specifying background of VOCs already emitted in cabin. Investigation consisted of three main stages: sampling, preparation of samples to analysis and chemical analysis of VOCs concentration with gas chromatography.

In order to simulate a driving conditions two cars were used. Tested vehicle (at the back) and emitting vehicle (ahead). Engine of emitting car was idling and subsequently operating with rotation speed about 2500–3000 rpm. The windows of the car behind were closed and ventilation system was working at the first level. Distance between cars was 70 cm (Fig. 1). This is the distance that is kept by cars in the real, urban conditions in congestion.



Fig. 1. Setting the vehicles relation to each other during measurement

Materials and methods

Parameters of vehicles used for the experiment are listed in Table 1.

Table 1

Basic parameters of tested vehicles

Mark and type	Mazda 3 Exclusive+	Opel Corsa C
Category	Passenger car	
Year of production	2011	2001
Fuel type	gasoline	gasoline
Engine capacity [ccm]	1598	973
Engine power [hp]	105	58

The first step of research was sampling which was performed in a chassis dynamometer hall. It let to eliminate the atmospheric conditions, especially the wind, which would affect the dilution of the emitted exhausts. From time to time the external fan was turned on which caused that conditions of the simulation were similar to outdoor. It also protect the working engine from excessive heating. Before the measurement, the samples of VOCs background were taken. Samples were taken in two places: out of the car, near air inlet and inside the cabin, where driver has head (Fig. 2) [6]. For sampling semi-automatic exhauster ASP-2 II was used. It is 2-channels device, so it was possible to sampling at the same time inside and outside. VOCs were adsorbed inside tubes filled with active carbon. The time of sampling was the same in both cases, background and right measurement and was 3 hours and the flow was 30 dm³/h. Samples for the measurement were taken directly after sample for background.



Fig. 2. Sampling locations

The result was set of 4 samples: outdoor background, outdoor measurement, background inside and measurement inside the cabin. The next steps were preparing the samples to chemical analysis and gas chromatography analysis. Sample preparation consisted on desorption of sediment on the active carbon VOCs with carbon disulfide

used as a solvent. Chromatographic analysis was performed with aid gas chromatograph Varian 450-GC with FID detector, capillary column Varian VF-WAXms (30m × 0.25 mm ID DF: 0.25 μm) and autosampler. Analysis of the VOCs were conducted with the following parameters:

- oven temperature (column) – 110°C during 10 minutes,
- inlet temperature – 250°C,
- FID temperature – 250°C,
- split – 1:20,
- volume of injection – 1 mm³.

Results and discussion

Chromatography analysis were qualitative and quantitative. As the result of measurements different VOCs and their concentrations were identified. The concentrations given from chromatograph analysis in ppm (parts per million) of VOCs in 2 cm³ of solvent (carbon disulfide) had to be converted to mg/m³ in air. Subsequently the last step was calculating how many VOCs have gotten into car cabin during the measurement by subtraction of the background VOCs concentrations from VOCs concentration adsorbed during the measurement. Identified outside and inside VOCs are presented in Table 2.

Table 2

VOCs identified outside and inside Mazda's car cabin

BO	BI	MO	MI
<i>n</i> -pentane	<i>n</i> -pentane	<i>n</i> -pentane	<i>n</i> -pentane
2-propanol	2-propanol	benzene	2-propanol
toluene	toluene	toluene	benzene
ethylbenzene	ethylbenzene	ethylbenzene	toluene
<i>p</i> -, <i>m</i> -xylene	<i>p</i> -, <i>m</i> -xylene	<i>p</i> -, <i>m</i> -xylene	ethylbenzene
cumene	cumene	cumene	<i>p</i> -, <i>m</i> -xylene
<i>o</i> -xylene	<i>p</i> -cymene	<i>o</i> -xylene	cumene
<i>p</i> -cymene		<i>p</i> -cymene	<i>o</i> -xylene
			<i>p</i> -cymene

BO – background outside, BI – background inside, MO – measure outside, MI – measure inside.

Percentage of identified VOCs inside car cabin in background (a) and the measurement (b) are presented in Fig. 3. The highest share in each of sample (background and the measurement) inside the car cabin had light hydrocarbons expressed as *n*-pentane. Also 2-propanol had high percentage in both samples. As can be observed, amount of light hydrocarbons in the measurement is lower than in background. It means that during the congestion simulating conditions into the cabin heavier hydrocarbons like xylene, cumene, ethylbenzene are entered.

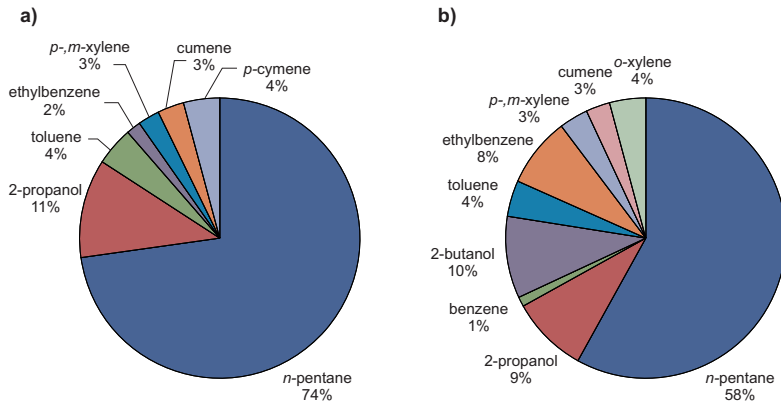


Fig. 3. Percentage of VOCs inside car cabin identified in: a) background, b) right measurement

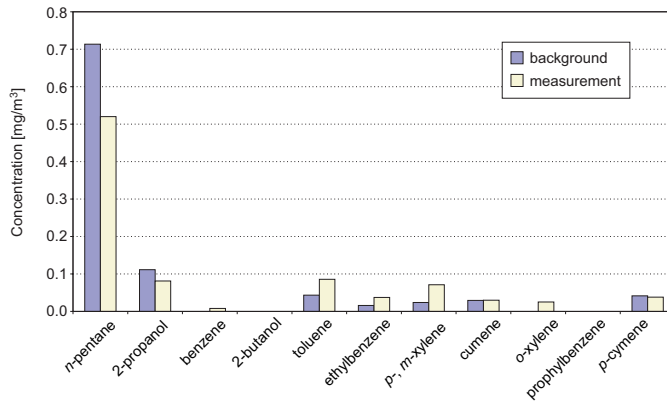


Fig. 4. Concentration of VOCs identified inside the car cabin before (background) and in the measurement

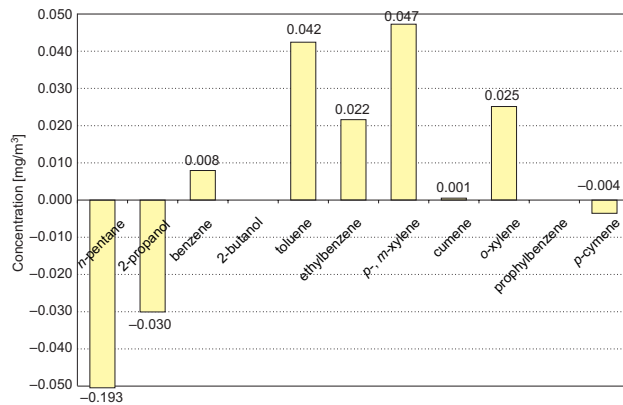


Fig. 5. Difference between VOCs concentration values identified before (background) and during measurement – the amount of VOCs getting inside cabin during simulated conditions

As it could be seen in Fig. 4, concentration of the VOCs majority is higher after measurement than in background. A few of them (*eg* benzene) appears after the simulation, so it means that during test pollutants was getting into the cabin. In Fig. 5 amount of VOCs entered into vehicle cabin during 3-hours simulation is presented.

Summary and conclusions

The research consisted on concentration of VOCs getting into the passenger car cabin determination. The tested car was new (2011), exploited car Mazda 3 and the emitting car was Opel Corsa C. In chromatography analysis 9 different VOCs were identified: *n*-pentane, 2-propanol, benzene, toluene, ethylbenzene, *para*-, *meta*- and *ortho*-xylene, cumene and *p*-cymene.

Measured values of pollutants concentration inside the cabin wasn't very high and couldn't cause immediate reactions of the organism. None of the concentrations exceeded any exposure limit, but, what is important, long-term exposure even on the low concentration of the VOCs (especially on the benzene) could be toxic. It should be also note that the measurements were carrying out in the simulation conditions with one emitting car. In real, traffic conditions, in which participate a lot of different vehicles, amount of pollutants getting into the cabin could be much higher. VOCs identified in the background measurement, indicates that in new car could be another source of those pollutants – the materials used for made cabin equipment [7]. To avoid exposure to VOCs inside the car cabin it is beneficial to ventilate the interior by open both of doors from time to time (on opposite sides) when stationary or both of windows during driving.

Acknowledgments:

The results presented in the paper was provided and developed during the POIG.01.04.00-02-154/13 and POIG.04.05.02-00-030/12-00 projects realization.

References

- [1] Chłopek Z. Badania modelu globalnej emisji spalin z silników pojazdów drogowych. *Chem Inż Ekol.* 1999;6(8):719-735.
- [2] Yang S, He LY. Fuel demand, road transport pollution emissions and residents' health losses in the transitional China. *Transport Res Part D: Transport Environ.* 2016;42:45-59. DOI: 10.1016/j.trd.2015.10.019
- [3] Badyda AJ, Dąbrowiecki P, Czechowski PO, Majewski G, Doboszyńska A. Traffic-related air pollution and respiratory tract efficiency. *Adv Exp Med Biol.* 2015;834:31-8. DOI: 10.1007/5584_2014_13.
- [4] Zawiślak M. Application of computational fluid dynamics in the assessment of the spread of toxic compounds emitted by a diesel engine inside a vehicle. *J Polish CIMAC.* 2014;9(2):197-205.
- [5] Pope CA, Burnett RT, Thun MJ, Calle EE, Krewski D, Ito K, Thurston GD. Lung Cancer, Cardiopulmonary Mortality, and Long-term Exposure to Fine Particulate Air Pollution. *JAMA Network.* 2002;287:9:1132-1141. DOI: 10.1001/jama.287.9.1132.
- [6] ISO 12219-3:2012, Interior air of road vehicles – Part 3: Screening method for the determination of the emissions of volatile organic compounds from vehicle interior parts and materials – Micro-scale chamber method, [www: http://www.iso.org/iso/catalogue_detail.htm?csnumber=54866](http://www.iso.org/iso/catalogue_detail.htm?csnumber=54866).

- [7] Geiss O, Tirendi S, Barrero-Moreno J, Kotzias D. Investigation of volatile organic compounds and phthalates present in the cabin air of used private cars. *Environ Int.* 2009;35(8):1188-1195. DOI:10.1016/j.envint.2009.07.016.

EKSPOZYCJA KIEROWCY PRZEBYWAJĄCEGO WEWNĄTRZ KABINY NOWEGO POJAZDU NA LOTNE ZWIĄZKI ORGANICZNE

¹ Katedra Inżynierii Pojazdów, Wydział Mechaniczny, Politechnika Wroclawska, Wrocław

² Dr. Schneider Automotive Polska Sp.z o.o., Janowice Wielkie

³ Katedra Konstrukcji i Badań Maszyn, Wydział Mechaniczny, Politechnika Wroclawska, Wrocław

Abstrakt: W obecnych czasach motoryzacja stanowi jedną z głównych gałęzi przemysłowych. Dynamiczny rozwój motoryzacji, poza wieloma walorami społecznymi i cywilizacyjnymi, jest powodem licznych problemów, przekładających się w mniejszym lub większym stopniu na zdrowie i życie ludzi. Transport jest jednym z głównych źródeł emisji zanieczyszczeń do powietrza, szczególnie w aglomeracjach miejskich. Co więcej, rozwój motoryzacji sprawia również, że ludzie spędzają w samochodach coraz więcej czasu. W warunkach miejskich natężenie ruchu jest znacznie wyższe niż poza miastem. Często powstają zatory drogowe. Spaliny, których składnikami są również lotne związki organiczne, dostając się do wnętrza pojazdów uczestniczących w zatorze drogowym, stanowią poważne zagrożenie dla kierowców tych pojazdów oraz ich pasażerów. W nowych pojazdach dodatkowym źródłem lotnych związków organicznych mogą być elementy wyposażenia wnętrza kabiny.

W pracy przedstawiono wyniki badań stężeń lotnych związków organicznych wewnątrz kabiny nowego, eksploatowanego samochodu osobowego. Zidentyfikowano również źródła lotnych związków organicznych znajdujących się wewnątrz pojazdu oraz dokonano oceny narażenia kierowcy.

Słowa kluczowe: wnętrze kabiny pojazdu, jakość powietrza wewnętrznego, lotne związki organiczne

Małgorzata KUTYŁOWSKA¹

PREDICTION OF WATER CONDUITS FAILURE RATE – COMPARISON OF SUPPORT VECTOR MACHINE AND NEURAL NETWORK

PRZEWIDYWANIE WSKAŹNIKA AWARYJNOŚCI PRZEWODÓW WODOCIĄGOWYCH – WEKTORY NOŚNE ORAZ SIECI NEURONOWE

Abstract: This paper presents the possibility of applying support vector machines (SVMs) and artificial neural networks (ANNs), based on radial basis functions to predict the failure rate of water conduits. The SVM method is an algorithm for carrying out regression and classification, taking into account a nonlinear decision space. This hyperplane divides the whole area in such a way that objects of different affiliation are separated from one another. In the case of ANNs, each of the neurons models a Gaussian response surface. The information from the inputs is transmitted to a basis function and each neuron calculates the Euclidean distance between the input, reference and output vectors. The failure rate of distribution pipes and house connections was predicted on the basis of operational data for the years 2001–2012. In both the methods the independent variables were: the length, diameter and year of construction of the distribution pipes and the house connections. The computations were carried out using the Statistica 12.0 software. The SVM-RBF model for the house connections and the distribution pipes had respectively 14 SVMs (including 7 localized SVMs) and 56 SVMs (including 46 localized SVMs). The ANN-RBF model contained 8 and 27 hidden neurons for respectively the distribution pipes and the house connections.

Keywords: regression methods, pipelines, modelling, radial basis functions

1. Introduction

Water distribution systems are the critical underground infrastructure components because they perform the strategic functions in broadly understood municipal engineering. In the current terrorist threat context [1], the necessity to ensure the proper protection and management of water supply systems is increasingly often highlighted. These are undoubtedly vital issues which together with reliability analyses, water demand analyses and the properly planned modernization of the pipelines and the whole

¹ Faculty of Environmental Engineering, Wrocław University of Science and Technology, Wybrzeże S. Wyspiańskiego 27, 50–370 Wrocław, Poland, phone: +48 71 320 40 84, email: malgorzata.kutyłowska@pwr.edu.pl

water supply infrastructure should be and currently are the subject of numerous studies and projects. Research on the technical condition, failure frequency and operational reliability of water conduits and the associated water losses is highly advanced in Poland and abroad [2–7]. The research findings indicate that such studies need to be continued in order to gain deeper knowledge in this field, especially with regard to mathematical modelling, which owing to the development of computing techniques is constantly improved and uses increasingly more accurate modelling methods [8]. Mathematical prediction and modelling have become very popular in broadly understood environmental engineering [9–13], which is an inducement to apply them to the study of the failure frequency of water distribution systems. So far such regression methods as: support vector machines (SVM), artificial neural networks (ANN) [14], K-nearest neighbours (KNN) [15] and regression and classification trees [16] have been used to determine failure rates.

The main aim of this study was to demonstrate that it is possible to apply a regression method based on support vector machines to predict the failure rate of water supply pipelines and to compare the results obtained in this way with the results of modelling this rate by means of RBF (radial basis functions) artificial neural networks. Besides also some prediction examples using other kernel functions of SVM models (linear, polynomial and sigmoidal) will be presented to achieve wider comparison area. Thanks to such a comparison it will be possible to determine the optimal modelling method for the currently operated water supply networks. A variant of the failure rate prediction method presented here has been successfully applied by Aydogdu and Firat [17], which induced the author to take up this subject as applied to the Polish water distribution network. The results presented here are complementary to the results of modelling the failure rate by SVM, reported in [18] where all the kinds of kernel functions were analyzed and other predictors were used. It is also examined whether the water supply pipeline failure rate prediction methods proposed in this paper can be an alternative to typical mathematical models.

1.1. Support vector machines

The support vector machines (SVM) method is an algorithm for regression and classification with a nonlinear decision space taken into account. This hyperplane divides the whole area in such a way that objects of different affiliation are separated from one another. It is also necessary to keep a maximum margin of error, *ie* the distance from the separating plane. The number of support vector machines determines the complexity of the relations between dependent and independent variables [19]. In the case of a qualitative analysis of such a dependent variable as the failure rate of water conduits, no classification, but regression is performed. Four kinds of SVMs, characterized by four types of kernel functions: linear, polynomial, sigmoidal and radial basis functions (RBF), are distinguished [19]. The notion of kernel functions derives from investigations of linear vector spaces. In the case of the problem considered here, RBF-SVM models, *ie* based on solely radial basis functions, were built and compared with ANN models. Nevertheless predictions results using other kernel functions are also

displayed to show wider modelling point of view. But the straight comparison (SVM vs. ANN) could be only performed between models based on the same kernel functions (RBF). In the course of an regression analysis a relation between the dependent variable and the independent variables (predictors) is sought. This relation should possibly most accurately generate a dependent variable value for new cases (testing sample data), ie ones which the SVM model has not “seen” before, having been trained on a training sample. The mapping function $\varphi(x)$ is called kernel function which meets Mercer condition and feature map for Mercer kernel is as follows [20]:

$$k(x, y) = \varphi(x) \varphi(y) \quad (1)$$

The kernel functions are described by the equations (2–5), respectively for linear, polynomial, sigmoidal and RBF [20]:

$$k(x, y) = (x \cdot y) \quad (2)$$

$$k(x, y) = (s(x \cdot y) + \gamma)^d \quad (3)$$

$$k(x, y) = \tanh(s(x \cdot y) + \gamma) \quad (4)$$

$$k(x, y) = \exp\left(-\frac{\|x - y\|^2}{2\sigma^2}\right) \quad (5)$$

where: γ – a learning rate,
 x – independent variable,
 y – dependent variable.

The prediction function is calculated from the relation [19]:

$$y(X) = w^T \varphi(x) + b \quad (6)$$

where: b – bias,
 w – weight vector,
 φ – mapping function.

1.2. RBF artificial neural networks

Since the theory of artificial neural networks is described in detail in the literature on the subject [21], only the most basic information on RBF artificial neural networks is provided here. Unlike the multilayer perceptron, RBF ANNs contain radial neurons (performing a function radially changing around a given centre in the vicinity of which nonzero values are assumed). Each such neuron models a Gaussian response surface. The information from the inputs is transmitted to the radial basis function and each neuron calculates the Euclidean distance between the input, reference and output vectors. It is essential that there are enough radial neurons so that they can accurately correlate the function with the sought solution. The solutions based on RBF artificial

neural networks are slow-speed and require a considerable storage area, which is sometimes a serious limitation [19]. RBF ANNs are trained as follows. Training proceeds in two steps [19]: first RBFs are arranged using the input signals and then weights between the RBFs and the output neurons are determined. Consequently, no iterative process is required, which is evidence of the absence of typical training epochs. The characteristic feature of RBF artificial neural networks is that the RBFs are determined on the basis of the input vector and after the weights are added up the result is fed to the output. The location and width of the basis functions and the weights linking them with the output signals are of major importance in RBF artificial neural networks [19].

2. Experimental methodology

The failure rate (λ , fail./km · a) of the distribution pipes and the house connections in a selected Polish town was predicted using the RBF-SVM method and the RBF-ANN method. The two approaches were based on radial basis functions. Moreover some prediction results using other kernel functions (linear, polynomial and sigmoidal) are displayed to make a comparison more accurate. Operational data for the years 2001–2012 obtained from the town's water company were used for modelling. In the case of SVM modelling, the whole data set was randomly divided into two equal (50%) subsets. The training sample and the testing sample had 147 data each for the house connections and respectively 124 and 125 data for the distribution pipes. First a model was built using the training data and then it was tested on an "unseen" sample. In the case of ANNs, the procedural algorithm was slightly different due to the peculiarities of this kind of modelling. The artificial neural network learning process consisted of several stages: a training stage (50% of the data), followed by a testing stage (25% of the data) and finally, the validation (25% of the data) of the created models. In the considered case, the whole data set (294 data for the house connections and 249 data for the distribution pipes) was used to train the ANN. The division into a training sample, a testing sample and a validating sample was random. Using the ANN algorithm one can also make prognosis based on unseen data. Such a prognosis was made using a separately created set of operational data. Models were built for separately the distribution pipes and the house connections. The computations were carried out using the Statistica 12.0 software.

Since the SVM method is a kind of nonparametric regression, the correlations between the dependent variables (the predicted value) and the independent variable need not to be known. V -fold cross validation was used to find the optimal model parameters. In this type of cross validation, data are divided into V randomly selected disjoint parts. Using the $V-1$ parts of data as training examples the dependent variable is predicted and the prediction error is calculated on the basis the residual sum of squares. The procedure is executed for all the V data segments. Then a model quality measure is determined on the basis of the averaged errors of the particular cycles. The optimal model parameters are selected during a quality analysis. The parameters determined in the course of the V -fold cross validation are: gamma, capacity, epsilon and the number

of support vector machines (including localized vectors) [19]. Tenfold ($V = 10$) cross validation was used in the considered problem, whereby it was possible to select proper values for such parameters (learning constants) as capacity (C) and epsilon (ϵ), since they are not *a priori* known. In the case of artificial neural networks, model parameters (eg the number of hidden neurons and the type of activation functions) are determined during ANN training using a proper training algorithm. Between ten and twenty ANN models, for which the number of hidden neurons ranged from 1 to 30, were tested. The model characterized by the smallest mean-square error and the best fit between the real data and the predicted ones was selected. The results presented later in this paper are for this selected optimal ANN model.

In both the methods the independent variables were: length (L_r, L_p), diameter (D_r, D_p) the year of construction (Y_r, Y_p) of the distribution pipes and the house connections. The same independent variables had been used by Aydogdu and Firat [17] to model the failure rate of water conduits by means of a combination of SVM and fuzzy logic. It should be noted that the average length of the pipelines was used in the calculations. This approach to failure rate determination (using the average length) is suggested in the literature on the subject [2]. The real (experimental) failure rate was calculated from the well-known relation [2, 3]:

$$\lambda = \frac{N(t)}{L \cdot \Delta t} \quad (7)$$

where: $N(t)$ – the number of failures of linear objects in time interval Δt , units;
 L – the average length of pipelines in time Δt , km;
 Δt – the observation time, year.

3. Results and discussion

The parameters of the built SVM-RBF and ANN-RBF models for the different types of water conduits are presented in Table 1. The validation error was one of the considerations for selecting an SVM model most accurately predicting the failure rate. The validation error for the distribution pipes and the house connections amounted to respectively 0.08 and 0.11. Nevertheless, the failure rate prediction on the basis of the testing sample was not satisfactory from the predicted/real data fit point of view. Moreover, the number of SVMs for the distribution pipes was high and as much as 82% of them were localized SVMs, ie with weights equal to \pm the capacity value (Table 1), indicating a more complicated model structure. In the case of any kind of modelling, one should answer the question whether the aim is to obtain a perfect data fit at any cost, ie at the expense of model architecture complication, or rather to reveal the correlations between the dependent and independent variables. The latter approach enables one to find out whether the independent variables (predictors in the case of the SVM method) show significant correlations with the dependent variable, even if the estimate carries a predefined admissible error.

Table 1

Parameters of SVM-RBF and ANN-RBF models

Type of conduit/parameter	Distribution pipes	House connections
SVM model		
Gamma	0.333	0.333
Capacity (C)	3	1
Epsilon (ϵ)	0.2	0.5
Number of support vectors (localized)	56 (46)	14 (7)
Cross-validation error	0.081	0.110
ANN model		
Number of hidden neurons	8	27
Activation functions: hidden/output layer	Gaussian/linear	Gaussian/linear
Training algorithm	RBFT	RBFT
Correlation coefficient (learning/prognosis step)	0.956/0.859	0.997/0.897
Determination coefficient (learning/prognosis step)	0.914/0.737	0.994/0.805

In the case of the ANN models, Pearson's correlation coefficient (R), a determination coefficient (R^2) and a relative mean-square prediction error (amounting to about 20% for the distribution pipes and the house connections) would be compared. The error is rather high in comparison with the results of failure rate modelling by, *eg* artificial neural networks based on the multilayer perceptron [22]. But in the cited paper there was an additional input signal – the pipeline material, which (besides the perceptron structure) could have contributed to the closer convergence between the real and predicted data. Also in [23], where hourly water demand histograms were predicted, RBF ANNs were found to be less useful than the multilayer perceptron. Despite the fact that there were three times more hidden neurons in the house connections model than in the distribution pipes model (Table 1), the prediction results are worse and characterized by larger discrepancies between the real and predicted data (Figs 1 and 2). Because of the nature of RBF ANNs, the activation functions and the training method were pre-imposed, which also can have a bearing on modelling quality in comparison with, *eg* artificial neural networks using the multilayer perceptron, where it is possible to use

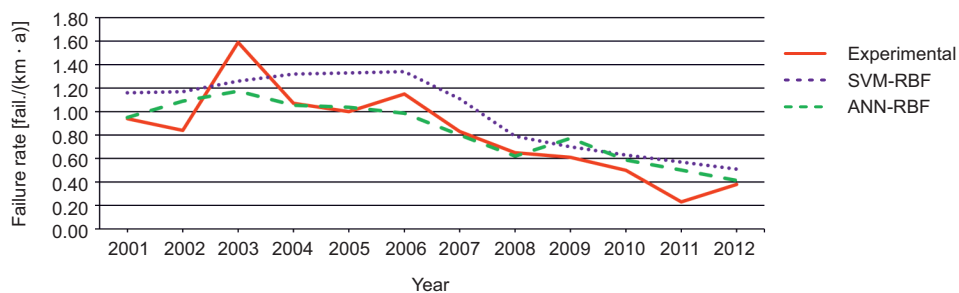


Fig. 1. Prediction results of house connections' failure rate – testing-SVM/prognosis-ANN

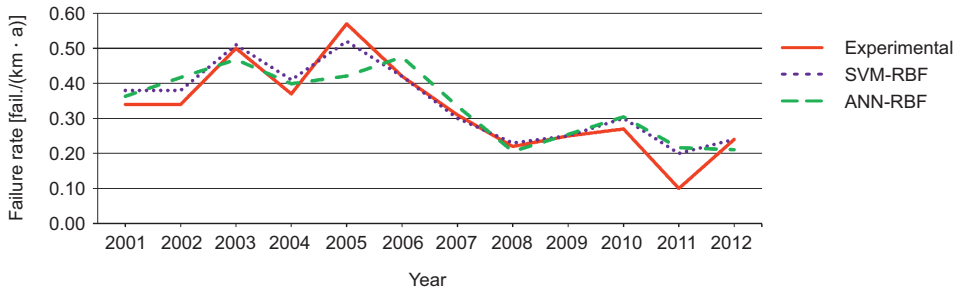


Fig. 2. Prediction results of distribution pipes’ failure rate – testing-SVM/prognosis-ANN

several different functions, such as the sigmoidal function, the exponential function and so on [22].

The failure rate prediction results for the learning sample are presented in Table 2 while the ones for the testing sample (the SVM model) and the prognosis stage (the ANN model) are shown in Figs 1 and 2.

Table 2

Results of failure rate prediction – learning step

Year	House connections			Distribution pipes		
	Experimental	ANN-RBF	SVM-RBF	Experimental	ANN-RBF	SVM-RBF
2001	0.94	0.95	1.17	0.34	0.36	0.38
2002	0.84	0.84	1.16	0.34	0.36	0.38
2003	1.59	1.58	1.26	0.50	0.47	0.48
2004	1.07	1.07	1.32	0.37	0.39	0.41
2005	1.00	1.00	1.32	0.57	0.48	0.52
2006	1.15	1.15	1.33	0.42	0.42	0.42
2007	0.83	0.80	1.12	0.31	0.30	0.33
2008	0.65	0.63	0.79	0.22	0.21	0.22
2009	0.61	0.62	0.70	0.25	0.25	0.24
2010	0.50	0.50	0.63	0.27	0.26	0.24
2011	0.23	0.33	0.57	0.10	0.21	0.20
2012	0.38	0.38	0.51	0.24	0.25	0.24

It is necessary to draw this distinction between the testing sample for the SVM model and the prognosis stage for the ANN model since the testing sample data and the prognosis stage data were unknown to the given model. Only in this way, by analyzing the results obtained for the data set unseen by the model, one can assess the quality of the model and its applicability to dependent variable (failure rate) prediction. Moreover, in the Table 3 and 4 the results prediction in learning step and main parameters of the models using other kernel functions (linear, polynomial and sigmoidal) are displayed, respectively. The main aim of this work was to compare the modelling results of ANN

and SVM models based on radial basis function. The information shown in the Table 3 and 4 should be rather treated as supplement. The analysis of the Table 3 shows that for distribution pipes SVM model based on sigmoidal function has the best convergence with experimental data in learning step ($R^2 = 0.85$). Slightly different situation is observed concerning house connections. For these conduits sigmoidal and polynomial functions were responsible for the best agreement (learning step) between predicted and experimental values of failure rate, R^2 equalled to 0.87 and 0.84, respectively. The whole comparison of prediction results using all kernel functions was described in [18] for another water distribution system. In this work only basic information concerning other kernel functions are stated.

Table 3

Results of failure rate prediction (other kernel functions) – learning step

Year	House connections			Distribution pipes		
	SVM-linear	SVM-poly-nomial	SVM-sigmoidal	SVM-linear	SVM-poly-nomial	SVM-sigmoidal
2001	1.04	1.04	0.95	0.43	0.43	0.39
2002	1.04	1.04	0.84	0.43	0.43	0.40
2003	1.18	1.21	1.20	0.47	0.47	0.51
2004	1.22	1.07	1.10	0.45	0.43	0.39
2005	1.24	1.06	0.93	0.49	0.48	0.53
2006	1.25	1.14	1.22	0.45	0.43	0.40
2007	0.99	1.03	0.85	0.33	0.40	0.37
2008	0.66	0.78	0.65	0.22	0.27	0.24
2009	0.58	0.63	0.52	0.21	0.26	0.22
2010	0.50	0.52	0.50	0.20	0.27	0.12
2011	0.43	0.33	0.50	0.15	0.22	0.04
2012	0.38	0.37	0.51	0.17	0.20	0.23

An analysis of Table 2 clearly shows that there is better agreement between the ANN-RBF model training results and the real failure rate λ values than in the case of the SVM-RBF model used for the house connections. For the distribution pipes the differences in failure rate predictions between the two modelling methods are not so significant and one can say that the two methods are equally effective, as indicated by the fact that coefficients $R = 0.96$ and $R^2 = 0.92$ are identical for both methods. Considerable errors (over 100%) occur in the estimates of the failure rate for the distribution mains only in 2011, which is undoubtedly due to the fact that this rate is very much different from the rates for the other analyzed years. A similar error occurs in the predictions of the failure rate for the house connections in 2011. Therefore the question arises: what should be done in the case of divergent data? Should they be included in order not to disrupt the continuity of the analysis of operational data, as it was done in this paper, or rather completely rejected? However, one should take into account the kind of analyzed problem. The modelling of the technical condition and

failure rate of a water distribution network should not omit or exclude some years from the analysis simply because of divergent data. The information about the failure rate level in a given year is based on pipeline failures which really occurred. Therefore if some years were neglected in the analysis, this would result in an incomplete picture of the reality. Whereas models based on all the available data make it possible to obtain a complete picture, albeit not always a very accurate one.

Table 4

Parameters of SVM models based on other kernel functions

Type of conduit/parameter	Distribution pipes	House connections
SVM-linear		
Gamma	—	—
Capacity (C)	10	2
Epsilon (ϵ)	0.4	0.3
Number of support vectors (localized)	36 (27)	50 (46)
Cross-validation error	0.094	0.112
SVM-polynomial		
Gamma	0.333	0.333
Capacity (C)	10	5
Epsilon (ϵ)	0.4	0.3
Number of support vectors (localized)	40 (33)	52 (48)
Cross-validation error	0.124	0.136
SVM-sigmoidal		
Gamma	0.333	0.333
Capacity (C)	10	10
Epsilon (ϵ)	0.1	0.1
Number of support vectors (localized)	116 (110)	123 (119)
Cross-validation error	0.093	0.119

The analysis of the Table 4 shows that SVM models based on other kernel functions are more complicated due to *eg* higher capacity value, higher value of parameter ϵ (linear and polynomial functions) and more support vectors (also localized). The aim of the modelling is not only to get convergent prediction results, but also to achieve relatively simple model structure and its parameters. The choosing of the optimal model (concerning SVM modelling) should be based not only on agreement between experimental and predicted values, but also on analyzing the cross-validation error and the model architecture described by *eg* number of support vectors (also localized) and capacity. The enough huge data base is also the problem during the modelling. In some cases the number of available operating parameters or number of registered cases (received from water utilities) is too low to build the model responsible for prediction of failure rate with satisfactory convergence with real data. The models proposed in this paper consist of basic operating data. In the future it seems to be reasonable to widen the vector of independent variables to create more general models.

Similar correlations (as the ones described above concerning RBF models) between real and predicted data were obtained at the testing stage (the SVM model) and the prognosis stage (the ANN model), as shown in Figs 1 and 2. In the case of the house connections, more convergent results are generated by the ANN model, but for some years (eg 2003, 2006 and 2009) the differences are much larger than the ones observed at the learning stage. Despite many divergences, the trend in the variation of the predicted values is similar to the trend in the variation of experimental values. In the years 2006–2008 a similar pattern is observed for the SVM model, but most of the λ values are much higher than the real ones.

The prediction of the failure rate of the distribution pipes (Fig. 2) by the SVM method and the ANN method was characterized by acceptable agreement between the predicted and experimental results in both cases. The Pearson's correlation coefficient for the SVM model and the ANN model amounted to respectively 0.96 and 0.86, indicating that the SVM method is slightly better for predicting the failure rate of distribution pipes than the ANN method. The opposite is true for house connections. It should also be noted that the results of predicting the failure rate of the distribution pipes and the house connections (Table 2, Figs 1 and 2) by means of the SVM-RBF model are very similar for both the learning sample and the testing sample. Whereas the results of learning and prognosis by the ANN-RBF method show larger discrepancies for both types of pipelines. Even though at the learning stage the agreement between the real and predicted results is satisfactory, the prediction process (using new data) carries a larger (but still acceptable from the engineering point of view) error. This is evidence of greater effectiveness of RBF-based training by means of SVMs than ANNs. However, at the current stage of the research it cannot be explicitly indicated which of the methods is better and should be widely adopted in the modelling of the failure rate of water distribution networks. Further research in this area is needed, also on operational data from other water companies, permitting more in-depth analyses and broader generalizations.

The prediction results on testing sample concerning house connections and distribution pipes using other kernel functions by means of SVM model are displayed in the Figs 3 and 4. Similarly as in learning step, polynomial and sigmoidal functions were

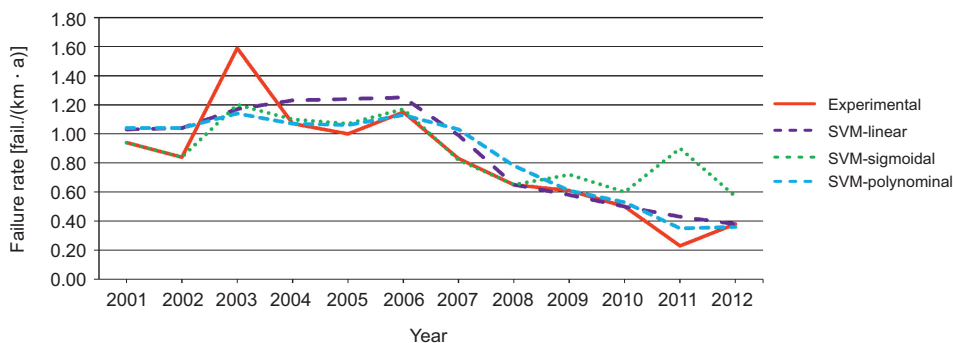


Fig. 3. Prediction results of house connections' failure rate – testing

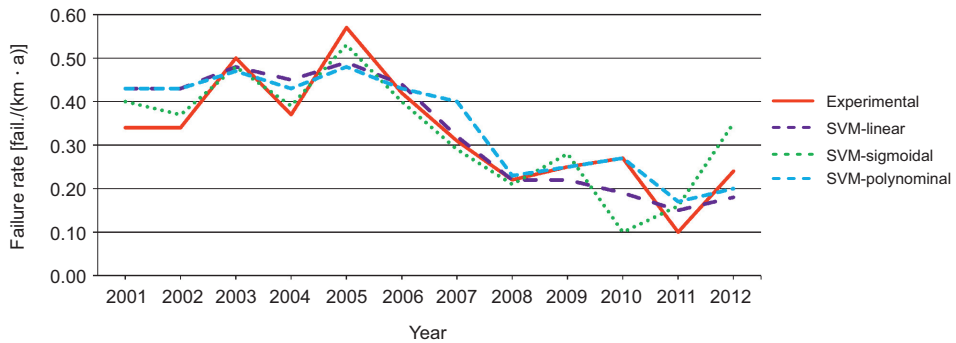


Fig. 4. Prediction results of distribution pipes' failure rate – testing

responsible for the optimal convergence between predicted and experimental values of indicator λ . It is necessary to remember that modelling only tries to imitate the reality. It is obvious that prediction results could not be exactly the same as experimental data. The problem is what error level is permitted and assumed at the very beginning of the modelling. Operating data have sometimes a lot of mistakes. If it is possible one should cooperate with exploiters to explain inaccuracy and to complete lack of parameters.

Such basic independent variables as: pipeline length, diameter and construction year were used to model the failure rate of the water supply pipelines. The weights of the connections between neurons were determined for the selected ANN model. The ANN-RBF model, describing the failure rate of the house connections, was characterized by the weakest connection between hidden neuron no. 19 and the output signal. The weight of this connection amounted to -0.09 . The highest connection weight value (1.00) was observed between the input neuron (diameter) and hidden neuron no. 8. This supports the thesis, advanced in numerous publications [2, 3, 24, 25], that the failure rate of a pipeline is correlated with its diameter. The ANN-RBF model for the distribution pipes had a connection between hidden neuron no. 2 and the output signal (λ), with a weight of -4.13 . This means that the situation was similar as in the case of the house connections. The strongest connection was characterized by a weight of 0.90 and occurred between the input signal (length) and hidden neuron no. 3. This means that the total length of a pipeline of this type for a given year plays a significant role in the modelling of the failure rate of distribution pipes. In the case of the SVM model, weights which should be considered jointly with another model parameter, *ie* capacity, were determined for the particular SVMs. If the weight of a given SVM is close to the value of $\pm C$, this means that this SVM lies relatively near the hyperplane. If the weight is equal to $\pm C$, the given SVM lies directly on the hyperplane boundary and it is then referred to as a localized SVM. The SVM-RBF model for the house connections had capacity $C = 1$ and the weights of its 14 SVMs were in a range of -1.00 – 1.00 . There were 7 localized SVMs. The other SVMs had weights ranging from -0.86 to 0.76 . The SVM-RBF model for the distribution mains had capacity $C = 3$ and the weights of 56 SVMs were in a range of -3.00 – 3.00 . There were 46 localized SVMs. The weights of the other SVMs ranged from -2.94 to 2.76 .

4. Conclusions

This paper has presented the results of the prediction of the failure rate of the distribution pipes and house connections in one of the Polish towns, based on operational data for the years 2001–2012, by means of support vector machines and artificial neural networks. The subject seems to be of importance for the correct and quick estimation of the reliability level. The created SVM-RBF and ANN-RBF models can be useful in cases when it is necessary to determine the failure rate in order to take a quick decision concerning the planned repairs of conduits. The obtained prediction results indicate that both the methods can be used to estimate the failure rate of municipal systems. But, similarly as in the case of other methods, a relatively large database must be available in order to identify the relevant correlations (training/learning) and then to test the model. One should bear in mind that each modelling carries a prediction error. When selecting an optimal model one should not only consider the achievement of the best possible convergence, but also assess the effect of an inaccurate estimate. The consequences of a failure of, *eg* distribution pipes are incomparably more massive and severe than any damage to house connections.

The results of prediction concerning other kernel functions are also satisfactory. The SVM models for the distribution pipes using linear, polynomial and sigmoidal kernel functions were characterized by the weights (without localized vectors) in the range -8.14 to 6.63 , -9.70 to 9.04 and -9.25 to 9.95 , respectively. In relation to house connections the weights without localized vectors varied in the range -1.86 to -0.23 , -3.26 to 2.69 and -9.89 to 3.09 , respectively.

The optimal SVM-RBF model had gamma coefficient amounted to 0.33 for both the distribution pipes and the house connections while capacity C and the number of SVMs were respectively 3 and 4 times greater in the case of the model describing the failure rate of the distribution pipes. The error of the V -fold cross validation amounted to 0.081 and 0.110 for the model describing the failure rate of respectively the distribution pipes and the house connections. The input signals and the predictors, respectively, in both the ANN method and the SVM method were the length, diameter and year of laying the water conduit in the ground. The optimal ANN-RBF model contained 8 and 27 hidden neurons for respectively distribution pipes and house connections. The correlation and determination coefficients are slightly higher at the stage of learning the artificial neural network than during prognosis. The obtained modelling results can be in still better agreement with the real data. This would increase the quality of the decisions concerning, *eg* the planning of replacements and renewals of pipeline sections. The accuracy of the modelling can be increased by adding more predicators of, *eg* the conduit material, the number of failures or the pressure prevailing in the pipeline, to the vector of independent variables. However, it is not always possible to obtain such data due to the fact that water companies do not record all their operational information. It should be noted that the situation is improving by the year and the operators increasingly often use the GIS database, which facilitates data acquisition and analysis. Therefore, further studies aimed at determining such independent variables which will be proper parameters for the correct prediction of the failure rate by SVMs and ANNs are needed.

Acknowledgment

The work was realized within the allocation No. B50519 awarded for Faculty of Environmental Engineering Wrocław University of Science and Technology by Ministry of Science and Higher Education. The grant was allocated for scientific researches of young scientists in years 2015–2016.

References

- [1] Pietrucha-Urbaniak K. *Glob Network Environ Sci Technol J.* 2014;16(5):893-900. http://journal.gnest.org/sites/default/files/Submissions/gnest_01414/gnest_01414_published.pdf
- [2] Hotłoś H. Ilościowa ocena wpływu wybranych czynników na parametry i koszty eksploatacyjne sieci wodociągowych [Quantitative assessment of the effect of some factors on the parameters and operating costs of water-pipe networks]. Wrocław: Wrocław University of Technology Publishing House; 2007.
- [3] Kwietniewski M, Rak J. Niezawodność infrastruktury wodociągowej i kanalizacyjnej w Polsce [Reliability of water supply and wastewater disposal infrastructure in Poland]. Warszawa: Monographs of the Civil Engineering Committee at the Polish Academy of Sciences, Studies in Engineering No. 67; 2010.
- [4] Iwanek M, Kowalski D, Kwietniewski M. Badania modelowe wpływu wody z podziemnego rurociągu podczas awarii [Model studies of a water outflow from an underground pipeline upon its failure]. *Ochr Środ.* 2015;37(4):13-17. http://www.os.not.pl/docs/czasopismo/2015/4-2015/Iwanek_4-2015.pdf
- [5] Zimoch I, Szymbik-Gralewska. Zastosowanie zintegrowanej metody analizy niezawodnościowo-ekonomicznej w zarządzaniu przewymiarowaną infrastrukturą wodociągową [Application of integrated reliability-economic analysis in management of oversized water supply infrastructure]. *Ochr Środ.* 2015;37(4):25-30. http://www.os.not.pl/docs/czasopismo/2015/4-2015/Zimoch_4-2015.pdf
- [6] Tscheikner-Gratl F, Sitzenfrei R, Rauch W, Kleidorfer M. *Struct Infrastruct Eng.* 2016;12(3):366-380. DOI: 10.1080/15732479.2015.1017730.
- [7] Piratla KR, Yerri SR, Yazdekhasti S, Cho J, Koo D, Matthews JC. *Proc Eng.* 2015;118:727-734. DOI: 10.1016/j.proeng.2015.08.507
- [8] Scheidegger A, Leitao JP, Scholten L. *Water Res.* 2015;83:237-247. <http://dx.doi.org/10.1016/j.watres.2015.06.027>.
- [9] Cieżak W, Cieżak J. *Environ Prot Eng.* 2015;41(2):179-186. DOI: 10.5277/epe150215.
- [10] Kaźmierczak B, Wdowikowski M. *Periodica Polytechnica Civ Eng.* 2016;60(2):3-5-312. DOI 10.3311/PPci.8341.
- [11] Tchórzewska-Cieślak B. *Environ Prot Eng.* 2011;37(3):111-118. http://epe.pwr.wroc.pl/2011/3_2011/12tchorzewska.pdf
- [12] Zimoch I, Łobos E. Application of the Theil statistics to the calibration of a dynamic water supply model. *Environ Prot Eng.* 2010; 36(4):105-116. http://epe.pwr.wroc.pl/2010/zimoch_4-2010.pdf
- [13] Kolasa-Więcek A. *Ecol Chem Eng S.* 2013;20(2):419-428. DOI: 10.2478/eces-2013-0030.
- [14] Nishiyama M, Filion Y. *Can J Civ Eng.* 2014;41(10):918-923. DOI: dx.doi.org/10.1139/cjce-2014-0114.
- [15] Kutylowska M. Prediction of failure rate of water pipes using K-nearest neighbours method. Proceedings of the IWA 8th Eastern European Young Water Professionals Conference Gdańsk, Poland, 12-14 May, 2016, 93-94. http://iwa-ywp.eu/wp-content/uploads/2016/06/Book_of_abstracts.pdf
- [16] Bevilacqua M, Braglia M, Montanari R. *Reliability Eng Syst Saf.* 2003; 79(1):59-67. <http://www.sciencedirect.com/science/article/pii/S0951832002001801>
- [17] Aydogdu M, Firat M. *Wat Resour Manage.* 2015;29:1575-1590. DOI: 10.1007/s11269-014-0895-5.
- [18] Kutylowska M, Orłowska-Szostak M. Przewidywanie wskaźnika awaryjności przewodów wodociągowych za pomocą metody wektorów nośnych [Forecasting failure rate of water pipes using support vector machines]. In: Kuś K, Piechurski F, editors. *Nowe technologie w sieciach i instalacjach wodociągowych i kanalizacyjnych*. Gliwice: 2016.
- [19] *Statistica 12.0., Electronic Manual.*
- [20] Guo YM, Wang XT, Liu C, Zheng YF, Cai XB. *Maint and Reliability.* 2014;16(1):85-91. <http://www.ein.org.pl/pl-2014-01-14>.
- [21] Suzuki K. *Artificial neural networks. Architectures and applications.* Chicago: InTech; 2013.
- [22] Kutylowska M. *Eng Fail Anal.* 2015;47:41-48. <http://dx.doi.org/10.1016/j.engfailanal.2014.10.007>.

- [23] Siwon Z, Cieżak W, Cieżak J. Modele neuronowe szeregów czasowych godzinowego poboru wody w osiedlach mieszkaniowych [Neural network models of hourly water demand time series in housing areas]. *Ochr Środ.* 2011;33(2):23-26.
http://www.os.not.pl/docs/czasopismo/2011/2-2011/Siwon_2-2011.pdf
- [24] Pelletier G, Mailhot A, Villeneuve JP. *J Wat Resour Plann and Manage.* 2003;129(2):115-123.
DOI: 10.1061/(ASCE)0733-9496(2003)129:2(115).
- [25] Tabesh M, Soltani J, Farmani R, Savic D. *J Hydroinformatics.* 2009;11(1):1-17.
DOI: 10.2166/hydro.2009.008.

PRZEWIDYWANIE WSKAŹNIKA AWARYJNOŚCI PRZEWODÓW WODOCIĄGOWYCH – WEKTORY NOŚNE ORAZ SIECI NEURONOWE

Wydział Inżynierii Środowiska
Politechnika Wroclawska, Wrocław

Abstrakt: W pracy przedstawiono możliwość zastosowania metody wektorów nośnych (SVM) oraz sztucznych sieci neuronowych (SSN) opartych na radialnych funkcjach bazowych do przewidywania wskaźnika intensywności uszkodzeń przewodów wodociągowych. Metoda wektorów nośnych jest algorytmem, za pomocą którego dokonuje się regresji i klasyfikacji z uwzględnieniem nieliniowej przestrzeni decyzyjnej. Ta hiperpłaszczyzna dzieli cały obszar w taki sposób, że obiekty o różnej przynależności są od siebie oddzielone. Natomiast w przypadku sieci neuronowych każdy z neuronów modeluje tzw. gaussowską powierzchnię odpowiedzi. Informacje z wejść przekazywane są funkcji bazowej, a każdy neuron oblicza odległość euklidesową między wektorami wejściowymi, wzorcowymi i wyjściowymi. Przewidywanie wskaźnika intensywności uszkodzeń przewodów rozdzielczych i przyłączy wykonano na podstawie danych eksploatacyjnych z lat 2001–2012. W przypadku obydwu metod zmiennymi niezależnymi były: długość, średnica oraz rok budowy przewodów rozdzielczych i przyłączy. Obliczenia przeprowadzono w programie Statistica 12.0. Model SVM dla przyłączy i przewodów rozdzielczych posiadał odpowiednio 14 wektorów nośnych, w tym 7 związanych oraz 56 w tym 46 związanych. Model SSN zawierał 8 i 27 neuronów ukrytych odpowiednio w odniesieniu do przewodów rozdzielczych i przyłączy.

Słowa kluczowe: metody regresyjne, rurociągi, modelowanie, radialne funkcje bazowe

Elżbieta BEZAK-MAZUR^{1*} and Dagmara ADAMCZYK¹

ADSORPTION OF MIXTURE OF TWO DYES ON ACTIVATED CARBON

ADSORPCJA MIESZANINY DWÓCH BARWNIKÓW NA WĘGLU AKTYWNYM

Abstract: Activated carbon is known as adsorbent of various contaminants from wastewater and air. The aim of the work was to estimate sorptive capacity of activated carbon in the removal of dyes, which are contaminants from textile wastewaters. The mixture of two dyes, methyl blue and naphthol green B was selected for investigations and WDeX activated carbon, virgin and regenerated, was chosen as adsorbent. The dye concentration, in both cases, was 200 mg/dm³. Sorptive capacities of activated carbon were expressed as values of surface sorption, which in case of fresh activated carbon was 60 mg/g, and after regeneration – ranged from 8 mg/g to 13 mg/g. The experimental data adsorption isotherms were defined and adsorption theoretical model, such as that of Freundlich or Langmuir, was selected. The highest removal efficiency in case of methyl blue was 94% for virgin carbon, the lowest – 75% (carbon after the fourth regeneration). The highest removal efficiency in case of naphthol green B was 78% for carbon after the fourth regeneration, the lowest – 55% (carbon after the first regeneration). The experimental data show that activated carbon can be used for the decontamination of dyes from textile wastewater. Model tests, however, need to be verified on real wastewater samples.

Keywords: Dye adsorption, activated carbon, Fenton reagent, methyl blue, naphthol green B

Introduction

Water covers 71% of the Earth's surface and constitutes 65% of human body mass. Contaminated water becomes a health hazard and a threat to the whole water ecosystem. River, lake and sea pollution originate in man's activities [1]. Those result, among others, in the generation of wastewater from textile, paper-making and leather industries. It contains a lot of organic compounds, including dyes. The latter constitute a major problem in dyeing wastewater treatment because of their complex structure.

¹ Department of Environmental Engineering and Protection, Faculty of Environmental Engineering, Geomatics and Power Engineering, Kielce University of Technology, al. Tysiąclecia Państwa Polskiego 7, 25–314 Kielce, Poland, phone: +48 41 34 24 535.

* Corresponding author: ebezak@tu.kielce.pl

Additionally, physical and chemical properties of dyes make them sparingly biodegradable, toxic, carcinogenic and mutagenic compounds [2–4]. Dye is observable even at very low concentration, which is detrimental to the aesthetic value of waters [5].

Three types of methods: chemical, biological and physical, are used to remove dyes from wastewater. The methods include, among others, coagulation and /or flocculation, membrane technologies (dialysis, reverse osmosis), modern oxidation methods (Fenton reaction, hydrogen peroxide method, UV radiation), biochemical oxidation and adsorption (activated carbons, inorganic adsorbents) [6–9].

According to the literature on the subject, activated carbons are employed as adsorbents of gaseous and liquid contaminants of air and wastewater, also to purify water and as catalysts [10, 11]. The choice of activated carbon as a sorbent depends on its sorptive capacity which changes, depending mainly on the properties of pores, *ie* their surface area and size [12]. Spent activated carbons are regenerated by means of thermal and chemical processes. Oxidation is one of chemical regeneration methods. Presently, modern oxidation methods, termed Advanced Oxidation Processes (AOP), are used. One of them is Fenton reagent which oxidises organic pollutants with hydroxyl radical $\text{OH}\cdot$, generated in the reaction medium, the oxidation potential of which amounts to 2.70 V. Activated carbons are catalysts of the formation of hydroxyl radicals. At the same time, carbons oxidize the pollutants adsorbed on carbon surface. Other oxidizing media include, among others, ozone, UV radiation, ultrasound, TiO_2 and hydrogen peroxide [13, 14].

Relying on the possibility of using activated carbons as sorbents of choice, reported in the literature on the subject, the authors undertook model investigations into selected dyes sorption on WDex activated carbon. The previous works [15, 16] of the authors concerned the possibility of sorption of naphthol green B and methyl blue, the present work deals with the sorption of the mixture of the dyes mentioned above.

The aim of the investigations, like in the earlier works, was to check the sorptive properties of activated, virgin and regenerated, WDex carbon, on which the mixture of two dyes, namely of methyl blue (C.I. 42780) and naphthol green B (C.I. 10020) was adsorbed. The spent WDex activated carbon was chemically regenerated with Fenton reagent, which is an excellent oxidizer.

Material and methods of investigations

Activated carbon characteristics

In the experiments, virgin WDex activated carbon, manufactured by Gryfskand company, was used. Activated carbon is employed, among others, in water purification. According to the literature [9], its sorptive capacity, *ie* specific surface area ($1050 \text{ m}^2/\text{g}$), pore volume ($1.20 \text{ cm}^3/\text{g}$) and iodine number (943 mg/g) indicate that this activated carbon can be an excellent sorbent.

Dye characteristics

In the experiment, two dyes were used, namely methyl blue and naphthol green B, of which a mixture was made.

The first dye, methyl blue, alternatively called cotton blue, is one of triamino triphenylmethane dyes, of the following molecular formula: $C_{37}H_{27}N_3Na_2O_9S_3$. This compound is easily soluble in water but weakly soluble in ethanol. Depending on pH, the dye can be either acidic or basic (Fig. 1). The molar mass of the compound is 799.8 g/mol [17].

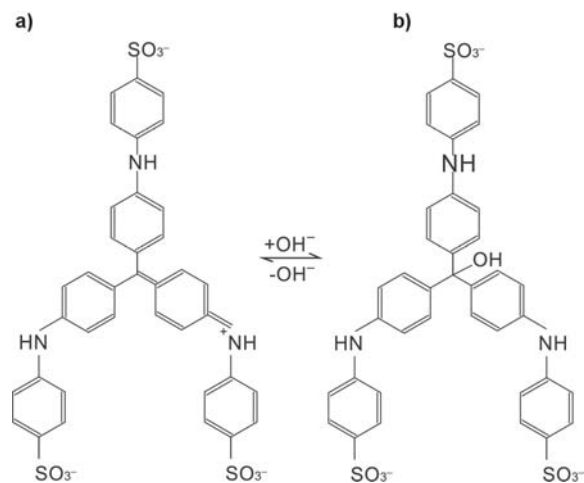


Fig. 1. Acidic a) and basic b) forms of methyl blue

Naphthol green B was the other dye (Fig. 2), the molecular formula of which is $C_{30}H_{15}FeN_3Na_3O_{15}S_3$. Its molar mass is 878.79 g/mol. This dye is very well soluble in water [18].

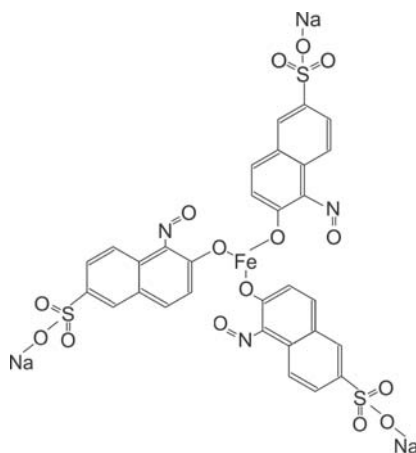


Fig. 2. Naphthol green B

Course of the experiment

Adsorption on virgin activated carbon

Virgin W Dex activated carbon was placed in conical flasks (0.2 g, 0.5 g, 1 g, 1.5 g, 2 g, respectively). Then 100 cm³ volumes of the solution of the mixture of the dyes, *ie* of methyl blue and naphthol green B, having the concentration of 200 mg/dm³ each, were added to the flasks. The contents were shaken for six hours. After that time, the phases, *ie* the dye solution and the spent sorbent, were separated. W Dex activated carbon was then washed with distilled water and dried in a dryer.

Adsorption on regenerated activated carbon

Following the adsorption process, W Dex activated carbon was regenerated using Fenton reagent. The latter was prepared in the following way: distilled water was poured into 1 dm³ beaker, then concentrated sulphuric acid(VI) was added, in such a way so that pH ranged around 3. To so prepared solution, 10 cm³ of FeSO₄ · 7 H₂O (the amount of ferrum ions 9.27 mg) and 1.5 cm³ of hydrogen peroxide were added. W Dex activated carbon was treated with Fenton reagent solution (500 cm³) prepared in a way described above, then it was stirred for 15 min. Activated carbon was then washed with distilled water, afterwards the regeneration process was repeated. Thus regenerated activated carbon was used again to adsorb dyes mixture on it.

Determination of dye concentration

Spectrophotometric method was used to determine the concentration of dyes. Marcel Media UV/VIS Spectrophotometer was employed. First, spectra of naphthol green B and methyl blue were recorded. Naphthol green B has the $\lambda = 715$ nm wavelength maximum, whereas for methyl blue, the maximum is the $\lambda = 591$ nm wavelength. Following the sorption process, samples of dyes were taken from a conical flask using a pipette and placed into a plastic cell. Then they were put into the spectrophotometer. The concentration of the dye, measured for pre-set wavelength, *ie* $\lambda = 715$ nm and $\lambda = 591$ nm for naphthol green B and methyl blue, respectively, was read on the computer monitor.

Results and discussion

At the first stage of investigations adsorption, A , was computed following formula [19]:

$$A = \frac{(c_0 - c_i) \cdot V}{m_c}$$

where: c_0 and c_i – dye initial and equilibrium concentration, respectively;
 V – solution volume;
 m_c – mass of dry activated carbon.

On the basis of calculated values of surface sorption, it was possible to plot sorption isotherms (Fig. 3–5). The highest surface sorption on virgin carbon for methyl blue and naphthol green B was 60 mg/g and 26 mg/g, respectively. As regards regenerated carbon, it ranged from 8 mg/g to 14 mg/g for methyl blue, and from 16 mg/g to 19 mg/g for naphthol green B.

Sorption isotherm presented in Figs. 3, 4, and 5 indicate that surface sorption for activated carbon decreased with subsequent regeneration cycles. After the first regeneration with Fenton reagent, surface sorption for methyl blue amounted to 12 mg/g, after the second regeneration cycle – to 9 mg/g. On the other hand, for naphthol

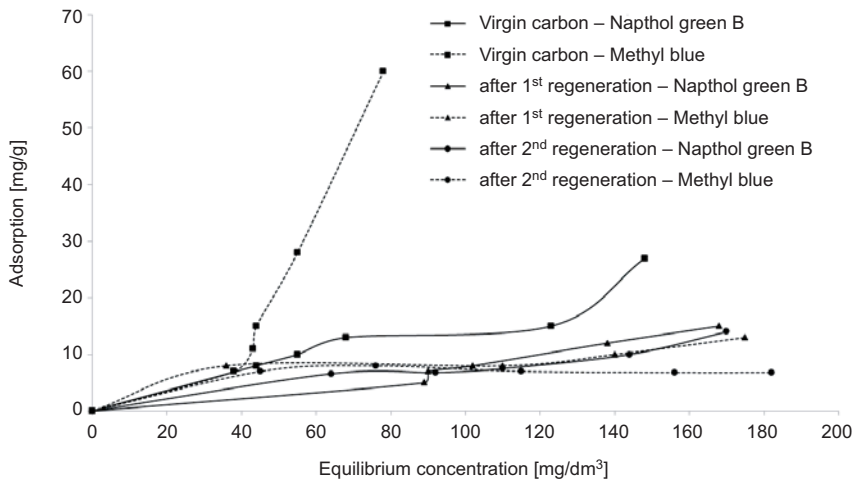


Fig. 3. Sorption isotherms for methyl blue and naphthol green B on virgin carbon and after the first and second regeneration

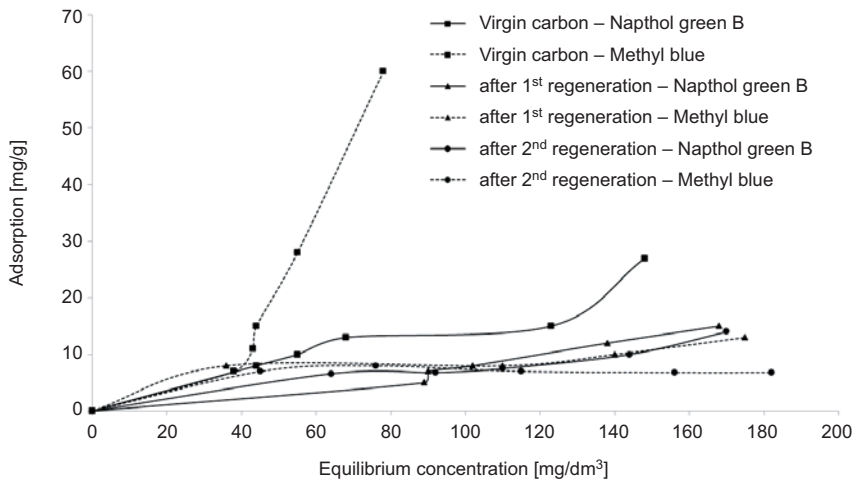


Fig. 4. Sorption isotherms for methyl blue and naphthol green B on virgin carbon and after the third and fourth regeneration

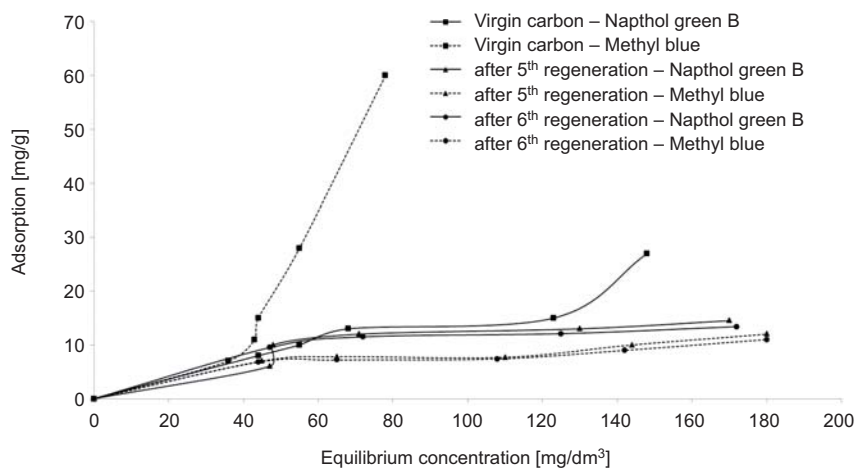


Fig. 5. Sorption isotherms for methyl blue and naphthol green B on virgin carbon and after the fifth and sixth regeneration

green B, after the first regeneration, surface sorption was 17 mg/g, after the second regeneration – it was 16 mg/g.

After the third and fourth regeneration cycle, surface sorption (Fig. 4.) for methyl blue was 12 mg/g and 11 mg/g, respectively, whereas for naphthol green B – 19 mg/g and 17 mg/g.

Sorption isotherms on virgin carbon and carbon after the fifth and sixth regeneration, presented in Fig. 5, showed that after the fifth and sixth regeneration, adsorption for methyl blue amounted to approx. 11 mg/g, and for naphthol green B – approx. 16 mg/g.

Experimental data indicate that WDeX activated carbon has good sorptive properties. Regeneration with Fenton reagent, however, slightly deteriorates sorptive properties of activated carbon. A change in activated carbon sorptive properties after regeneration definitely must be related to the Fenton reagent oxidizing action on carbon surface, where modification of surface functional groups occurs.

It was also noted that regeneration process was significantly limited due to a loss of carbon mass. In the course of experiment out of the original sorbent mass of 15.057 g, only 11.159 g were left, which makes a loss of 25.89% (Table 1).

Table 1

Changes in carbon parameters during the experiment

Sorbent type	Mass [g]	Mass loss [%]
Virgin carbon	15.057	
Carbon after the first regeneration	13.562	9.93
Carbon after the second regeneration	12.295	18.34
Carbon after the third regeneration	12.034	20.07
Carbon after the fourth regeneration	11.667	22.51
Carbon after the fifth regeneration	11.498	23.64
Carbon after the sixth regeneration	11.159	25.89

At the next stage of investigations, an attempt was made to fit an adsorption model to experimentally obtained isotherms. Two models, *ie* Freundlich equation and Langmuir equation, were used to analyse adsorption isotherms.

The Langmuir equation [20], applied to determine adsorption results, is based on the assumption that the adsorption maximum corresponds to the sorbent surface being saturated with adsorbed molecules of constant energy, and additionally, no migration of adsorbed substance on the sorbent plane takes place. The Langmuir equation can be presented in the following form:

$$\frac{c}{A} = \frac{1}{a_m \cdot k} + \frac{1}{a_m} \cdot c$$

where: c – dye concentration in the solution,
 A – adsorption,
 k – a constant related to adsorption heat,
 a_m – adsorbed surface.

The Freundlich isotherm [21] is the earliest developed relation that expressed sorption equation. The Freundlich model follows the formula:

$$A = K \cdot c^{1/n}$$

where: K – the Freundlich constant,
 $1/n$ – the Freundlich exponent, or in the logarithmic form:

$$\log A = \log K + \frac{1}{n} \log c$$

An exemplary Langmuir isotherm for activated carbon after the fourth regeneration for methyl blue is presented in Fig. 6.

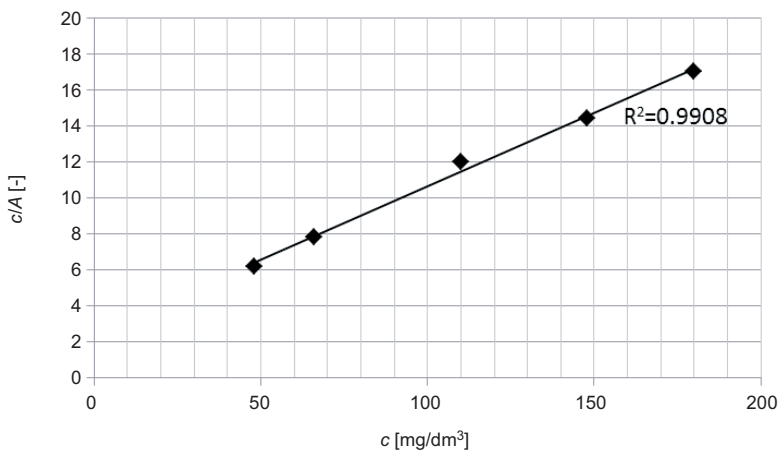


Fig. 6. Langmuir isotherm for WDex activated carbon after the fourth regeneration – methyl blue

An exemplary Freundlich isotherm for activated carbon after the fourth regeneration for naphthol green B is shown in Fig. 7.

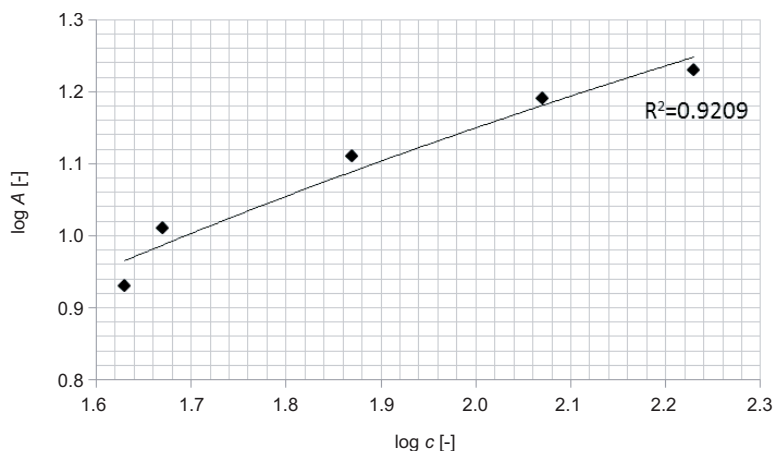


Fig. 7. Freundlich isotherm for WDex activated carbon after the fourth regeneration – naphthol green B

It should be noted that the higher is the value of the correlation coefficient (R^2), the better is the fit of the theoretical model to the experimental isotherm.

On the basis of calculated correlation coefficients (Table 2, Table 3), it can be stated that for methyl blue adsorption on virgin carbon, the Freundlich model better describes experimental data. In turn, correlation coefficients of the Langmuir model indicate its better fit to the experimental data after successive regeneration cycles (from the first to the sixth one).

Table 2

Parameters of Freundlich and Langmuir isotherms for methyl blue

Activated carbon	Freundlich isotherm			Langmuir isotherm		
	k	n	R^2	a_m	k	R^2
Virgin	0.0002	0.346	0.918	-12.5	-0.011	0.618
After the first regeneration	2.84	1.93	0.804	16.95	0.015	0.878
After the second regeneration	5.87	13.16	0.949	9.09	0.132	0.999
After the third regeneration	3.04	3.96	0.878	13.69	0.029	0.961
After the fourth regeneration	3.09	4.24	0.915	12.19	0.033	0.991
After the fifth regeneration	3.23	4.24	0.870	12.82	0.032	0.974
After the sixth regeneration	3.05	3.96	0.870	13.51	0.028	0.965

For naphthol green B, correlation coefficients show that the Langmuir model better describes the results after the fourth, fifth and sixth regeneration cycles. On the contrary, the Freundlich model is better fitted to the results of surface sorption on virgin carbon and on carbon after the first, second and third regeneration cycles.

It can be stated that both theoretical models are definitely capable of describing the experimental data obtained in the course of investigations.

Table 3

Parameters of Freundlich and Langmuir isotherms for naphthol green B

Activated carbon	Freundlich isotherm			Langmuir isotherm		
	k	n	R^2	a_m	k	R^2
Virgin	0.28	1.13	0.911	125.00	0.001	0.137
After the first regeneration	0.007	0.66	0.910	-20.40	-0.003	0.459
After the second regeneration	0.20	1.22	0.891	76.92	0.001	0.148
After the third regeneration	0.48	1.44	0.926	43.48	0.004	0.559
After the fourth regeneration	1.21	3.36	0.921	26.31	0.011	0.961
After the fifth regeneration	1.66	2.25	0.870	24.27	0.016	0.945
After the sixth regeneration	1.59	2.18	0.841	22.22	0.015	0.950

Dye adsorption on W Dex activated carbon is also presented with a graph of the dependence of selected dye removal percentage on subsequent regeneration cycles g (Fig. 8.). The highest percentage of removal was 94% (virgin carbon) and 78% (carbon after the fourth regeneration), for methyl blue and naphthol green B, respectively. On the other hand, the lowest removal percentage was obtained for methyl blue in the fourth regeneration cycle (75%), and for naphthol green B in the carbon first regeneration cycle (55%).

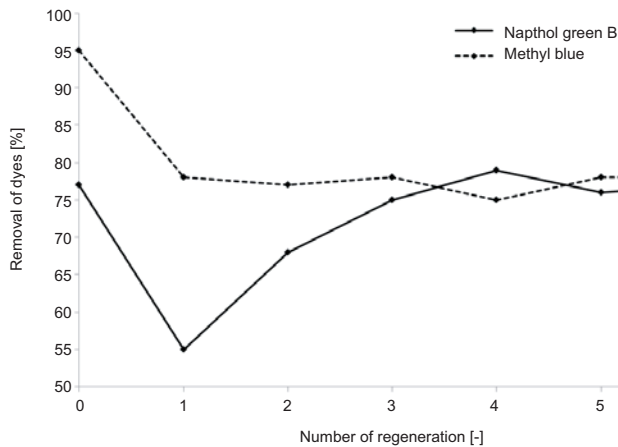


Fig. 8. Percentage of both dyes removal for virgin and regenerated activated carbon for $m_c = 2$ g

Conclusions

Summing up model investigations into selected dyes described above, that is naphthol green B and methyl blue, it can be stated that:

- W Dex activated carbon demonstrates high sorptive capacity, which is implied by surface sorption values for virgin carbon: 60 mg/g (methyl blue) and 26 mg/g (naphthol green B),
- the maximum removal percentage for methyl blue amounted to almost 94% (virgin carbon), for naphthol green B that was 78% (carbon after the fourth regeneration),
- Fenton reagent used for regeneration made it possible to maintain carbon sorptive capacity,
- Fenton reagent causes the oxidation of the adsorbed substance and the carbon matrix, and also changes in the properties of carbon,
- a disadvantageous phenomenon that accompanies sorption on regenerated carbon is a sorbent mass loss, which after six regeneration cycles amounts to almost 26%.

Acknowledgements

The work reported herein has been undertaken as part of project N N205 1993 33 funded by the Ministry of Science and Higher Education. The costs of the conference participation for the PhD student were covered from the budget of the Programme for the Development of Teaching Potential of the Kielce University of Technology – “Education to success”, Contract UDA-POKL.04.01.01-00-175/08-02, co-financed from the European Social Fund, Priority 4, Measure 4.1, Activity 4.1.1.

References

- [1] Sonune A, Ghate R. Developments in wastewater treatment methods. *Desalination*. 2004;167:55-63. DOI: 10.1016/j.desal.2004.06.113.
- [2] Pereira MFR, Soares SF, Órfão JJM, Figueiredo JL. Adsorption of dyes on activated carbons: influence of surface chemical groups. *Carbon*. 2003;41:811-821. DOI: 10.1016/S0008-6223(02)00406-2.
- [3] Zhu M, Lee L, Wang H, Wang Z. Removal of an anionic dye by adsorption/precipitation processes using alkaline white mud. *J Hazard Mater*. 2007;149:735-741. DOI: 10.1016/j.jhazmat.2007.04.037.
- [4] Namasivayam C, Kavitha D. Removal of Congo Red from water by adsorption onto activated carbon prepared from coir pith, an agricultural solid waste. *Dyes Pigm*. 2002;54:47-58. DOI: 10.1016/S0143-7208(02)00025-6.
- [5] Kima T, Park Ch, Yang J, Kima S. Comparison of disperse and reactive dye removals by chemical coagulation and Fenton oxidation. *J Hazard Mater*. 2004;B112:95-103. DOI: 10.1016/j.jhazmat.2004.04.008.
- [6] Demirbas A. Agricultural based activated carbons for the removal of dyes from aqueous solutions: A review. *J Hazard Mater*. 2009;167:1-9. DOI: 10.1016/j.jhazmat.2008.12.114.
- [7] Shen D, Fan J, Zhou W, Gao B, Yue Q, Kang Q. Adsorption kinetics and isotherm of anionic dyes onto organo-bentonite from single and multisolite systems. *J Hazard Mater*. 2009;172:99-107. DOI: 10.1016/j.jhazmat.2009.06.139.
- [8] Pengthamkeerati P, Satapanajaru T, Singchan O. Sorption of reactive dye from aqueous solution on biomass fly ash. *J Hazard Mater*. 2008;153:1149-1156. <http://www.sciencedirect.com/science/article/pii/S0304389407013659>.
- [9] Attia AA, Rashwan WE, Khedr SA. Capacity of activated carbon in the removal of acid dyes subsequent to its thermal treatment. *Dyes Pigm*. 2006;69:128-136. DOI:10.1016/j.dyepig.2004.07.009.
- [10] Wang X, Zhu N, Yin B. Preparation of sludge-based activated carbon and its application in dye wastewater treatment. *J Hazard Mater*. 2008;153:22-27.
- [11] Wang S, Zhu ZH. Effects of acidic treatment of activated carbons on dye adsorption. *Dyes Pigm*. 2007;75:306-314. DOI: 10.1016/j.dyepig.2006.06.005
- [12] Tamai H, Yoshida T, Sasakib M, Yasudaa H. Dye adsorption on mesoporous activated carbon fiber obtained from pitch containing yttrium complex. *Carbon*. 1999;37:983-989. DOI: 10.1016/S0008-6223(98)80013-4.

- [13] Dąbek L, Ozimina E, Picheta-Oleś A. Dye removal efficiency of virgin activated carbon and activated carbon regenerated with Fenton's reagent. *Environ Protect Eng.* 2012;38:5-13. DOI: 10.5277/epe.
- [14] Dąbek L, Ozimina E. Usuwanie zanieczyszczeń organicznych z roztworów wodnych metodą pogłębio-nego utleniania. (Removal of organic pollution from methylene blue on activated carbon through advanced oxidation processes) *Ochr Środ Zasob Natural.* 2009;41:369-376.
- [15] Bezak-Mazur E, Adamczyk D. Adsorption Naphtol Green B on Activated Carbon F 300 (Investigation of adsorption methylene blue on activated carbon). *Ecol Chem Eng A.* 2012,19(9):1123-1131. DOI:10.2428/ecea.2012.19(09)108.
- [16] Bezak-Mazur E, Adamczyk D. Badanie adsorpcji błękitu metylowego na węglu aktywnym [The investigation of adsorption methylene blue on activated carbon]. *Zesz Nauk Polit Rzesz.* 2011;58(4):17-26.
- [17] <http://stainsfile.info/StainsFile/dyes/42780.htm>.
- [18] <http://stainsfile.info/StainsFile/dyes/10020.htm>.
- [19] Kumar KV, Kumaran A. Removal of methylene blue by mango seed kernel powder. *Biochem Eng J.* 2005;27:83-93. DOI: 10.1016/j.bej.2005.08.004.
- [20] Malik PK. Dye removal from wastewater using activated carbon developed from sawdust: adsorption equilibrium and kinetics. *J Hazard Mater.* 2004;B113:81-88. DOI: 10.1016/j.jhazmat.2004.05.022.
- [21] Al-Degs YS, El-Barghouthi MI, El-Sheikh AH, Walker GM. Effect of solution pH, ionic strength, and temperature on adsorption behaviour of reactive dyes on activated carbon. *Dyes Pigm.* 2008;77:16-23. DOI: 10.1016/j.dyepig.2007.03.001.

ADSORPCJA MIESZANINY DWÓCH BARWNIKÓW NA WĘGLU AKTYWNYM

Katedra Inżynierii i Ochrony Środowiska, Wydział Inżynierii Środowiska, Geomatyki i Energetyki
Politechnika Świętokrzyska w Kielcach

Abstrakt: Węgiel aktywny jest znany jako adsorbent różnych zanieczyszczeń znajdujących się w ściekach i powietrzu. W pracy podjęto próbę oceny zdolności sorpcyjnych węgla aktywnego w odniesieniu do barwników będących zanieczyszczeniami ścieków farbiarskich. Do badań wybrano mieszaninę dwóch barwników, błękitu metylowego i zieleni naftolowej B, a jako sorbent węgiel aktywny W Dex świeży i regenerowany. Stężenie obu barwników wynosiło 200 mg/g. Zdolności sorpcyjne węgla świeżego wyrażone wielkością adsorpcji właściwej wyniosły 60 mg/g, a po regeneracji – od 8 mg/g do 13 mg/g. Z danych eksperymentalnych wykreślono izotermy sorpcji oraz dopasowano teoretyczny model adsorpcji tj. model Freundlicha lub Langmuira. Najwyższy procent usunięcia dla błękitu metylowego wyniósł 94% dla węgla świeżego, a najniższy – 75% (węgiel po IV regeneracji). Najwyższy procent usunięcia dla zieleni naftolowej B wyniósł 78% dla węgla po IV regeneracji, a najniższy – 55% (węgiel po I regeneracji). Uzyskane wyniki wskazują, iż zastosowany sorbent zarówno w postaci świeżej, jak i zregenerowanej może być stosowany w procesach usuwania barwników ze ścieków farbiarskich. Jednak badania modelowe muszą zostać sprawdzone na realnych próbkach ścieków.

Słowa kluczowe: Adsorpcja barwników, węgiel aktywny, odczynnik Fentona, błękit metylowy, zieleń naftolowa B

Krzysztof FRĄCZEK¹, Dariusz ROPEK¹
and Anna LENART-BORON^{1*}

THE EFFECT OF HEAVY METALS ON THE GROWTH OF WATERBORNE *Escherichia coli* OF MUNICIPAL LANDFILL ORIGIN

WPLYW METALI CIĘŻKICH NA WZROST *Escherichia coli* IZOLOWANYCH Z WÓD POCHODZĄCYCH ZE SKŁADOWISKA ODPADÓW KOMUNALNYCH

Abstract: The aim of this study was to assess the sensitivity of *Escherichia coli* isolates originating from a municipal waste landfill to the selected heavy metals. The analyses were conducted using environmental strains, isolated from surface water – a stream flowing along the landfill and from leachate and the observations were compared to the reaction of a reference strain EC ATCC 25922. The growth rate of bacterial cultures was evaluated in the liquid medium supplemented with 0.02; 0.1 and 0.5 mg · dm⁻³ of heavy metal salts: chromium, zinc, cadmium, copper, lead and mercury. The bacterial growth was examined turbidimetrically every 24 hours for 5 days. The performed study showed differences between the examined isolates in their response to the addition of the heavy metals in the liquid medium. Additionally, varied intensity of the heavy metals' effect on bacterial growth was observed, with the weakest growth inhibition being recorded in the case of lead, while chromium and mercury causing the greatest growth inhibition of bacterial strains.

Keywords: municipal waste landfill, *Escherichia coli*, heavy metals, municipal waste

There are many environmental consequences of growing population as well as developing industry, among which there is increasing production of waste, which is accumulated in both industrial and municipal landfills. In 2014 more than 10 thousand Mg of municipal waste was produced with 268 kg of waste produced by an average Polish citizen [1]. However, what is significant, is that an increasing amount of waste is being recycled in various ways, resulting on the other hand in decreasing amount and

¹ Department of Microbiology, University of Agriculture in Kraków, al. A. Mickiewicza 24/28, 30–059 Kraków, Poland, phone: +48 12 662 44 02, email: rrfracuse@cyf-kr.edu.pl

² Department of Agricultural Environment Protection, University of Agriculture in Kraków, al. A. Mickiewicza 21, 31–120 Kraków, Poland, phone: +48 12 662 44 02, email: rropek@cyf-kr.edu.pl

* Corresponding author: annalenart82@gmail.com

share of waste being deposited in landfills. In 2014, 5.4 thousand Mg of collected waste (ie 52.6%) was landfilled, while in 2013 this amount reached almost 6 thousand Mg and constituted 63.1% of the total amount of waste collected [1]. Depending on the amount and composition of waste deposited, there are various components that may be leached out and enter groundwater, including polycyclic aromatic compounds (PAHs) and heavy metals [2].

Heavy metals are among major toxicants of the environment, which are also one of the most persistent pollutants of water. They are both difficult to degrade and they can accumulate in the food chain [3]. Even though some heavy metals, such as copper, iron, manganese, or zinc are essential elements that serve as micronutrients, may function as components of enzymes, catalysts of certain biochemical reactions and stabilize protein structures in bacterial cell walls [4], still the requirements of living organisms for those essential heavy metals are usually very low [5]. On the other hand, many other heavy metals, including cadmium, lead or mercury, have no biological role [4] and may become potentially toxic to living organisms – microorganisms in particular [5]. The toxicity of such metals is manifested among others by the displacement of essential heavy metals from their native binding sites [4]. The excess of both groups of heavy metals may result in damaging cell membranes, altering enzyme specificity, etc. [5]. Common heavy metals that have been identified in polluted water include arsenic, copper, cadmium, lead, chromium, nickel, mercury and zinc [3]. The presence of heavy metals in landfills and landfill leachate is due to different kinds of waste being deposited, such as electronic waste, painting or used batteries [6]. Environmental contamination with heavy metals can cause various alterations to the microbial community of a given environment, including the reduction of microbial biomass or biodiversity [7]. Toxic effects of these contaminants may lead to changes in the microbial community structure and increase the level of physiological adaptation or tolerance, resulting in the selection of heavy metal-resistant species or strains [8, 9].

Microbial survival in contaminated environments depends on their biochemical properties, various adaptation mechanisms, including morphological changes within their cells, which may be associated with chromosomal genes or located on plasmids [10]. Microorganisms developed a wide variety of mechanisms aiming at reducing the impact of these contaminants on their cells, including efflux transporters that excrete the excess metal outside their cells [11].

Another threat to the quality of surface water and groundwater in the neighborhood of landfills is the possibility of their contamination with different groups of microorganisms, including pathogenic and opportunistic bacteria, such as coliforms, *Escherichia coli*, *Staphylococcus* spp. or *Salmonella* spp. [12]. This is due to the fact that the municipal landfills collect various types of mixed waste, including disposable napkins, sanitary towels, hypodermic needles or syringes [13]. Also the presence of large amount of organic matter in landfills may promote an increase in the number of some enteric bacteria [14]. In general, contamination of surface water and groundwater, including increased levels of both chemical compounds and microbial indicators of pollution, is a serious problem throughout the world, as it affects drinking water resources [15]. Landfill leachate may be one of major sources of water contamination – even though

landfills have developed their preventive measures in the form of liners, waste had been deposited without proper protection for several years. The quality of landfill leachate is affected by four main factors, including the composition of waste deposited and its size distribution, the age of landfill, its mode of operation and the geometric parameters [16]. As a result of leachate contamination, municipal landfills may significantly deteriorate the quality of surface water and groundwater quality in their neighborhood [17].

With respect to the previously mentioned issues, a study was undertaken primarily in order to determine the heavy metal contamination and the prevalence of selected microbial indicators of sanitary quality in both leachate and surface water in the vicinity of a municipal landfill. The secondary aim of this study was to assess the effect of some heavy metals on the growth of waterborne strains of *E. coli* isolated from the mentioned landfill.

Material and methods

The object of the field stage of the study were samples of surface water and leachate collected within and in the vicinity of the municipal landfill site in Tarnow, launched in 1985. Surface water samples for microbiological analyses were collected from a small stream flowing along the landfill, while leachate samples were collected directly from the leachate collector located within the landfill. Immediately after collection, the samples were transported to the laboratory of the Department of Microbiology, University of Agriculture in Krakow. The bacteriological analyzes included enumeration of total number of mesophilic bacteria (TS agar, 37°C, 48 h), psychrophilic bacteria (TS agar, 20°C, 72 h), as well as coliforms and *Escherichia coli* (Endo agar, 37°C and 44°C, 48 h). Total number of mesophilic and psychrophilic bacteria was assessed using the serial dilutions method and the results were presented as the number of cfu per 1 cm³ of water, while the number of coliforms and *E. coli* was analyzed using the filtration method and the results were presented as cfu per 100 cm³. The results were presented as means from three replicates. The species identification of the *E. coli* isolates was confirmed based on Gram staining and biochemical API tests (BioMerieux, Marcy l'Etoile, France).

Additionally, concentrations of the following heavy metals were evaluated in the leachate and surface water samples: Pb, Cu, Cd, Zn were determined using Inductively Coupled Plasma Mass Spectrometry [18], Cr(VI) – spectrophotometrically [19] and Hg was determined using Atomic Absorption Spectroscopy [20].

Another stage of the study comprised the investigation of the effect of lead, cadmium, copper, zinc, chromium and mercury on three *E. coli* strains – one derived from the surface water sample (E1), the second one derived from leachate (E2) and a reference strain (EC ATCC 25922). Bacteria were cultured on a liquid medium (nutrient broth) in Erlenmeyer flasks protected with gauze tampons. The broth was prepared from dry bullion and distilled water. Aqueous solutions of metal salts were added to the nutrient broth. It was sterilized at 100°C in the Koch apparatus. The following concentrations of metal ions concentration were added to the medium: 0.02,

0.1 and 0.5 mg · dm⁻³. The cold nutrient broth was inoculated with bacteria and left at 24°C for 5 days (120 h). The growth of bacteria was controlled turbidimetrically after each 24 hrs using Shimadzu UV-1201V spectrometer with 520 nm wavelength, referring to McFarland standards. Samples of bullion inoculated with bacteria but without addition of metal salts served as control. The experiment was repeated three times.

Data were analyzed using Statistica v. 10 (StatSoft, USA). Basic descriptive statistics were calculated as well as Pearson correlation coefficient between the prevalence of waterborne bacteria and the concentrations of heavy metals in water samples. One-way ANOVA analysis was employed to verify the significance of differences between the reaction of the tested *E. coli* strains to different heavy metal salts and their concentrations.

Results and discussion

Collection of waste in landfills has been considered as being opposite to sustainability in various aspects, as it is both waste of resources and constitutes health and environmental hazards [21]. For instance, water that enters landfills forms leachate that can carry pollutants to their surroundings, which may result in pollution of groundwater, thus affecting the quality of water used as drinking resources, and can deteriorate surface water quality [22, 23]. However, the concentration of heavy metals in landfill leachate and surface water collected in the direct vicinity of the considered landfill was very low. As compared to the Regulation of the Minister of Environment [24] for the classification of bodies of surface water and environmental quality standards for priority substances, there was no transgression of permissible values, therefore the tested samples were considered clean in terms of heavy metal concentration.

On the other hand, the examined surface water and leachate samples contained large amounts of bacteria, including potential pathogens such as coliforms and *Escherichia coli* (Table 1).

Table 1

The concentration of heavy metals and bacterial abundances
in the examined surface water and leachate samples

Parameter	Leachate	Surface water
Pb [mg · dm ⁻³]	0.1	< 0.004
Cd [mg · dm ⁻³]	0.018	< 0.0003
Cu [mg · dm ⁻³]	0.02	0.005
Zn [mg · dm ⁻³]	0.16	< 0.05
Cr VI [mg · dm ⁻³]	0.015	< 0.0004
Hg [mg · dm ⁻³]	< 0.00005	< 0.00005
Psychrophilic bacteria [cfu · cm ⁻³]	725400	86450
Mesophilic bacteria [cfu · cm ⁻³]	398000	70000
Coliforms [cfu · 100 cm ⁻³]	1340	240
<i>Escherichia coli</i> [cfu · cm ⁻³]	490	20

The presence of the latter two groups, *ie* coliforms and *E. coli*, is a commonly used indicator of water contamination with *eg* feces [25]. Comparing the number of coliforms in the tested surface water with the limit values given by the Regulation of the Minister of Environment [26], which divides surface waters into 5 classes of purity, among others depending on the concentration of coliforms, shows that the tested water sample should be qualified as 2nd class of purity, indicating good quality of water, with low anthropogenic impact. What is obvious, much larger numbers of microbial indicators of contamination were observed in leachate from the landfill.

The selected isolates of *E. coli* were tested for their tolerance against different essential and non-essential heavy metals. Figures 1–6 show the changes in the density of liquid bacterial cultures with the addition of the heavy metals selected for the analysis (*ie* lead, chromium, zinc, copper, cadmium and mercury, respectively) at three concentrations – 0.02; 0.1 and 0.5 mg · dm⁻³. Changes in the density of *E. coli* culture in control liquid medium – without heavy metals – are shown in Fig. 7. It could be observed that the number of bacterial cells decreased in day 5 even in control cultures, but the minimum cell density, recorded for the reference *E. coli* strain (ATCC 25922) was almost 2550 · 10⁶ cfu · cm⁻³. These values were higher in a few cases, *ie* all concentrations of lead (Fig. 1a–c), the smallest concentration of zinc (Fig. 3a) and in the case f reaction of the leachate-derived isolate of *E. coli* to the smallest concentration of chromium (2780 · 10⁶ cfu · cm⁻³, Fig. 2a). As shown in Figures 1–6, the reaction of bacterial cultures to the tested six heavy metals was different, with chromium and mercury having most severe inhibiting effect while lead (all concentrations) and zinc (0.02 and 0.1 mg/dm³) appeared to be the least toxic to *E. coli* strains. These results are similar to the ones obtained by Mariscal et al [27] in their studies on the toxicity of several heavy metals to *E. coli* measured by fluorescent bioassay, or Spain [28], who observed much higher minimum inhibitory concentrations for lead and zinc (5 and 1 mM, respectively) than for chromium and mercury (0.2 and 0.01 mM, respectively). These observations can be caused by the fact that zinc is among the essential trace elements, for instance it plays a role in forming complexes such as zinc fingers in DNA and acts as a component in cellular enzymes [29]. Also Abskharon et al [5] in their studies on the resistance of *E. coli* strains isolated from wastewater sites to different heavy metals observed that chromium had the greatest inhibiting effect on *E. coli* strains that were tested in their research. It can also be noticed that the density of bacterial cultures gradually decreased with increasing concentration of heavy metals, which is not surprising and in agreement with observations of other researchers [5, 30–32]. Also the reaction of individual isolates to the addition of heavy metals to the liquid medium was statistically significant ($p < 0.05$, F values: leachate 12.54; surface water 14.54 and reference strain 17.37).

Microbial survival in polluted environments depends on their biochemical and structural properties, as well as their adaptability to severe environmental conditions, including morphological changes of cells and modifications of metal speciation [5, 10, 33]. Also the increased resistance of microorganisms to xenobiotics, including heavy metals results among others from exposure to the contaminated environment which causes selection for strains developing the resistance mechanisms [5, 28].

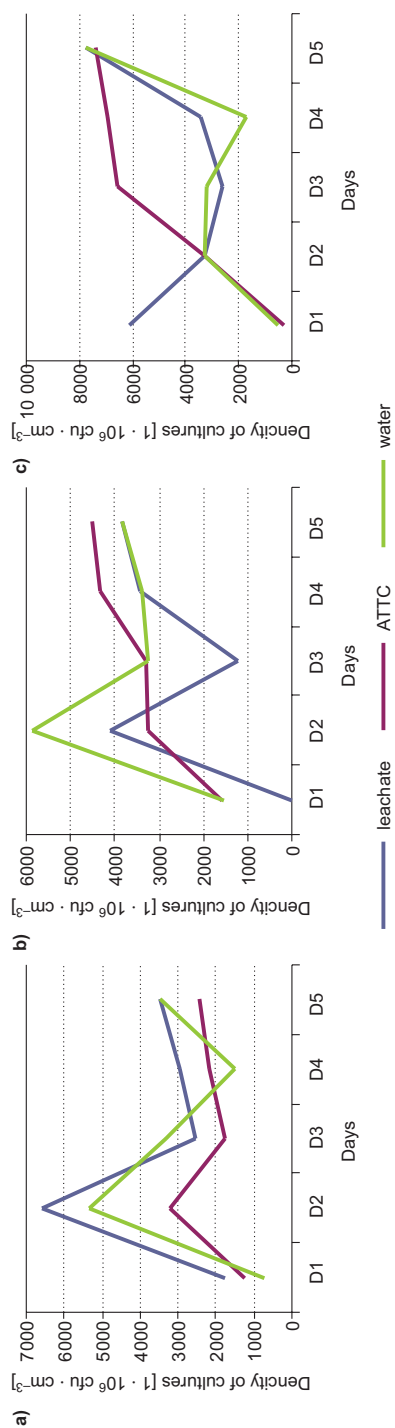


Fig. 1. Changes in the density of bacterial cultures in response to the addition of lead in the concentration of a) 0.02 mg \cdot dm $^{-3}$; b) 0.1 mg \cdot dm $^{-3}$ and c) 0.5 mg \cdot dm $^{-3}$

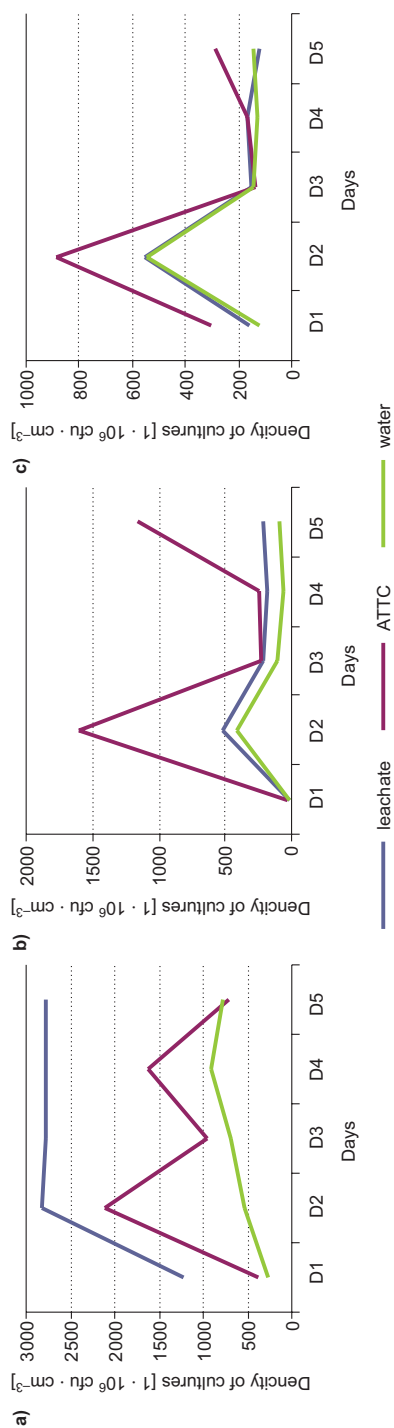


Fig. 2. Changes in the density of bacterial cultures in response to the addition of chromium in the concentration of a) 0.02 mg \cdot dm $^{-3}$; b) 0.1 mg \cdot dm $^{-3}$ and c) 0.5 mg \cdot dm $^{-3}$

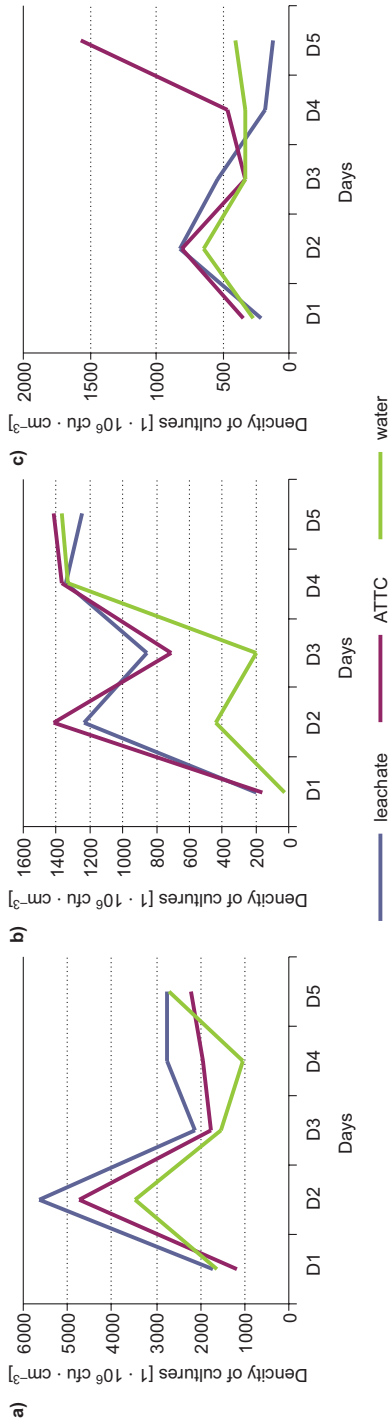


Fig. 3. Changes in the density of bacterial cultures in response to the addition of zinc in the concentration of a) 0.02 $\text{mg} \cdot \text{dm}^{-3}$; b) 0.1 $\text{mg} \cdot \text{dm}^{-3}$ and c) 0.5 $\text{mg} \cdot \text{dm}^{-3}$

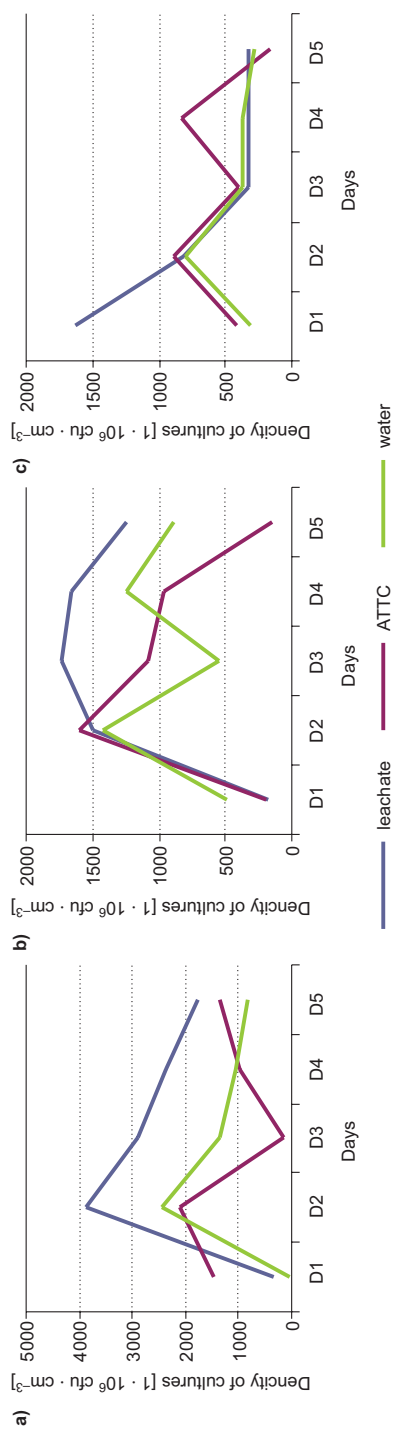


Fig. 4. Changes in the density of bacterial cultures in response to the addition of copper in the concentration of a) 0.02 $\text{mg} \cdot \text{dm}^{-3}$; b) 0.1 $\text{mg} \cdot \text{dm}^{-3}$ and c) 0.5 $\text{mg} \cdot \text{dm}^{-3}$

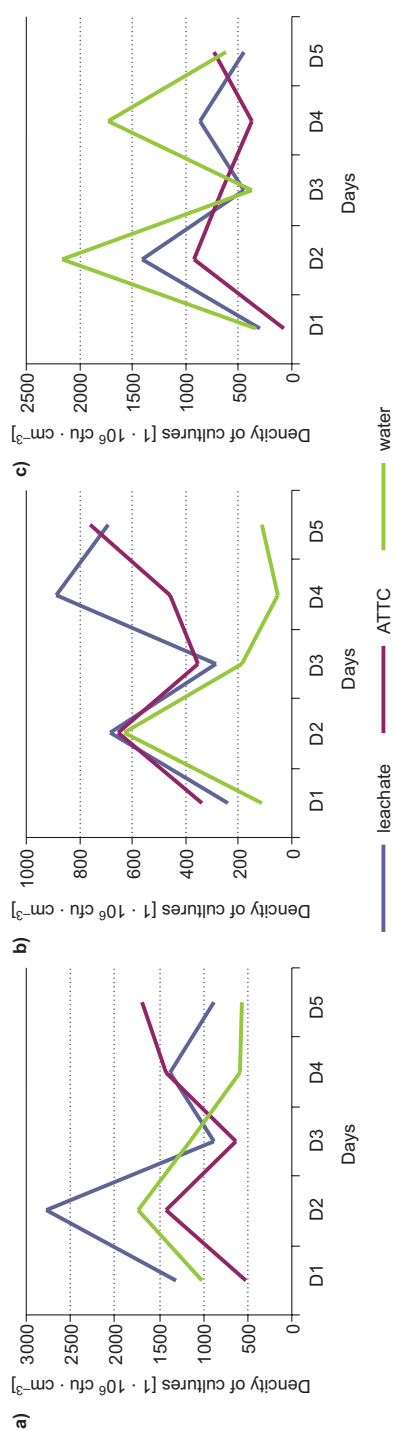


Fig. 5. Changes in the density of bacterial cultures in response to the addition of cadmium in the concentration of a) 0.02 mg \cdot dm $^{-3}$; b) 0.1 mg \cdot dm $^{-3}$ and c) 0.5 mg \cdot dm $^{-3}$

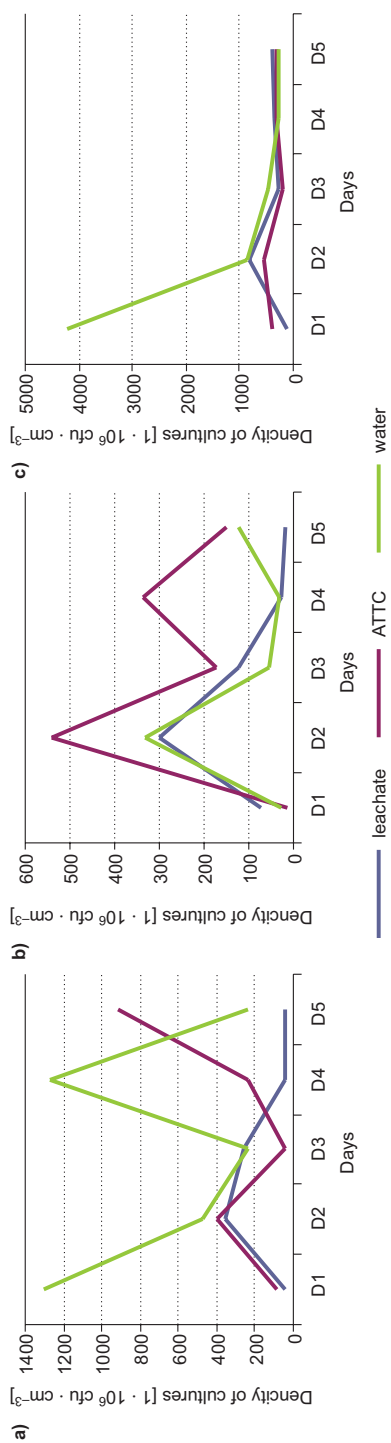


Fig. 6. Changes in the density of bacterial cultures in response to the addition of mercury in the concentration of a) 0.02 mg \cdot dm $^{-3}$; b) 0.1 mg \cdot dm $^{-3}$ and c) 0.5 mg \cdot dm $^{-3}$

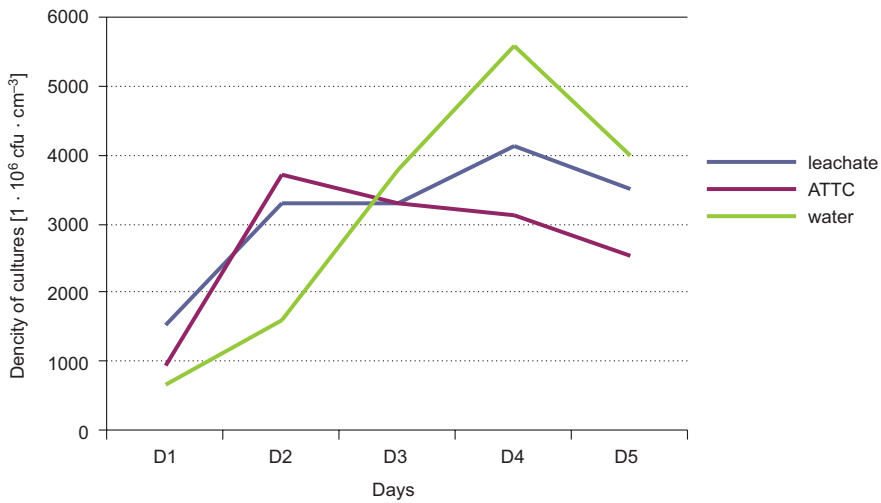


Fig. 7. Changes in the density of bacterial cultures in control cultures

Conclusions

Results of this study show that the values of heavy metal concentrations in both landfill leachate and surface water collected in its direct vicinity meet the environmental standards, so it can be concluded that the current operation mode of the landfill does not result in chemical contamination of the surrounding environment. On the other hand, very high concentrations of bacterial contaminants indicate that the considered landfill may not only pose significant biological threat to the neighboring water resources, but also may have negative health effect on the landfill workers or residents of nearby areas.

The performed tests on the reaction of waterborne *E. coli* isolates derived from the landfill leachate and the nearby surface water sample showed that the bacterial reaction to the effect of different heavy metals varied strongly. The isolate of *E. coli* derived from the landfill leachate did not show increased resistance to the presence of heavy metals in the liquid medium, except for the smallest concentration of chromium and copper. In general, it can be stated that as compared to the control culture, the tested heavy metals inhibited or decreased the growth rate of *E. coli* strains, and this effect increased with raising concentrations of metals in the medium. Addition of chromium and mercury caused the most severe growth inhibition of tested bacterial strains. Even though some of the tested metals act as important trace elements, most of them have toxic effects on microorganisms.

Acknowledgement

The study was supported by the Ministry of Science and Higher Education in Poland (Project no. N N305 227237).

References

- [1] Adamczyk I, Różańska B, Sobczyk M. Infrastruktura komunalna w 2014 r. (Community infrastructure in 2014) Główny Urząd Statystyczny. Warszawa; 2015. <http://stat.gov.pl/obszary-tematyczne/infrastruktura-komunalna-nieruchomosci/nieruchomosci-budynki-infrastruktura-komunalna/infrastruktura-komunalna-w-2014-r-,3,12.html>.
- [2] Domska D, Warechowska M. The effect of the municipal waste landfill on the heavy metals content in soil. *Contemp. Probl Manage Environ Protect.* 2009;4:95-105. http://www.uwm.edu.pl/environ/vol04/vol_04_chapter06.pdf.
- [3] Akpor OB, Muchie M. Remediation of heavy metals in drinking water and wastewater treatment systems: Processes and applications. *Int J Phys Sci.* 2010; 5(12):1807-1817. http://www.academic-journals.org/article/article1380814369_Akpor%20and%20Muchie.pdf.
- [4] Bruins MR, Kapil S, Oehme FW. Microbial resistance to metals in the environment. *Ecotoxicol Environ Saf.* 2000;45:198-207. DOI: 10.1006/eesa.1999.186.
- [5] Abskharon RNN, Hassan SHA, Gad El-Rab SMF, Shoreit AAM. Heavy metal resistant *E. coli* isolated from wastewater sites in Assiut City, Egypt. *Bull Environ Contam Toxicol.* 2008;81:309-315. DOI 10.1007/s00128-008-9494-6.
- [6] Adeolu AO, Ada OV, Gbenga AA, Adebayo OA. Assessment of groundwater contamination by leachate near a municipal solid waste landfill. *Afr J Environ Sci Technol.* 2011;5(11):933-940. DOI: 10.5897/AJEST11.272.
- [7] Wyszowska J, Kucharski J, Borowik A, Boros E. Response of bacteria to soil contamination with heavy metals. *J Elementol.* 2008;13:443-453. <http://www.uwm.edu.pl/jold/poj1332008/jurnal-15.pdf>.
- [8] Tobor-Kapłon MA, Bloem J, Romkens PFAM, d'Ruiter PC. Functional stability of microbial communities in contaminated soils. *Oikos.* 2005;111:119-129. DOI: 10.1111/j.0030-1299.2005.13512.x.
- [9] Lenart-Boroń A, Wolny-Kołodka K. Heavy metal concentration and the occurrence of selected microorganisms in soils of a steelworks area in Poland. *Plant Soil Environ.* 2015;61(6):273-278. DOI: 10.17221/217/2015-PSE.
- [10] Wuertz S, Mergeay M. The impact of heavy metals on soil microbial communities and their activities. In: van Elsland JD, Trevors JT, Wellington EMH (eds). *Modern soil microbiology*. New York: Marcel Dekker; 1997.
- [11] Nies DH. Efflux-mediated heavy metal resistance in prokaryotes. *FEMS Microbiol Rev.* 2003;27:313-339. DOI: [http://dx.doi.org/10.1016/S0168-6445\(03\)00048-2](http://dx.doi.org/10.1016/S0168-6445(03)00048-2).
- [12] Grisey E, Belle E, Dat J, Mudry J, Aleya L. Survival of pathogenic and indicator organisms in groundwater and landfill leachate through coupling bacterial enumeration with tracer tests. *Desalination.* 2010;261(1-2):162-168. DOI:10.1016/j.desal.2010.05.007.
- [13] Flores-Tena FJ, Guerrero-Barrera AL, Avelar-Gonzalez FJ, Ramierz-Lopez EM, Martinez-Saldaña MC. Pathogenic and opportunistic Gram-negative bacteria in soil, leachate and air in San Nicolas landfill at Aguascalientes, Mexico. *Rev Latinoam Micr.* 2007;49:25-30. http://www.medigraphic.com/pdfs/lamicro/mi-2007/mi07-1_2e.pdf
- [14] Palmisano AC, Barlaz MA. *Microbiology of solid waste*. Boca Raton: CRC Press; 1996.
- [15] Röling WFM, van Breukelen BM, Braster M, Lin B, van Verseveld HW. Relationships between Microbial Community Structure and Hydrochemistry in a Landfill Leachate-Polluted Aquifer. *Appl Environ Microbiol.* 2001; 67(10):4619-4629. DOI: 10.1128/AEM.67.10.4619-4629.2001.
- [16] Szpadt R. Usuwanie i oczyszczanie odcieków ze składowisk odpadów komunalnych. (Removal and treatment of leachate from municipal landfill sites) *Przegl Komunal.* 2006;12:60-66. <http://e-czytelnia.abrys.pl/przeglاد-komunalny/2006-12-256/dodatki-zeszyty-komunalne-2968/usuwanie-i-oczyszczanie-odciekow-ze-skladowisk-odpadow-komunalnych-6964>.
- [17] Frączek K, Ropek D. Municipal waste dumps as the microbiological threat to the natural environment. *Ecol Chem Eng S.* 2011;18:93-110. [http://tchie.uni.opole.pl/freeECE/S_18_1/FraczekRopek_18\(S1\).pdf](http://tchie.uni.opole.pl/freeECE/S_18_1/FraczekRopek_18(S1).pdf)
- [18] Voica C, Kovacs MH, Dehelean A, Ristoiu D, Iordache A. ICP-MS determinations of heavy metals in surface waters from Transylvania. *Rom J Phys.* 2012;75:1184-1193. http://www.nipne.ro/rjp/2012_57_7-8/1184_1193.pdf
- [19] Ferng WB, Parker GA. Spectrophotometric determination of Chromium as the chromium-peroxo-4-(2-pyridylazo)resorcinol complex. *Fresenius Z Anal Chem.* 1980;304:382-384. <http://download.springer.com/static/pdf/172/art%253A10.1007%252FBF00480608.pdf?originUrl=http%3A%2F%2Flink.springer.com>

- %2Farticle%2F10.1007%2FBF00480608&token2=exp=1456483196~acl=%2Fstatic%2Fpdf%2F172%2Fart%25253A10.1007%25252FBF00480608.pdf%3Dhttp%253A%252F%252Flink.springer.com%252Farticle%252F10.1007%252FBF00480608*~hmac=8a2f75e1c369dc78cfa7e83acbe8158c74a0d71d93c9ee56652702954abf5f6e.
- [20] ISO 12846 Water quality – Determination of mercury – Method using atomic absorption spectrometry (AAS) with and without enrichment. International Organization for Standardization, Geneva, Switzerland; 2012. http://www.iso.org/iso/iso_catalogue/catalogue_tc/catalogue_detail.htm?csnumber=51964.
- [21] Ettler V, Mihaljevic M, Matura M, Skalova M, Sebek O, Bezdicka P. Temporal variation of trace elements in waters polluted by municipal solid waste landfill leachate. *Bull Environ Contam Toxicol*. 2008;80:274-279. DOI: 10.1007/s00128-008-9361-5.
- [22] Pablos MV, Martini F, Fernandez C, Babin MM, Herraiz I, Miranda J, et al. Correlation between physicochemical and ecotoxicological approaches to estimate landfill leachates toxicity. *Waste Manage*. 2011;31:1841-1847. DOI: 10.1016/j.wasman.2011.03.022.
- [23] Vaverková M, Adamcová D. Evaluation of landfill pollution with special emphasis on heavy metals. *J Ecol Eng S*. 2014;15(4):1-6. DOI: 10.12911/22998993.1094972.
- [24] The Minister of Environment Regulation dated November 9th 2011, for the classification of bodies of surface water and environmental quality standards for priority substances (Journal of Laws of 2011, No. 257, item 1545). <http://isap.sejm.gov.pl/DetailsServlet?id=WDU20112571545>.
- [25] World Health Organization, Guidelines for drinking-water quality, 3rd, Recommendations, Vol. 1, WHO, Geneva, 2004. http://www.who.int/water_sanitation_health/dwq/GDWQ2004web.pdf.
- [26] The Minister of Environment Regulation dated February 11th 2004 for the classification of surface water and groundwater quality, methods of conducting of monitoring, the interpretation of the results and the presentation of these water quality. (Journal of Laws of 2004, No. 32, item 284). <http://isap.sejm.gov.pl/DetailsServlet?id=WDU20040320284>.
- [27] Mariscal A, Garcia A, Carnero M, Gómez J, Pinedo A, Fernández-Crehuet J. Evaluation of the toxicity of several heavy metals by a fluorescent bacterial bioassay. *J Appl Toxicol*. 1995;15(2):103-107. DOI: 10.1002/jat.2550150208.
- [28] Spain A. Implications of microbial heavy metal resistance in the environment. *Rev Undergraduate Res*. 2003;2:1-6. https://www.researchgate.net/publication/235641003_Implications_of_bacterial_resistance_against_heavy_metals_in_bioremediation_A_review.
- [29] Nies DH. Microbial heavy metal resistance. *Appl Microbiol Biotechnol*. 1999;51:730-750. <http://link.springer.com/article/10.1007/s002530051457>
- [30] Hassen A, Saidi N, Cherif M, Boudabous A. Resistance of environmental bacteria to heavy metals. *Bioresour Technol*. 1998;64:7-15. DOI:10.1016/S0960-8524(97)00161-2
- [31] Filali BK, Taoufik J, Zeroual Y, Dzairi FZ, Talbi M, Blaghen M. Wastewater bacterial isolates resistant to heavy metals and antibiotics. *Curr Microbiol*. 2000;41:151-156. DOI: 10.1007/s0028400.
- [32] Hussein H, Farag S, Kandil K, Moawad H. Tolerance and uptake of heavy metals by *Pseudomonads*. *Process Biochem*. 2005;40:955-961. DOI:10.1016/j.procbio.2004.04.001.
- [33] Ehrlich HL. Microbes and metals. *Appl Microbiol Biotechnol*. 1997;48:687-692. DOI:10.1007/s002530051116.

WPLYW METALI CIĘŻKICH NA WZROST *Escherichia coli* IZOLOWANYCH Z WÓD POCHODZĄCYCH ZE SKŁADOWISKA ODPADÓW KOMUNALNYCH

¹ Katedra Mikrobiologii

² Katedra Ochrony Środowiska Rolniczego
Uniwersytet Rolniczy im. Hugona Kołłątaja w Krakowie

Abstrakt: Celem pracy była ocena wrażliwości izolatów *Escherichia coli*, pochodzących ze składowiska odpadów komunalnych na działanie wybranych metali ciężkich. Badaniu poddano izolaty środowiskowe, pochodzące z wody powierzchniowej – strumienia płynącego wzdłuż składowiska oraz z odcieków, a także szczep wzorcowy EC ATCC 25922. Ocenie poddano tempo wzrostu kultur bakteryjnych w podłożu płynnym z dodatkiem 0,02; 0,1 oraz 0,5 mg · dm⁻³ soli metali ciężkich: chromu, cynku, kadmu, miedzi, ołowiu i rtęci.

Wzrost bakterii badano turbidymetrycznie w odstępach 24-godzinnych przez okres 5 dni. Na podstawie przeprowadzonych badań stwierdzono różnice pomiędzy badanymi izolatami w ich reakcji na obecność badanych metali ciężkich w podłożu. Zaobserwowano także różną intensywność działania metali, przy czym najsłabsze zahamowanie wzrostu bakterii stwierdzono w przypadku ołowiu, natomiast najsilniejszy efekt hamujący miały chrom i rtęć.

Słowa kluczowe: składowisko odpadów komunalnych, *Escherichia coli*, metale ciężkie, odpady komunalne

Gabriela KAMIŃSKA¹, Mariusz DUDZIAK^{1,*},
Jolanta BOHDZIEWICZ¹ and Edyta KUDLEK¹

EFFECTIVENESS OF REMOVAL OF SELECTED BIOLOGICALLY ACTIVE MICROPOLLUTANTS IN NANOFILTRATION

OCENA SKUTECZNOŚCI USUWANIA WYBRANYCH SUBSTANCJI AKTYWNYCH BIOLOGICZNIE W PROCESIE NANOFILTRACJI

Abstract: This study addressed the removal efficiency of five different compounds classified as biologically active compounds *ie* benzo(a)pyrene (BaP), anthracene (ANT), diclofenac (DCL), pentachlorophenol (PCP), octylphenol (OP) in nanofiltration. They were removed from deionized water solution (500 µg/dm³) and comparatively from synthetic and municipal effluent. It was found that the efficiency of the nanofiltration depends on significantly both on type of membrane and the environmental matrix and physic-chemical properties of the compounds contained in the treated feed. The highest retention was observed for benzo(a)pyrene removed from deionized water. In this case, the retention of BaP varied from 99.82% to 99.94%. For other compounds (excluding octylphenol) we observed an inverse trend, higher retention degrees were obtained when the synthetic or real effluent were filtered. This study documented a complex mechanism of separation of low molecular weight organic micropollutants in nanofiltration, which could be a result of intermolecular interactions, sieve effect and adsorption. In addition, in the last part we compare our experimental data with predicted retention coefficients, which were computed from models for predicting retention of micropollutants in nanofiltration.

Keywords: biologically active compounds, nanofiltration

Introduction

The group of biologically active substances include polycyclic aromatic hydrocarbons, pharmaceuticals, pesticides and the other substances used in industry *eg* bisphenol A and octylphenol. Their negative impact on living organisms has been repeatedly documented [1–5]. Among individuals exposed to toxic substances we can observe, aside the lethal effects, growth and development disruptions or hormonal irregularities [6–8].

¹ Institute of Water and Wastewater Engineering, Silesian University of Technology, ul. Konarskiego 18, 44–100 Gliwice, Poland, phone: +48 32 237 16 98, fax: +48 32 237 10 47.

* Corresponding author: mariusz.dudziak@polsl.pl

At the same time, many of these substances have been identified by European Parliament in Water Framework Directive as particularly dangerous and priority. Initially 33 compounds were designated as particularly dangerous, among which were octylphenol, pentachlorophenol, anthracene and many others [9]. Currently the list of priority substances or priority hazardous has been extended with 12 new compounds [10]. Moreover, to ensure good chemical state of surface waters, for some of these substances environmental quality standards were established, which should be achieved by the end of 2021, and for the 33 priority substances and by the end of 2027, for newly identified compounds [11].

In this light, it is advisable to conduct research to enhance cheap and effective methods of micropollutants removal from effluent waters. Process that guarantees effective separation of low molecular weight organic compounds is nanofiltration (NF) [12–15]. Thanks to using compact nanofiltration membranes with pore size in active layer usually not exceeding 2 nm, retained compounds have the molecular weight in the range of 150–500 Da [16]. In addition, nanofiltration membrane surface is additionally charged. Therefore, mechanism of separation and mass transport in NF is complex and results from occurring various effects and processes in filtration. Separation mechanism can therefore be based on both the molecular sieve effect, which is typical for ultrafiltration, as well as diffusion and dilution effects occurring mainly in reverse osmosis process or an electrostatic interaction and adsorption [15–16]. Physicochemical properties of membrane and separated pollutants decide which mechanism is dominant. They determine in direct way the type and strength of interactions between membrane surface and substances contained in feed [17].

Knowledge of micropollutants separation mechanisms in nanofiltration process has become a basis for developing retention models. They allow in very high accuracy predict the retention of particular feed ingredients. One of the simplest and earliest method of forecasting retention coefficients is diagram proposed in work [18]. Depending on the membrane properties and pollutants, authors presented a method of approximating retention coefficient of pollutants in high pressure membrane techniques. It shows that in the first place you should take into account the molecular weight of the compound and the molecular weight cut off (MWCO) of membrane, followed by the pKa of compound and pH of the feed. It should also be considered that the degree of removal of the compound is dependent on hydrophobic nature and the size ratio of diameter of retained particles into the membrane pore size. Newer micropollutants retention models are based on statistical analyses, allowing more accurately identify the most important factors affecting their retention. In work [19] derived equation that allows to calculate the retention of organic micropollutants in NF process according to value of the log D and geometry of the molecule, and the retention degree of the divalent ions. Similar results were shown by the research of the retention of estrogenic compounds. In this case, the variables in equation allowing to estimate the retention size were: molecular weight of the compound, the retention coefficient of NaCl and absorbance value of treated water [17].

The purpose of presented study was to determine the efficiency of nanofiltration process in removal of biologically active substances of various origin (PAHs, pesticides,

EDCs). It dealt with the influence of membrane nanofiltration type and the aqueous matrix on the efficiency of their removal. In the second part, obtained results were used for validation of the micropollutants retention models available in the literature.

Materials and methods

Chemicals

Chemical standards of benzo(a)pyrene (BaP), anthracene (ANT), (2), diclofenac (DCL), pentachlorophenol (PCP), octylphenol (OP) were supplied by Sigma Aldrich. Stock solution of individual standards (1 mg/cm³) were prepared in methanol for PCP, OP and DCL or acetone for BaP and ANT. The structural and physicochemical properties of selected micropollutants are shown in Table 1.

Table 1

Physicochemical properties of selected biologically active substances

Compound	Molecular weight ^a [g/mole]	Log K_{ow} ^b [-]	Length ^b [nm]	Width ^b [nm]	Depth ^b [nm]	Eqwidth ^b [nm]	Log D^d [-]
Pentachlorophenol (PCP)	266.34	4.40	0.59	0.55	0.15	0.28	2.45
4-tert-octylphenol (OP)	206.32	4.12	0.87	0.79	0.40	0.56	5.47
Diclofenac (DCL)	296.15	4.51	0.96	0.90	0.26	0.48	1.37
Benzo(a)pyrene (BaP)	252.31	6.35	1.10	0.78	0.06	0.23	6.35
Anthracene (ANT)	178.22	4.45	0.90	0.51	0.39	0.49	4.68

^a <https://pubchem.ncbi.nlm.nih.gov/compound/2336>; ^b calculated with ChemBio3D Ultra 12.0; ^c geometric mean of width and depth; ^d ACD/Labs Percepta Platform.

The concentration of selected biologically active compounds was determined using solid phase extraction (SPE) and HPLC analysis at a wavelength of λ : 220 nm (for PCP, DCL, OP), 254 nm for ANT and 250 nm for BaP. For SPE, glass columns filled with C18 phase (Supelco) were used.

Preparation of feeds

To investigate the retention of selected biologically active compounds from aquatic solutions, artificial solutions made of deionized water were prepared. Comparatively, synthetic and real effluents were used. Synthetic effluent was prepared by diluting in the tap water the following organic substances: (0.152 g/dm³ of broth; 0.226 g/dm³ of peptone) and inorganic substances (0.007 g/dm³ of NH₄Cl; 0.0075 g/dm³ of NaCl; 0.002 g/dm³ of CaCl · 6H₂O; 0.04 g/dm³ of MgSO₄ · 7H₂O; 0.016 g/dm³ of K₂HPO₄; 0.04 g/dm³ of KH₂PO₄) and then solution was vaccinated (1 cm³/dm³) with surface water containing natural bacteria. Finally, obtained solution was aerated for 5 days in order to guarantee a biodegradation of high molecular weight compounds. In all types of feed concentration of micropollutants was maintained at constant level of 500 µg/dm³ by adding sufficient volume of stock solutions.

Membranes and filtration run

Nanofiltration was carried out in a membrane cell equipped with a magnetic stirrer (volume 0.4 dm³, membrane filtration area 0.00385 m²), operating in a dead-end mode at the transmembrane pressure 2 MPa. Prior to the first application, the membranes were conditioned by means of filtration of deionized water. Setup used in nanofiltration is illustrated in Fig. 1.

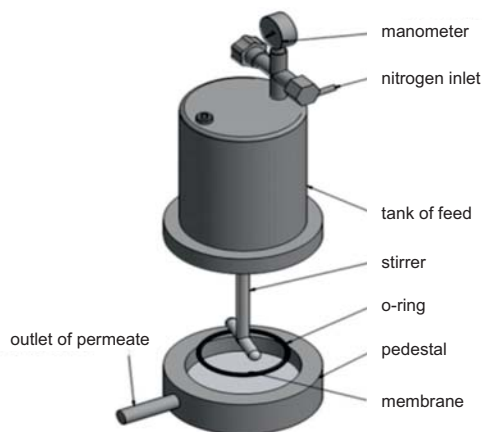


Fig. 1. Dead-end nanofiltration unit

Four types of commercial nanofiltration membranes were used in nanofiltration process. Their properties are shown in Table 2.

Table 2

Characteristics of nanofiltration membranes

Symbol	DK	HL	NF-90	NF-270
Manufacturer	GE	GE	Dow Filmtec	Dow Filmtec
Material ^a	Thin film			
MWCO ^b [Da]	150–300	150–300	150	200
Salt retention – NaCl ^b [%]	63	44	47	87
Salt retention – MgSO ₄ ^{2b} [%]	94	98	97	99
Contact angle ^c [°]	37	25	63	17
Volume deionized water flux ^d , $J_v \cdot 10^6$ [m ³ · m ⁻² · s ⁻¹]	16.47	42.42	47.03	33.28

^a Data provided by manufacturer; ^b own measurements: NaCl and MgSO₄ of 1 g/dm³ at $\Delta P = 2$ MPa; ^c own measurements by means of goniometer; ^d own measurements at $\Delta P = 2$ MPa.

Before nanofiltration, membranes were stored in deionized water for 24 h, then they were conditioned with deionized water. After that, initial deionized water flux (J_w) was measured. During nanofiltration, the volume of permeate was measured and then

permeate flux (J_v) and volume reduction factor (VRF) were computed according to equation 1 and 2 respectively. Fouling behavior was described by means of relative permeate flux from equation 3.

$$J_{v/(w)} = \frac{V_p}{S \cdot t} \quad (1)$$

$$VRF = \frac{V_p}{V_n} \cdot 100\% \quad (2)$$

$$\alpha_v = \frac{J_v}{J_w} \quad (3)$$

where: $J_{v/(w)}$ – permeate/deionized water flux;
 VRF – volume reduction factor;
 α_v – relative volume permeate flux;
 S – membrane area;
 t – time of permeate collection;
 V_p ; V_n – volume of permeate and feed respectively.

External validation of models for predicting retention of micropollutants by nanofiltration membranes

In the last stage of this study, the experimental data were used as data set for external validation of available in literature models for predicting retention of micropollutants by nanofiltration membranes. The first model, designated as M1, assumes that the retention of micropollutants should be predicted with molecular weight of compounds, NaCl retention coefficient and a certain indicators describing physicochemical properties of feed. The equation of this model was the following [16]:

$$R = 42.894 + 0.083 M_w + 0.193 SR_{NaCl} + 74.120 ABS \quad (4)$$

where: M_w – molecular mass;
 SR_{NaCl} – sodium chloride retention;
 ABS – absorbance (UV_{254}) was at the level of 0.0; 0.061 and 0.218 for deionized water, synthetic effluent and real effluent respectively.

In the second model (M2 symbol), retention was predicted by means of geometrical dimensions of molecule, hydrophobic-hydrophilic properties of micropollutants and membrane $MWCO$. The equation of M2 retention model is written as [20]:

$$R = 265.150 \text{ eqwidth} - 117.356 \text{ depth} + 81.662 \text{ length} - 5.229 \log D - 0.272 MWCO - 62.565 \quad (5)$$

where: $MWCO$ – molecular weight cut off of membrane – when $MWCO$ is between 150–300 Da, proper value is average *ie* 225 Da [20].

Fitting of models to experimental data were determined by means of mean relative estimation error according to the equation:

$$MRE = \frac{1}{n} \sum_{t=1}^n \left| \frac{y_t - y_p}{y_t} \right| \cdot 100\% \quad (6)$$

where: MRE – mean relative estimation error;
 n – number of samples;
 y_t – experimental value of retention;
 y_p – estimated value of retention.

In addition, strength of relationship between a certain parameters used for prediction of retention and experimental retention coefficient was determined. This was done by calculation of correlation coefficient according to equation 7.

In that, we could explain the discrepancy between the existing experimental retention coefficients and computed from M1 and M2 models.

$$r = \frac{\sum_{i=1}^n (x_i - \bar{x})(y_i - \bar{y})}{\sqrt{\sum_{i=1}^n (x_i - \bar{x})^2 \sum_{i=1}^n (y_i - \bar{y})^2}} \quad (7)$$

where: x_i, y_i – values of variables X and Y respectively for i observations;
 n – numer of observations;
 \bar{x}, \bar{y} – arithmetic mean for observed values of each variable.

Results and discussion

Effect of membrane type on micropollutants removal and nanofiltration performance

Effectiveness of nanofiltration in micropollutants removal from artificial solution of deionized water is presented in Fig. 2. Retention coefficients of anthracene and benzo(a)pyrene indicated almost complete their removal for all tested membranes. That can be explained by very hydrophobic properties of PAHs, normally described by $\log K_{ow}$. Retention of PCP, DCL and OP was more dependent on membrane type. Their retention coefficients were in the range 75.9–92.3%; 89.9–98.9% and 21.4–96.9% for pentachlorophenol, octylphenol and diclofenac. The highest retention was obtained with HL and NF-90 membranes. Different separation properties of tested nanofiltration membranes are probably caused by their different hydrophilic-hydrophobic properties, which are determined by contact angle. The higher contact angle is, the more hydrophobic is membrane and more intensive adsorption of pollutants on membrane surface. In many studies, relationship between hydrophobicity of membranes and degree of adsorption of micropollutants during nanofiltration was proved [16, 21, 22].

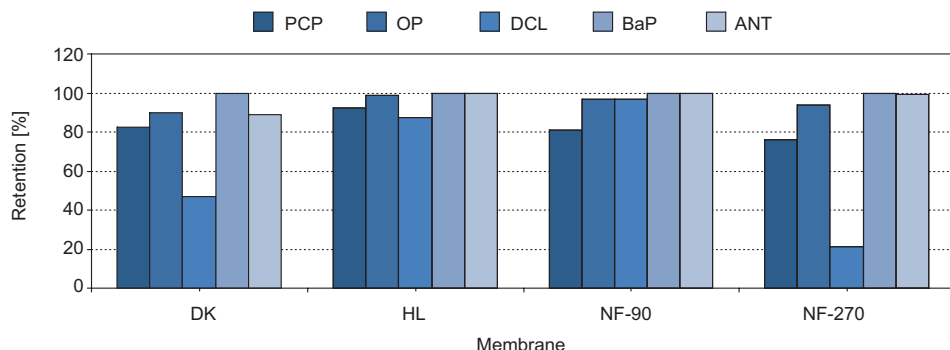


Fig. 2. Impact of membrane on retention of micropollutants (feed: deionized water)

Therefore, adsorption is considered as one of mechanisms of separation in high pressure membrane techniques [18, 23]. Take into account, effect of membranes type and their properties on effectiveness of micropollutants removal, normally we should consider also *MWCO* of membranes. However, due to similar value of *MWCO* of tested NF membranes we assume that sieve effect in separation mechanism of micropollutants was comparable in that case.

Figure 3 shows effect of volume reduction factor on relative permeate flux during nanofiltration of artificial solution of deionized water for all tested membranes. It was found, that relative permeate flux slightly decreased with increase in VRF. α_v was in the range from 0.89 to 1.05. It means that, solution of deionized water with micropollutants as a feed did not cause significant fouling of nanofiltration membranes.

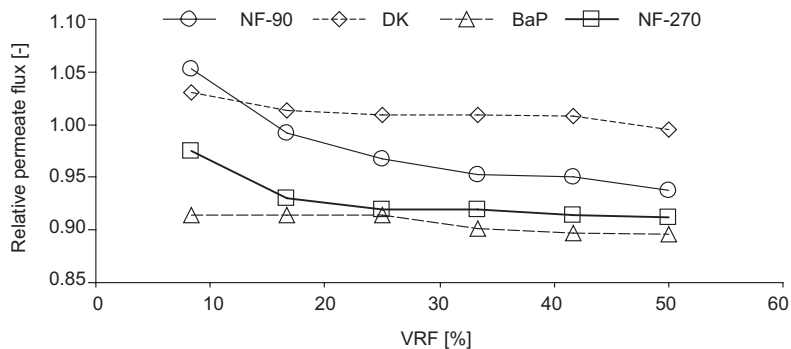


Fig. 3. Variation of relative permeate flux versus with VRF during the filtration of artificial solution of deionized water containing selected biologically active compounds

Effect of the water matrix on micropollutants removal and nanofiltration performance

Type of feed affected also the effectiveness of micropollutants removal in nanofiltration (Fig. 4). Retention coefficients of PCP for synthetic effluent were around 12%

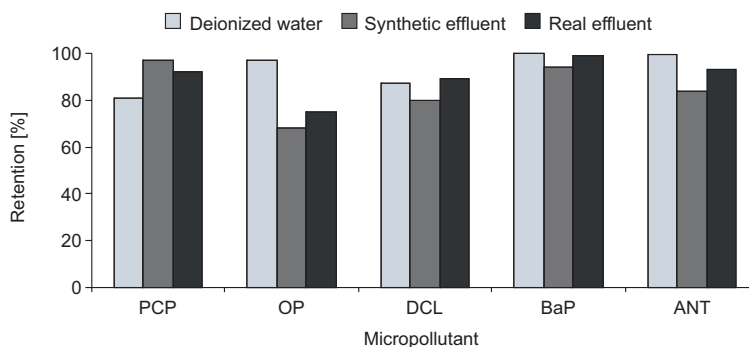


Fig. 4. Comparison of effectiveness of micropollutants removal from deionized water, synthetic and real effluents

and 17% higher than for artificial deionized water solution containing micropollutants. Opposite tendency was observed for OP, DCL, BaP and ANT. Effectiveness of removal of these micropollutants was the highest for artificial solution of deionized water and the lowest for synthetic effluent. Intervening effects were obtained while removal of micropollutants from synthetic effluent. These results indicate complex and dependent on many factors separation mechanisms of low molecular weight organic compounds in nanofiltration. Substances and pollutants contained in artificial and real effluent formed a filtration cake, that can be consider as additional separation layer – secondary membrane, enhancing removal of micropollutants. This effect was probably a reason of higher removal of pentachlorophenol from effluents than from artificial solution of deionized water. However, this effect did not affect the retention of OP, DCL, BaP and ANT. In case of the latter compounds, dominant mechanisms of separation could be adsorption. For effluent samples, adsorption of micropollutants was lower due to other organic and inorganic compounds normally present in wastewater. They could preferentially occupy active sorption sites on the membrane surface.

Taking onto consideration effect of feed type on nanofiltration performance (NF-90 membrane), it was found that a reduction of permeate flux versus increasing VRF was the lowest for filtration of deionized water solution and the highest for real effluent (Fig. 5a). In initial phase of nanofiltration of real effluent, permeate flux was around

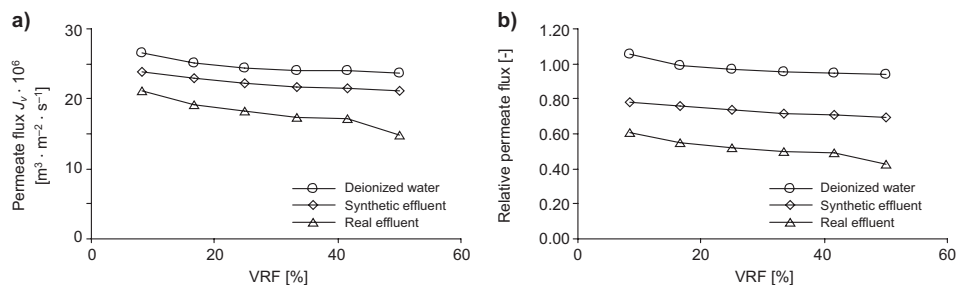


Fig. 5. Dependence of a) volume permeate flux and b) relative volume permeate flux versus VRF

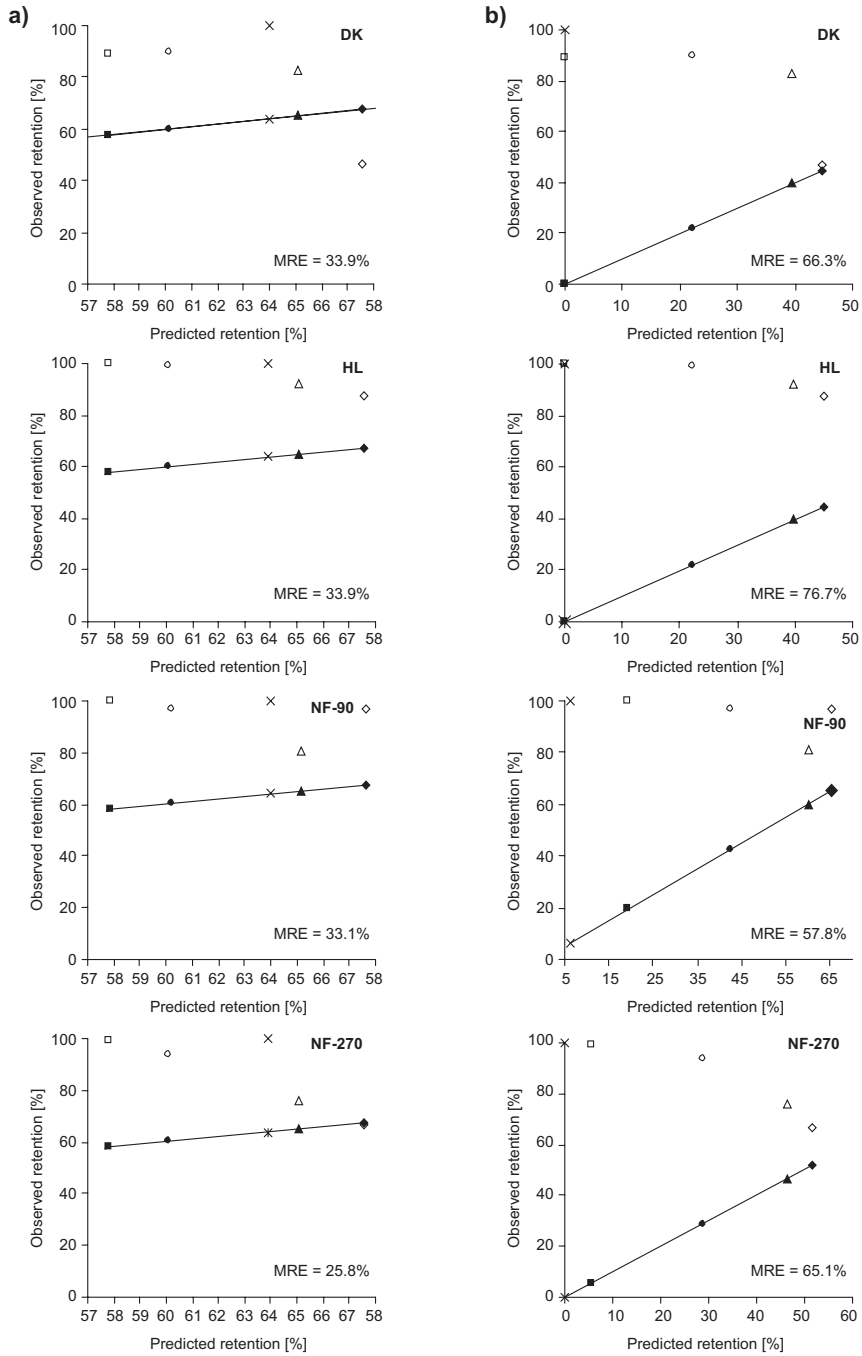


Fig. 6. Observed retention versus predicted retention computed from models: a) M1 and b) M2 (feed: deionized water with Δ – PCP, \circ – OP, \diamond – DCL, \times – BaP, \square – ANT)

20% lower in comparison to permeate flux for filtration of deionized water solution. Thus, organic and inorganic pollutants present in real and synthetic effluents caused more intensive fouling of NF-90 membrane. This is confirmed also by the values of relative permeate flux (Fig. 5b), which in case of more intensive coating the membrane surface with a layer of pollutants take significantly lower values.

Prediction of biologically active substances retention in nanofiltration based on mathematical models and statistical analysis

Relationship between observed and predicted retention coefficients of biologically active substances is presented in Fig. 6a and 6b. Based on MRE parameters, it was found that M1 model predicted the retention of micropollutants more precise than M2 model. More specifically, divergence between experimental and predicted retention coefficient computed from M1 model were in the range from 25% to 33%. While, computed from M2 model retention coefficients deviated from experimental data in the range of 57–76%.

Moreover, computed from M1 model retention coefficients were very similar to experimental data (observed retention coefficients) for synthetic and real effluents (Fig. 7). Precision of M1 model, described by MRE parameter reached 11 and 19% for synthetic and real effluent respectively. For comparison, for M2 model, MRE parameters were equaled 53 and 55% respectively.

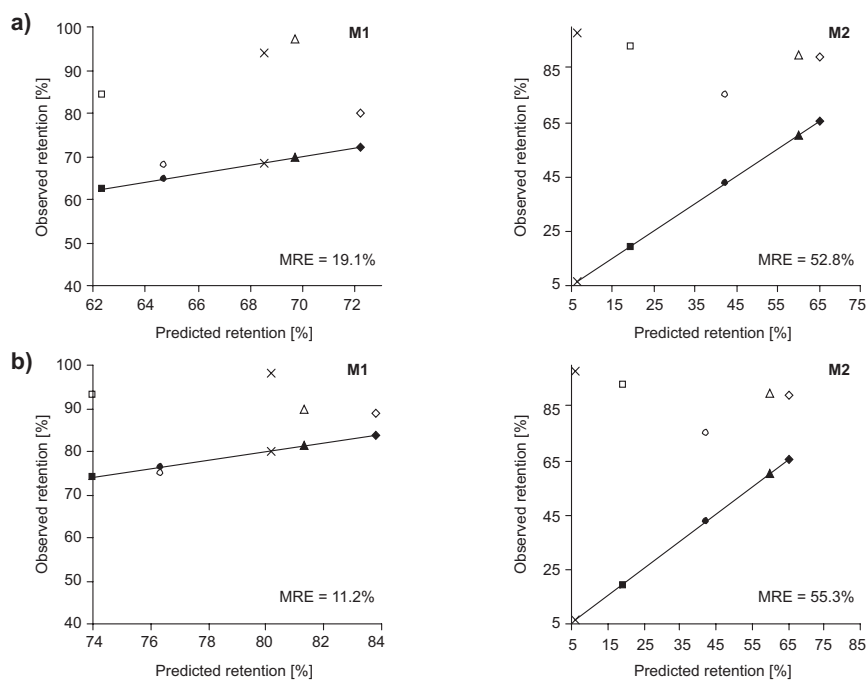


Fig. 7. Observed retention versus predicted retention for nanofiltration (membrane NF90) of a) synthetic and b) real effluents (with Δ – PCP, \circ – OP, \diamond – DCL, X – BaP, \square – ANT)

As was mentioned, computed from M1 model retention coefficients predicted retention better than M2 model for all considered feed types. Thus, retention of biologically active compounds was conditioned by molecular weight and also potential of membrane for monovalent ions separation and organics content in the feed. Mechanisms of micropollutants separation include not only sieve effect, dependent on size of micropollutants molecule and size of membrane pores, but also a few phenomena accompanying membrane filtration *eg* intermolecular interactions occurring between different feed ingredients. Potential of membrane for divalent ions retention (usually reached 96–99%) as well as parameters describing geometrical dimensions of compounds seem to be less important factors for predicting the micropollutants retention. Moreover, we did not observe positive correlation between parameters such as length, width and eqwidth of molecule and retention coefficients (Table 3).

Table 3

Correlation coefficient between retention and chosen structural and physicochemical parameters of micropollutants (deionized water)

Membrane	Length [nm]	Width [nm]	Eqwidth [nm]	$\log K_{ow}$ [-]
DK	0.085	-0.45	-0.37	0.40
HL	0.33	-0.33	0.51	0.32
NF90	0.91	0.40	0.33	0.34
NF270	0.42	-0.3	0.16	0.39

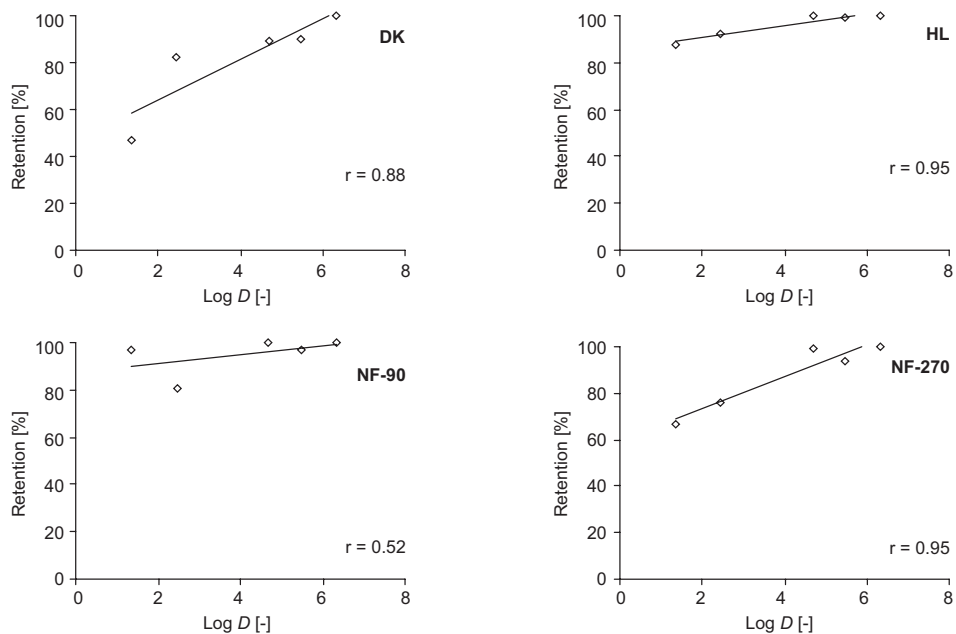


Fig. 8. Dependence of retention coefficients and $\log D$ of compounds (deionized water)

It was found that, the reason of slight divergences between computed from M1 model retention coefficients and experimental retention coefficients may be caused by omitted impact of adsorption of compounds on membrane surface during nanofiltration. It is confirmed by shown in Fig. 8 positive linear correlation between $\log D$ parameter (logarithm of the distribution coefficient (D) at a selected pH, assumed to be measured in octanol), and retention coefficients of biologically active substances.

Conclusions

Based on the carried out experiments can be concluded that:

- In nanofiltration of deionized water, retention of micropollutants was in the range from 21.5% to 99.82%. The removal efficiency of biologically active substances depends on the type of the nanofiltration membrane. The best results were obtained using the membrane of the symbols HL and NF-90.

- The highest removal efficiency was obtained for anthracene and benzo(a)pyrene, and the lowest for diclofenac. This effect could be due to a more hydrophobic nature of PAHs.

- Comparing the efficiency of removal of biologically active substances from deionized water and effluent – it has been found that the retention of all the compounds apart from PCP was higher during the filtration of deionized water than the effluent samples.

- The results confirm that the separation mechanism in the nanofiltration process is complex and dependent on both the properties of the membrane and separated material as well as the feed type.

- It was found that contaminants contained in synthetic and real wastewater caused significant fouling of the membrane NF-90. The observed reduction in the permeate flux ranged from 20% (initial phase of filtration) to 40% (the end of filtration) of the values obtained in the nanofiltration of deionized water.

- Model based on molecular weight of molecule and absorbance of feed as well as membrane potential for sodium chloride separation (M1 model) predicted well retention of biologically active substances with different properties. In comparison model based on potential of membrane for divalent ions retention and parameters describing geometrical dimensions of compounds (M2 model) was not applicable to predict retention selected in this study micropollutants.

Acknowledgements

The paper has been prepared within the frame of the National Science Centre project based on decision no DEC-2013/11/B/ST8/0439. Author Gabriela Kamińska obtained scholarship for preparing PhD thesis within the frame of the National Science Centre project based on decision no UMO-2014/12/T/ST8/00668.

References

- [1] Bolong N, Ismail A, Salim M, Matsuura T. Desalination. 2009;239:229-246.
DOI:10.1016/j.desal.2008.03.020.
- [2] Soares A, Guieysse B, Jefferson B, Cartmell E, Lester J. Environ Int. 2009;34:1033-1049.
DOI: 10.1016/j.envint.2008.01.004.

- [3] Schäfers C, Teigeler M, Wenzel A, Maack G, Fenske M, Segner H. *J Toxicol Env Heal A*. 2007;70:768-779. DOI:<http://dx.doi.org/10.1080/15287390701236470>.
- [4] Wang X, Miao Y, Zhang Y, Cheng Li Y, Wu M, Yu G. *Sci Total Environ*. 2013;447:80-89. DOI:10.1016/j.scitotenv.2012.12.086.
- [5] Patrolecco L, Ademollo N, Capri S, Pagnotta R, Polesello S. *Chemosphere* 2010;81:1386-1392. DOI: 10.1016/j.chemosphere.2010.09.027.
- [6] Mihaich E, Friederich U, Caspers N, Hall AT, Klecka G, Dimond S, et al. *Ecotox Environ Safe*. 2009;72:1392-1399. DOI: 10.1016/j.ecoenv.2009.02.005.
- [7] Mariel A, Alejandra B, Silvia P. *Environ Toxicol Phar*. 2014;38:634-642. DOI:10.1016/j.etap.2014.08.014.
- [8] Zhang L, Li Q, Chen L, Zhang A, He J, Wen Z, Wu L. *Ecotox Environ Safe*. 2015;112:137-143, DOI: 10.1016/j.ecoenv.2014.10.037.
- [9] Directive 2008/105/EC of the European Parliament and of the Council of 16 December 2008 on environmental quality standards in the field of water policy, amending and subsequently repealing Council Directives 82/176/EEC, 83/513/EEC, 84/156/EEC, 84/491/EEC, 86/280/EEC and amending Directive 2000/60/EC of the European Parliament and of the Council. <http://eur-lex.europa.eu/LexUriServ/LexUriServ.do?uri=OJ:L:2008:348:0084:0097:en:PDF>.
- [10] Directive 2013/39/EU of the European Parliament and of The Council of 12 August 2013 amending Directives 2000/60/EC and 2008/105/EC as regards priority substances in the field of water policy. <http://eur-lex.europa.eu/LexUriServ/LexUriServ.do?uri=OJ:L:2013:226:0001:0017:EN:PDF>.
- [11] Directive 2000/60/EC of the European Parliament and of the Council of 23 October 2000 establishing a framework for Community action in the field of water policy. http://ec.europa.eu/health/endocrine_disruptors/docs/wfd_200060ec_directive_en.pdf.
- [12] Hajibabania S, Verliefe A, McDonald J, Khdan S, Le-Clech P. *J Membrane Sci*. 2011;373:130-139. DOI:10.1016/j.memsci.2011.02.040.
- [13] Acero J, Benitez F, Teva F, Leal A. *Chem Eng J*. 2010;163:264-272. DOI:10.1016/j.cej.2010.07.060.
- [14] Hajibabania S, Verliefe A, McDonald J, Khdan S, Le-Clech P. *J Membrane Sci*. 2011;373:130-139. DOI:10.1016/j.memsci.2011.02.040.
- [15] Radjenovic J, Petrovic M, Ventura F, Barcelo D. *Water Res*. 2008;42:3601-361. DOI:10.1016/j.watres.2008.05.020.
- [16] Dudziak M. Separacja mikrozanieczyszczeń estrogenicznych wysokociśnieniowymi technikami membranowymi. (Separation of estrogenic micropollutants by high pressure membrane techniques). Gliwice: Politechnika Śląska (Silesian University of Technology); 2013.
- [17] Semião A, Schäfer A. *Membrane Sci*. 2013;431:244-256. DOI:10.1016/j.memsci.2012.11.080.
- [18] Schäfer A, Akanyeti I, Semião A. *Adv Colloid Interface Sci*. 2011; 164: 100-117. DOI: 10.1016/j.cis.2010.09.006.
- [19] Bellona C, Drewes JE, Xu P, Amy G. *Water Res*. 2004; 38: 2795-2809. DOI:10.1016/j.watres.2004.03.034
- [20] Yangali-Quintanilla V, Sadmani A, McConville M, Kennedy M, Amy G. *Water Res*. 2010;44:373-384. DOI: 10.1016/j.watres.2009.06.054
- [21] McCallum EA, Hyung H, Anh Do T, Huang C, Kim J. *J Membrane Sci*. 2008;319:38-43. DOI:10.1016/j.memsci.2008.03.014.
- [22] Yoon Y, Westerhoff P, Snyder S, Wert EJ. *Membrane Sci*. 2006; DOI:10.1016/j.memsci.2005.06.045.
- [23] Mohammad AW, Teow YH, Ang WL, Chung YT, Oatley-Radecliffe DL, Hilal N. *Desalination*. 2015;356:226-254. DOI:10.1016/j.desal.2014.10.043.

OCENA SKUTECZNOŚCI USUWANIA WYBRANYCH SUBSTANCJI AKTYWNYCH BIOLOGICZNIE W PROCESIE NANOFILTRACJI

Instytut Inżynierii Wody i Ścieków
Politechnika Śląska, Gliwice

Abstrakt: W ramach pracy podjęto badania nad oceną skuteczności usuwania pięciu różnych związków należących do grupy substancji aktywnych biologicznie, tj. benzo(a)pirenu (BaP), antracenu (ANT), diklofenaku

(DCL), pentachlorofenol (PCP) i oktylofenol (OP) w procesie nanofiltracji. Przedmiotem badań były modelowe roztwory tych substancji o stężeniu $500 \mu\text{g}/\text{dm}^3$ wykonane na bazie wody zdejonizowanej. Uzyskane wyniki badań porównano pod kątem skuteczności usuwania wybranych związków z syntetycznych i rzeczywistych odpływów z komunalnej oczyszczalni ścieków. Wykazano, że na skuteczność procesu nanofiltracji istotny wpływ ma rodzaj membrany nanofiltracyjnej, właściwości fizykochemiczne usuwanych związków, jak również rodzaj matrycy środowiskowej poddawanej oczyszczaniu. Najwyższą efektywność usuwania zaobserwowano dla benzopirenu w trakcie nanofiltracji wody zdejonizowanej. Współczynniki retencji wynosiły wówczas od 99,82% do 99,94%, co oznacza praktycznie jego całkowite usunięcie. Z kolei dla pozostałych związków z wyjątkiem oktylofenolu zaobserwowano odwrotną tendencję, wyższe współczynniki retencji uzyskano, gdy filtrowanym medium były ścieki syntetyczne lub rzeczywiste. Przeprowadzone badania udokumentowały złożony mechanizm separacji małocząsteczkowych mikrozanieczyszczeń organicznych w procesie nanofiltracji wynikający m.in. z oddziaływań międzycząsteczkowych, efektu sitowego, jak i adsorpcji. Dodatkowo, w ostatniej części pracy porównano uzyskane dane doświadczalne z przewidywanymi współczynnikami retencji, które zostały obliczone z modeli dotyczących przewidywania retencji mikrozanieczyszczeń w procesie nanofiltracji.

Słowa kluczowe: związki aktywne biologicznie, nanofiltracja

Milena RUSIN^{1*}, Janina GOSPODAREK¹
and Aleksandra NADGÓRSKA-SOCHA²

THE EFFECT OF PETROLEUM-DERIVED SUBSTANCES ON CHEMICAL COMPOSITION OF WINTER WHEAT

WPLYW SUBSTANCJI ROPOPOCHODNYCH NA SKŁAD CHEMICZNY PSZENICY OZIMEJ

Abstract: The aim of the study was to determine the effect of petrol, used engine oil and diesel fuel on the content of calcium, magnesium, iron, potassium and the selected heavy metals in the grain, straw and roots of winter wheat. The effect of bioremediation process on the abovementioned parameters was also determined. The experiment was conducted in 2014 on the area of the Experimental Station of the University of Agriculture in Krakow, situated in Mydlniki. In June 2010, the soil surface was artificially contaminated with petroleum-derived substances in quantity of 6000 mg per 1 kg of dry mass. Half of the objects were subjected to the bioremediation process by adding biopreparation ZB-01. The evaluation of nutrients content was conducted using flame absorption spectrometry. The results of the experiment showed that all used petroleum-derived substances most frequently contributed to the decrease in the content of selected nutrients in the grain of winter wheat. In other organs of plant the content of nutrients and heavy metals due to the presence of petroleum-derived substances in the soil was variable and depended on the type of used substances and on the analysed part of the plant. Application of biopreparation ZB-01 on soil contaminated with engine oil usually caused an increase in the content of analysed nutrients in the roots of plants, but also their decline in the straw. In other objects variables dependencies were noted, most frequently biopreparation had no significant effect on the content of heavy metals in the plants.

Keywords: petroleum-derived substances, bioremediation, nutrients, heavy metals, winter wheat

In recent years, the progressive economy industrialization and the increase of the level of antropopression have led to the intensive growth of petroleum-derived substances consumption, which carries the risk of entering these compounds to the environment. The most vulnerable to contamination are the soils located near petrol stations, garages, seaports, and other areas where the production or distribution of crude

¹ Department of Agricultural Environment Protection, University of Agriculture, al. A. Mickiewicza 21, 31-120 Kraków, Poland, phone: +48 12 662 44 02.

² Department of Ecology, University of Silesia, ul. Bankowa 12, 40-007 Katowice, Poland, phone: +48 32 359 19 15.

* Corresponding author: milena_rusin@wp.pl

oil is present [1]. Moreover, heavy agriculture machines are increasingly used, which leads to increase of diesel fuel consumption and therefore may lead to the contamination of cultivated soils. Incorrect transport, storage and inadequate care in the disposal of petroleum-derived substances are the main factors influencing the increase of environmental pollution with these compounds [2–4]. Petroleum-derived substances penetrate into the soil and contribute to its degradation by modifying the physico-chemical and biological properties [5, 6]. The presence of these xenobiotics in the soil results in inhibition of growth and development of many crops, disturbs the uptake of water and nutrients, and modifies the content of heavy metals in plant organs [7–10].

To purify the soil contaminated with petroleum-derived substances most commonly various techniques of bioremediation are used. For this purpose soil microorganisms are applied. They are supposed to reduce the concentration of contaminants to acceptable levels, convert petroleum hydrocarbons into non-toxic compounds or perform mineralization to carbon dioxide and water. Most commonly bacteria and fungi are used, as characterized by a large population size, rapid growth, and moreover, their metabolic products decompose pollutants [11–13].

The aim of the study was to determine the effect of petrol, used engine oil and diesel fuel on the content of selected nutrients (calcium, magnesium, iron, potassium) and heavy metals (cadmium, lead, zinc, nickel, copper, manganese) in the grain, straw and roots of winter wheat.

Material and methods

The plant material used for the laboratory analysis was obtained from the Experimental Station of the University of Agriculture in Krakow, located in Mydlniki (50°5'5,04"N 19°51'13,47"E). In November 2009, indigenous soil was placed in special containers of 1 m³ volume each, retaining the natural arrangement of layers. The containers were sunk in the ground so that their upper edge was at the same level as the surface of the soil. All containers had a pipe leading to the surface, enabling the excess of water to be pumped out, and three plastic tubes for suitable soil aeration, which is necessary for the correct course of bioremediation. The soil in the containers was left for eight months without any intervention in order to regain its natural biological functions. In June 2010, the soil surface was artificially contaminated with petrol, used engine oil, and diesel fuel in a quantity of 6000 mg of petroleum-derived substance per 1 kg of dry mass, by pouring it on the soil. After one week, half of the containers were subjected to the bioremediation process by adding biopreparation ZB-01, which was specially produced for this experiment and contained selected prokaryotic organisms, mainly bacteria from the following genera: *Bacillus*, *Pseudomonas*, *Moraxella*, *Stenotrophomonas*, *Acinetobacter*, *Corynebacterium*, *Methylobacterium*, *Alcaligenes*, *Oligella*, *Morganella*. The procedure of bioremediation was repeated in spring 2011. The non-contaminated soil was placed in identical containers and constituted the control treatment. The experiment was set in four repetitions in line with the randomised blocks method. In subsequent years, until 2013 the soil in the containers was left without any intervention to enable natural plant succession. The seeds of the Batuta variety of winter

wheat were sown in the containers in mid-October 2013, after earlier preparation of the soil (*ie* loosening and fertilizing). Pre-sowing soil fertilization with 'azofoska' was applied providing 5.44 gN, 2.56 gP₂O₅ and 7.64 gK₂O per container.

Plant material used to determine the content of selected nutrients and heavy metals was collected after the wheat harvest in early August 2014. In order to determine the nutrients (calcium, potassium, iron, magnesium) and heavy metal (copper, manganese, nickel, lead, zinc, cadmium) concentrations in plants parts, plant material was cleaned of any patches of deposited aphid honeydew and other surface contaminants, washed in tap, next in distilled water. It was then dried at 105°C. A portion of 0.25 g dried plant material was digested with 5 cm³ of HNO₃ at 110°C and then diluted to 10 cm³ with deionized water. Next, the metal content was measured using flame absorption spectrometry (Unicam 939 Solar) [14, 15]. The quality of the analytical procedure was checked using a reference material (Certified Reference Material CTA-OTL-1 Oriental Tobacco Leaves) with the same quantities of samples.

The obtained results were then subjected to analysis by STATISTICA 10.0 software. The significance of differences between the means were tested by two-factor variance analysis, and the means were differentiated by Fisher's LSD test at $\alpha = 0.05$.

Results

All used petroleum-derived substances contributed to a significant reduction in calcium, magnesium and iron contents in the grain of winter wheat (Table 1). Additionally, used engine oil and petrol resulted in a decrease in potassium content, respectively 920.01 mg · kg⁻¹ and 837.22 mg · kg⁻¹ compared to the control.

Table 1

The content of some nutrients in grain of winter wheat [mg · kg⁻¹]

Object	Ca	Mg	Fe	K
EO OR	328.17 ^{bc*}	648.30 ^a	38.73 ^{abc}	4616.92 ^a
EO R	435.29 ^{cd}	736.44 ^b	37.30 ^{ab}	5206.15 ^{cd}
DF OR	372.24 ^{cd}	759.54 ^{bc}	41.68 ^{abcd}	5616.57 ^d
DF R	324.24 ^{bc}	733.63 ^b	48.91 ^{cd}	5174.31 ^{bcd}
P OR	297.24 ^b	762.58 ^{bc}	32.15 ^a	4699.71 ^a
P R	179.39 ^a	718.28 ^b	47.94 ^{bcd}	4739.03 ^{ab}
C OR	541.28 ^c	843.27 ^d	61.70 ^c	5536.93 ^d
C R	368.24 ^c	803.13 ^{cd}	50.50 ^d	5025.16 ^{abc}

EO – soil contaminated with engine oil, DF – soil contaminated with diesel fuel, P – soil contaminated with petrol, C – control soil, OR – without bioremediation, R – with bioremediation. * Means in columns marked with the same letters do not differ significantly according to LSD test at $\alpha = 0.05$.

Biopreparation ZB-01 applied to the soil contaminated with engine oil resulted to a significant increase in the contents of magnesium and potassium in the grain of analysed plants, while in the case of control caused a decline in calcium, iron and

potassium contents. The grain obtained from plants growing in soil contaminated with petrol after the application of the biopreparation was characterized by a higher iron content but a lower calcium content compared to the object in which the bioremediation process was not applied. In the case of diesel fuel, there was no significant effect of using the biopreparation ZB-01 on the level of analysed nutrients in winter wheat grain.

All petroleum-derived substances used in the experiment resulted in a significant increase in the cadmium content in winter wheat grain (Table 2). Engine oil also contributed to the increase in the content of manganese by nearly $4 \text{ mg} \cdot \text{kg}^{-1}$ compared to the control, while diesel fuel – an increase in the contents of lead and nickel ($33 \text{ mg} \cdot \text{kg}^{-1}$ and $0.19 \text{ mg} \cdot \text{kg}^{-1}$ respectively). Grain of plants growing in soil contaminated with petrol was characterized by lower content of zinc (nearly $17 \text{ mg} \cdot \text{kg}^{-1}$) than the grain of plants obtained from control.

Table 2

The content of some heavy metals in grain of winter wheat [$\text{mg} \cdot \text{kg}^{-1}$]

Object	Cd	Pb	Zn	Ni	Cu	Mn
EO OR	0.37 ^{c*}	3.04 ^{bcd}	56.01 ^{cd}	0.17 ^{bc}	5.17 ^{bcd}	21.46 ^b
EO R	0.35 ^c	6.18 ^{cd}	56.61 ^d	0.23 ^d	5.62 ^{cd}	21.31 ^b
DF OR	0.45 ^d	7.42 ^{de}	53.52 ^{bcd}	0.31 ^c	5.87 ^d	19.14 ^{ab}
DF R	0.33 ^c	8.50 ^c	50.85 ^{bc}	0.31 ^c	5.56 ^{cd}	25.98 ^c
P OR	0.21 ^b	3.29 ^a	42.09 ^a	0.14 ^{abc}	4.04 ^a	20.33 ^{ab}
P R	0.25 ^b	3.99 ^{ab}	48.40 ^{abc}	0.18 ^{cd}	4.60 ^{abc}	19.00 ^{ab}
C OR	0.09 ^a	4.29 ^{abc}	59.01 ^d	0.12 ^{ab}	4.90 ^{abcd}	17.51 ^a
C R	0.21 ^b	4.29 ^{abc}	45.74 ^{ab}	0.09 ^a	4.31 ^{ab}	19.65 ^{ab}

Symbols as in Table 1. * Means in columns marked with the same letters do not differ significantly according to LSD test at $\alpha = 0.05$.

Used biopreparation usually had no significant effect on the content of selected heavy metals in wheat grain and only in object contaminated with engine oil it contributed to an increase in nickel content, in the object contaminated with diesel fuel – an increase in manganese content, but a decrease in cadmium content, while in control – an increase in cadmium content, but a decrease in the content of zinc.

All applied xenobiotics caused a significant increase in the iron content in wheat straw (Table 3). Straw of plants growing in soil contaminated with diesel fuel was additionally characterized by almost $520 \text{ mg} \cdot \text{kg}^{-1}$ higher calcium content compared to the control. Petrol contributed to a significant increase in the content of potassium in the straw simultaneously decreasing calcium and magnesium contents.

The use of the biopreparation on soil contaminated with petrol most often resulted in a significant decrease in content of selected nutrients in the analysed part of the plant (a decrease in the contents of magnesium and iron in the object contaminated with engine oil, a decrease in calcium, iron and potassium contents in the object contaminated with diesel fuel, a decrease in iron and potassium contents in the object contaminated with petrol and a decrease in calcium content in the control). However, it

Table 3

The content of some nutrients in straw of winter wheat [$\text{mg} \cdot \text{kg}^{-1}$]

Object	Ca	Mg	Fe	K
EO OR	2838.84 ^{bc}	512.57 ^{cd}	376.03 ^c	17956.08 ^{bc}
EO R	3000.18 ^c	462.14 ^{ab}	269.04 ^d	26830.23 ^d
DF OR	3081.05 ^c	519.50 ^d	133.30 ^c	18120.88 ^{bc}
DF R	2136.00 ^a	486.26 ^{abcd}	57.03 ^a	12341.05 ^a
P OR	2169.03 ^a	455.77 ^a	360.30 ^c	41934.27 ^c
P R	2145.74 ^a	612.64 ^c	127.02 ^c	15802.75 ^{ab}
C OR	2561.82 ^b	509.02 ^{bcd}	89.24 ^b	14681.78 ^{ab}
C R	2031.50 ^a	465.45 ^{abc}	78.55 ^{ab}	19931.02 ^c

Symbols as in Table 1. * Means in columns marked with the same letters do not differ significantly according to LSD test at $\alpha = 0.05$.

was noted, that biopreparation applied to the soil contaminated with engine oil caused a significant increase in potassium content in straw (by $8874.15 \text{ mg} \cdot \text{kg}^{-1}$), while in the case of soil contaminated with petrol – an increase in magnesium content (by $156.87 \text{ mg} \cdot \text{kg}^{-1}$), and in the case of control – an increase in potassium content (by $5249.24 \text{ mg} \cdot \text{kg}^{-1}$).

The engine oil led to an increase in the content of most analysed heavy metals in winter wheat straw (lead, zinc, nickel and manganese) (Table 4). Diesel fuel on the one hand, caused an increase in the nickel content by almost $0.3 \text{ mg} \cdot \text{kg}^{-1}$, but on the other hand, also led to a decline in zinc content by more than $10 \text{ mg} \cdot \text{kg}^{-1}$. Petrol caused a significant lead level increase, but also a decrease in the contents of zinc and manganese. Used petroleum-derived substances had no significant effect on the contents of cadmium and copper in the straw of analysed plants.

Table 4

The content of some heavy metals in straw of winter wheat [$\text{mg} \cdot \text{kg}^{-1}$]

Object	Cd	Pb	Zn	Ni	Cu	Mn
EO OR	0.89 ^a	15.71 ^{dc}	79.53 ^c	0.73 ^{bcd}	7.94 ^a	41.10 ^d
EO R	1.01 ^a	9.35 ^{bc}	83.21 ^c	0.90 ^c	9.83 ^b	34.73 ^{cd}
DF OR	0.93 ^a	6.62 ^{ab}	36.80 ^a	0.83 ^{dc}	8.26 ^a	21.84 ^b
DF R	1.00 ^a	10.59 ^{bc}	47.22 ^a	0.86 ^{dc}	7.69 ^a	53.10 ^c
P OR	0.81 ^a	17.13 ^c	41.28 ^a	0.65 ^{abc}	7.63 ^a	13.38 ^a
P R	0.96 ^a	12.37 ^{cd}	38.49 ^a	0.77 ^{cde}	8.35 ^a	32.42 ^c
C OR	0.79 ^a	5.07 ^a	58.08 ^b	0.54 ^a	7.91 ^a	27.97 ^{bc}
C R	0.90 ^a	6.87 ^{ab}	65.79 ^b	0.61 ^{ab}	7.81 ^a	58.57 ^c

Symbols as in Table 1. * Means in columns marked with the same letters do not differ significantly according to LSD test at $\alpha = 0.05$.

Biopreparation application on soil contaminated with diesel fuel, petrol and on control soil led to a significant increase in manganese content in the straw of winter wheat compared to the objects in which the bioremediation process was not applied. Moreover, the straw obtained from plants growing in soil contaminated with used engine oil after applying the biopreparation was characterized by the higher nickel and copper contents, in turn, lower lead content (as in the object contaminated with petrol) than the objects without the application of biopreparation.

Both diesel fuel and petrol caused an increase in iron content in the roots of winter wheat compared to the control (Table 5). However, used engine oil caused an almost twofold decrease in the content of this nutrient in the analysed part of plant. The roots of plants growing in soil contaminated with diesel fuel were also characterized by a higher content of magnesium, while the roots of plants growing in soil contaminated with petrol contained significantly less calcium and magnesium ($673.07 \text{ mg} \cdot \text{kg}^{-1}$ and $56.26 \text{ mg} \cdot \text{kg}^{-1}$ respectively) in relation to the control.

Table 5

The content of some nutrients in roots of winter wheat [$\text{mg} \cdot \text{kg}^{-1}$]

Object	Ca	Mg	Fe
EO 0R	3108.15 ^b	440.64 ^b	641.81 ^a
EO R	3772.83 ^c	498.44 ^c	1366.23 ^c
DF 0R	3199.68 ^b	551.48 ^d	1547.91 ^d
DF R	3003.90 ^b	496.79 ^c	1068.37 ^b
P 0R	2438.89 ^a	392.94 ^a	1459.01 ^{cd}
P R	2606.69 ^a	431.13 ^{ab}	1112.94 ^b
C 0R	3111.96 ^b	449.20 ^b	1118.94 ^b
C R	3265.60 ^b	447.91 ^b	1478.92 ^{cd}

Symbols as in Table 1. * Means in columns marked with the same letters do not differ significantly according to LSD test at $\alpha = 0.05$.

Biopreparation ZB-01 in the case of the object contaminated with engine oil caused a significant increase in calcium, magnesium and iron contents in plant roots. In the object contaminated with diesel fuel the most frequently inverse relationship was reported (a decrease of magnesium and iron contents after applying the biopreparation). Most often, biopreparation did not affect significantly the content of the analysed components in the case of control and object contaminated with petrol and only led to a decrease in iron content in plants growing in soil contaminated with petrol and increase the content of this element in the control object.

Both engine oil and diesel fuel caused a significant increase in the contents of cadmium, lead, zinc and manganese in the roots of analysed plant (Table 6). Both xenobiotics, also led to a decrease in copper content compared to the control (over $2 \text{ mg} \cdot \text{kg}^{-1}$). Moreover the roots of plants growing in soil contaminated with engine oil were characterized by a significantly higher content of nickel (by $0.38 \text{ mg} \cdot \text{kg}^{-1}$). There

was no significant effect of petrol on the contents of selected heavy metals in the roots of winter wheat.

Table 6

The content of some heavy metals in roots of winter wheat [$\text{mg} \cdot \text{kg}^{-1}$]

Object	Cd	Pb	Zn	Ni	Cu	Mn
EO OR	1.95 ^c	14.01 ^{cde}	127.30 ^d	1.29 ^b	12.24 ^a	130.31 ^b
EO R	1.96 ^c	17.06 ^c	144.02 ^c	1.33 ^b	13.31 ^{ab}	169.47 ^{cd}
DF OR	1.90 ^c	15.72 ^{dc}	115.12 ^d	1.18 ^{ab}	11.94 ^a	181.92 ^d
DF R	2.22 ^d	14.13 ^{cde}	80.47 ^{bc}	1.14 ^{ab}	14.30 ^{bc}	169.52 ^{cd}
P OR	1.38 ^a	11.31 ^{abc}	59.24 ^a	1.21 ^{ab}	13.02 ^{ab}	96.04 ^a
P R	1.59 ^b	9.83 ^a	66.58 ^a	0.97 ^a	15.00 ^{bc}	98.31 ^a
C OR	1.43 ^{ab}	10.17 ^{ab}	71.09 ^{ab}	0.91 ^a	14.56 ^{bc}	97.71 ^a
C R	1.64 ^b	13.00 ^{bcd}	88.18 ^c	1.07 ^{ab}	16.33 ^c	151.04 ^c

Symbols as in Table 1. *Means in columns marked with the same letters do not differ significantly according to LSD test at $\alpha = 0.05$.

Application of the biopreparation on the soil contaminated with engine oil and on control soil led to a significant increase in the contents of zinc and manganese in plant roots. In the case of soil contaminated with diesel fuel, it was noted, that the use of biopreparation increased the contents of cadmium and copper in the analysed parts of plant, in turn, the zinc content dropped. In the object contaminated with petrol, most often, used bioremediation process did not affect significantly the content of heavy metals in the roots of winter wheat and only caused an increase in cadmium content by $0.21 \text{ mg} \cdot \text{kg}^{-1}$ compared to the object, in which the biopreparation was not used.

Discussion

In conducted experiment petroleum-derived substances caused a decrease in calcium content in winter wheat grain and petrol also caused a decrease in the content of this nutrient in straw and roots of plants. Wyszowski and Wyszowska [8] showed, on the basis of their studies, that the engine oil causes a decrease in calcium content in the aerial parts of oats and maize. The dose of xenobiotic and used organic and mineral fertilization have the major effect on the strength of this interaction. These authors also showed that the engine oil usually causes a decrease in magnesium content and the doses above $6 \text{ g} \cdot \text{kg}^{-1}$ also contribute to the decrease in potassium content in plants, which corresponds to results of the present experiment, particularly with regard to the grain of winter wheat. Wyszowski et al [7] found that the engine oil in small doses ($1.696 \text{ g} \cdot \text{kg}^{-1}$) increases the contents of calcium, magnesium and potassium in the aerial parts and roots of yellow lupine. The discrepancies may be due to the fact of different plant species used in both experiments as well as the other types of soil used as the substrate, which may also have a significant effect on nutrient uptake by plants and was emphasized by these authors. Wyszowski and Ziolkowska [16] showed that petrol

and engine oil may cause a decrease in magnesium content in the aerial parts of oats. In our experiment, petrol also caused a decrease in the content of this micronutrient in all analysed parts of plant, while diesel fuel – the decline in winter wheat grain. The authors also showed that petrol contributes to a significant increase in potassium content in oats, which was also confirmed in our experience (petrol resulted in a significant decrease in potassium content in winter wheat straw). Wyszowski and Ziolkowska [17] found that a dose of petrol and engine oil amounting to $5 \text{ cm}^3 \cdot \text{kg}^{-1}$ results in a decrease in calcium and magnesium contents in the aerial parts of yellow lupine and maize. Petroleum-derived substances usually cause an increase of soil density, which leads to clogging of soil pores and, consequently, contributes to disturbances of water and nutrient uptake by plants. These substances may also block the transport of substances in plant cells, which may contribute to the limited growth and development of plants [18].

Rusin et al [10] found that engine oil and diesel fuel cause an increase in the contents of lead and manganese in leaves of broad bean. In our experiment mentioned substances also most often contributed to the increase in heavy metals content in the analysed parts of winter wheat. These authors also showed that diesel fuel can increase nickel content, engine oil – increase zinc content, while petrol – decrease zinc content in leaves, which also corresponds to the results of our experiment. Furthermore, Nwachi et al [19] showed that petroleum-derived substances cause an increase in lead content in the leaves of *Vernonia amygdalina*, *Talinum triangulare*, *Manihot esculenta* i *Xanthoxoma sagittifolium*. Many authors emphasize that the petroleum-derived substances contribute to the increase of heavy metals level in the soil [20–22], which may also explain the increase of their content in plant organs.

Available scientific literature provides scarce information about the effect of supported bioremediation on the content of nutrients and heavy metals in plants growing in soil contaminated with petroleum-derived substances. Nanekar et al [23] showed that adding an extra microorganisms (bioaugmentation) to the soil contaminated with petroleum-derived substances decreased the amount of total petroleum hydrocarbons in the soil, and also resulted in lowering lead content while increasing manganese content. In the present experiment, the application of ZB-01 biopreparation on the soil contaminated with both used engine oil and petrol decreased the lead content in winter wheat straw, and for all analysed objects caused an increase in manganese content in some parts of plant. Rusin et al [10] also showed that the use of biopreparation ZB-01 on soil contaminated with petrol contribute to the decline in lead content and most often to increase in manganese content in the leaves of broad bean. Microorganisms are often used for the purification of soil contaminated with petroleum-derived substances, which is associated with their ability to adapt to adverse conditions and the use of harmful compounds for their growth and development, which increases the rate of decomposition [12, 13].

Wyszowski and Ziolkowska [16] demonstrated that the addition of compost, bentonite and calcium oxide to soil contaminated with engine oil and petrol modifies the content of nutrients in plants. All substances introduced into the soil most often contributed to increase in calcium and magnesium contents in spring oilseed rape,

however, the bentonite may cause a decrease in calcium and magnesium contents, while calcium oxide – calcium content increase, but also decline in magnesium content in oats. Compost most often contributed to the increase in magnesium content in yellow lupine and an increase in calcium content in maize [17]. In the present experiment the effect of ZB-01 biopreparation was also variable and resulted both an increase and a decrease in the content of selected nutrients, which was dependent on the type of xenobiotic, and on the analyzed part of plant. Many authors emphasize that biostimulation of the soil and its proper aeration are determining factors in improving the soil purification from petroleum-derived substances [24, 25]. Moreover composted municipal organic wastes cause a decrease in content and phytotoxicity of petroleum hydrocarbons by up to 80% [26]. The addition of organic substances into the soil contaminated with other substances (*eg* heavy metals) may contribute to the increase in nutrient content in winter wheat grain [27].

Conclusions

1. All used petroleum-derived substances, most often, contributed to a significant reduction in selected nutrients content in the grain of winter wheat. In other plants' organs the nutrient content due to the presence of petroleum-derived substances in the soil was variable and depended on the type of the compound and on the analysed part of plant. Diesel fuel caused an increase in calcium content in the straw, and iron and magnesium contents in the roots, petrol – a decrease in calcium and magnesium contents in the straw and in the roots, but also an increase in the potassium content in the roots, while engine oil – a decrease in iron content in the roots. Moreover all used substances led to the increase in iron content in the straw of analysed plants.

2. The effect of petroleum-derived substances on the content of heavy metals in plants was also variable. Engine oil and diesel fuel caused an increase in the contents of cadmium, lead, zinc and manganese in the roots and an increase in the cadmium content in grain and nickel in straw but also led to a reduction in copper content in the roots. Petrol contributed to the increase in cadmium content in the grain and lead in the straw, but also to a decline in the zinc content in the grain and straw, and manganese in the straw.

3. Application of ZB-01 biopreparation on soil contaminated with engine oil, most often, caused an increase in content of the analysed nutrients in the roots of plants, but also their decline in the straw. In the case of soil contaminated with diesel oil biopreparation, most often, caused a decrease in their content in both straw and roots, in the case of soil contaminated with petrol – a decrease in calcium content in the grain, the decline in iron content in the roots and straw, but also an increase in calcium content in the grain and magnesium in the straw, while in control - a decrease in calcium content in the grain and straw, as well as iron in the grain and roots.

4. ZB-01 biopreparation usually had no significant effect on the content of heavy metals in plants, but most often affect an increase in the manganese content in all plant organs. In the case of other heavy metals biopreparation effect was also dependent on the type of metal and the analysed part of the plant.

Acknowledgements

The work was financed from designated subsidy to conduct research, development work and related tasks, contributing to the development of young scientists and University of Agriculture PhD students financed under competition procedure in 2015. No topic 4172.

References

- [1] Pala DM, de Carvalho DD, Pinto JC, Sant'Anna Jr GL. A suitable model to describe bioremediation of a petroleum-contaminated soil. *Int Biodeterior Biodegrad.* 2006;58(3-4):254-260. DOI: 10.1016/j.ibiod.2006.06.026.
- [2] Ayotamuno JM, Kogbara RB, Egwunem PN. A comparison of corn and elephant grass in the phytoremediation of a petroleum hydrocarbon polluted agricultural soil in Port Harcourt, Nigeria. *J Food Agric Environ.* 2006;4(3-4):216-222. https://www.researchgate.net/profile/Reginald_Kogbara2/publication/244995687_A_Comparison_of_Corn_and_Elephant_Grass_in_the_Phytoremediation_of_a_Petroleum-Hydrocarbon_Contaminated_Agricultural_Soil_in_PortHarcourt/links/0c96053567529627b8000000.pdf.
- [3] Das N, Chandran P. Microbial degradation of petroleum hydrocarbon contaminants: an overview. *Biotechnol Res Int.* 2011;1:1-13. DOI: 10.4061/2011/941810.
- [4] Jahangeer A, Kumar V. An overview on microbial degradation of petroleum hydrocarbon contaminants. *Int J Eng Techn Res.* 2013;1(8):34-37. https://www.erpublication.org/admin/vol_issue1/upload%20Image/IJETR011822.pdf.
- [5] Caravaca F, Rodán A. Assessing changes in physical and biological properties in soil contaminated by oil sludges under semiarid Mediterranean conditions. *Geoderma.* 2003;117:53-61. DOI: 10.1016/s0016-7061(03)00118-6.
- [6] Labud V, Garcia C, Hernandez T. Effect of hydrocarbon pollution on the microbial properties of a sandy and a clay soil. *Chemosphere.* 2007;66(10):1863-1871. DOI: 10.1016/j.chemosphere.2006.08.021.
- [7] Wyszowski M, Wyszowska J, Ziółkowska A. Effect of soil contamination with diesel oil on yellow lupine yield and macroelements content. *Plant Soil Environ.* 2004;50(5):218-226. <http://www.agriculturejournals.cz/publicFiles/52751.pdf>.
- [8] Wyszowski M, Wyszowska J. Effect of enzymatic activity of diesel oil contaminated soil on the chemical composition of oat (*Avena sativa* L.) and maize (*Zea mays* L.). *Plant Soil Environ.* 2005;51(8):360-367. <http://www.agriculturejournals.cz/publicFiles/50994.pdf>.
- [9] Iturbe R, Flores C, Castro A, Torres LG. Sub-soil contamination due to oil spills in zones surrounding oil pipeline-pump stations and oil pipeline right-of-ways in Southwest-Mexico. *Environ Monit Assess.* 2007;133(1-3):387-398. DOI: 10.1007/s10661-006-9593-y.
- [10] Rusin M, Gospodarek J, Nadgórska-Socha A. The effect of petroleum-derived substances on the growth and chemical composition of *Vicia faba* L. *Pol J Environ Stud.* 2015;24(5):2157-2166. DOI: 10.15244/pjoes/41378.
- [11] Dindar E, Şağban FOT, Başkaya H.S. Bioremediation of petroleum contaminated soil. *J Biol Environ Sci.* 2013;7(19):39-47. <http://jbes.uludag.edu.tr/PDFDOSYALAR/19/mak06.pdf>.
- [12] Haritash AK, Kaushik CP. Biodegradation aspects of Polycyclic Aromatic Hydrocarbons (PAHs): A review. *J Hazard Mater.* 2009;169(1-3):1-15. DOI: 10.1016/j.jhazmat.2009.03.137.
- [13] Milić JS, Beškoski VP, Ilić MV, Ali SAM, Gojgić-Cvijović GĐ, Vrvic MM. Bioremediation of soil heavily contaminated with crude oil and its products: composition of the microbial consortium. *J Serb Chem Soc.* 2009;74(4):455-460. DOI: 10.2298/jsc0904455m.
- [14] Azcue J, Murdoch A. Comparison of different washing, ashing, and digestion methods for the analysis of trace elements in vegetation. *Int J Environ Anal Chem.* 1994;57:151-162. DOI: 10.1080/03067319408027420.
- [15] Nadgórska-Socha A, Kafel A, Kandziora-Ciupa M, Gospodarek J, Zawisza-Raszka A. Accumulation of heavy metals and antioxidant responses in *Vicia faba* plants grown on monometallic contaminated soil. *Environ Sci Pollut Res.* 2013;20(2):1124-1134. DOI: 10.1007/s11356-012-1191-7.
- [16] Wyszowski M, Ziółkowska A. Effect of compost, bentonite and calcium oxide on content of some macroelements in plants from soil contaminated by petrol and diesel oil. *J Elem.* 2009;14(2):405-418. DOI: 10.5601/jelem.2009.14.2.21.

- [17] Wyszowski M, Ziółkowska A. Role of compost, bentonite and calcium oxide in restricting the effect of soil contamination with petrol and diesel oil on plants. *Chemosphere*. 2009;74(6):860-865. DOI: 10.1016/j.chemosphere.2008.10.035.
- [18] Osuagwu AN, Okigbo AU, Ekpo IA, Chukwurah PN, Agbor RB. Effect of crude oil pollution on growth parameters, chlorophyll content and bulbils yield in air potato (*Dioscorea bulbifera* L.). *Int J Appl Sci Technol*. 2013;3(4):37-42. http://www.ijastnet.com/journals/Vol_3_No_4_April_2013/4.pdf.
- [19] Nwaichi EO, Wegwu MO, Nwosu UL. Distribution of selected carcinogenic hydrocarbon and heavy metals in an oil-polluted agriculture zone. *Environ Monit Assess*. 2014;186(12):8697-8706. DOI: 10.1007/s10661-014-4037-6.
- [20] Okonokhua BO, Ikhajiagbe B, Anoliefo GO, Emende TO. The effects of spent engine oil on soil properties and growth of maize (*Zea mays* L.). *J Appl Sci Environ Manage*. 2007;11(3):147-152. DOI: 10.4314/jasem.v11i3.55162.
- [21] Santos-Echeandia J, Prego R, Cobelo-Garcia A. Influence of the heavy fuel spill from the Prestige tanker wreckage in the overlying seawater column levels of copper, nickel and vanadium (NE Atlantic ocean). *J Marine Syst*. 2008;72:350-357. DOI: 10.1016/j.jmarsys.2006.12.005.
- [22] Ujowundu CO, Kalu FN, Nwaoguikpe RN, Kalu OI, Ihejirika CE, Nwosunjoku EC, Okechukwu RI. Biochemical and physical characterization of diesel petroleum contaminated soil in southeastern Nigeria. *Res J Chem Sci*. 2011;1(8):57-62. <http://www.isca.in/rjcs/Archives/v1/i8/ISCA-RJCS-2011-184-10.pdf>.
- [23] Nanekar S, Dhote M, Kashyap S, Singh SK, Juwarkar AA. Microbe assisted phytoremediation of oil sludge and role of amendments: a mesocosm study. *Int J Environ Sci Technol*. 2015;12:193-202. DOI: 10.1007/s13762-013-0400-3.
- [24] Kauppi S, Sinkkonen A, Romantschuk M. Enhancing bioremediation of diesel-fuel-contaminated soil in a boreal climate: Comparison of biostimulation and bioaugmentation. *Int Biodeterior Biodegrad*. 2011;65:359-368. DOI: 10.1016/j.ibiod.2010.10.011.
- [25] Megharaj M, Ramakrishnan B, Venkateswarlu K, Sethunathan N, Naidu R. Bioremediation approaches for organic pollutants: A critical perspective. *Environ Int*. 2011;37:1362-1375. DOI: 10.1016/j.envint.2011.06.003.
- [26] Adekunle IM. Bioremediation of soils contaminated with Nigerian petroleum products using composted municipal wastes. *Biorem J*. 2011;15(4):230-241. DOI: 10.1080/10889868.2011.624137.
- [27] Leszczyńska D, Kwiatkowska-Malina J. The influence of organic matter on yield and quality of winter wheat *Triticum aestivum* spp. vulgare (L.) cultivated on soils contaminated with heavy metals. *Ecol Chem Eng S*. 2014;20(4):701-708. DOI: 10.2478/eces-2013-0048.

WPLYW SUBSTANCJI ROPOPOCHODNYCH NA SKŁD CHEMICZNY PSZENICY OZIMEJ

¹ Katedra Ochrony Środowiska Rolniczego
Uniwersytet Rolniczy im. Hugona Kołłątaja, Kraków

² Katedra Ekologii
Uniwersytet Śląski, Katowice

Abstrakt: Celem przeprowadzonych badań było określenie oddziaływania benzyny, przetworzonego oleju silnikowego i oleju napędowego na zawartość wapnia, magnezu, żelaza i potasu oraz wybranych metali ciężkich w ziarnie, słomie i korzeniach pszenicy ozimej. Dodatkowo określono oddziaływanie procesu bioremediacji na wyżej wymienione cechy. Doświadczenie zostało przeprowadzone w 2014 r. na obszarze Stacji Doświadczalnej Uniwersytetu Rolniczego w Mydlnikach, położonych niedaleko Krakowa. Jest to obszar, który w czerwcu 2010 r. został sztucznie zanieczyszczony substancjami ropopochodnymi w ilości 6000 mg na kg s m. gleby. Połowa z obiektów została poddana procesowi bioremediacji z użyciem preparatu ZB-01. Ocena zawartości składników pokarmowych w liściach roślin została przeprowadzona przy użyciu metody płomieniowej absorpcji atomowej. Na podstawie przeprowadzonych badań stwierdzono, że wszystkie zastosowane substancje ropopochodne najczęściej przyczyniały się do spadku zawartości wybranych składników pokarmowych w ziarnie pszenicy ozimej. W pozostałych organach roślinnych zawartość składników pokarmowych, jak również metali ciężkich spowodowana obecnością ropopochodnych w glebie była zmienna i zależała od rodzaju zastosowanego związku i od analizowanej części rośliny. Zastosowany

biopreparat ZB-01 na glebę zanieczyszczoną olejem silnikowym najczęściej powodował wzrost zawartości analizowanych składników pokarmowych w korzeniach roślin, ale także ich spadek w słomie, w pozostałych obiektach odnotowano zmienne zależności, najczęściej nie miał on jednak istotnego wpływu na zawartość metali ciężkich w roślinach.

Słowa kluczowe: substancje ropopochodne, bioremediacja, składniki pokarmowe, metale ciężkie, pszenica ozima

Karolina PETELA^{1*} and Andrzej SZŁĘK¹

ASSESSMENT OF PASSIVE COOLING IN RESIDENTIAL APPLICATION UNDER MODERATE CLIMATE CONDITIONS

OCENA MOŻLIWOŚCI STOSOWANIA PASYWNEGO CHŁODZENIA DO CELÓW DOMOWYCH W KLIMACIE UMIARKOWANYM

Abstract: In the face of environmental regulations, renewable energy systems are anticipated to become more attractive. Passive buildings may appear promising in terms of energy saving. The aim of the work is an investigation of energy effects of using radiative passive cooling. System analysed here bases on the radiative heat exchange with nocturnal sky. On every exposed surface, beyond the convection mechanism, a radiative heat exchange with the sky takes place. Analysis shows that passive cooling has a potential in cold production, however is sensitive to ambient conditions and that cold supply is inversely proportional to demands. Small value of average heat loss from the radiator makes the system independently unable to fulfil cooling demand, however may become an attractive, eco-friendly supplement to a conventional air-conditioner.

Keywords: passive cooling, nocturnal sky, solar collector, residential cooling

Introduction

The subject of limiting the use of non-renewable energy sources is still important, considering the continuous worldwide growth of electric energy usage and demand. One has to be aware of the tendency, that the use of electric energy increases in summer as well, which results from increasing use of air conditioning systems. Most commonly applied are compression chillers. However, in order to decrease the use of non-renewable energy, alternatives are needed. One of the possibilities is the application of commercially-spread sorption chillers. Their mode of operation is analogical to that of compression chiller, but the electric compressor is substituted by a colloquially named

¹ Faculty of Energy and Environmental Engineering, Institute of Thermal Technology, Silesian University of Technology, ul. Konarskiego 22, 44-100 Gliwice, Poland, phone: +48 32 237 10 31, +48 32 237 10 41, fax: +48 32 237 28 72, email: karolina.petela@polsl.pl, andrzej.szlek@polsl.pl

* Corresponding author: karolina.petela@polsl.pl

sorption compressor which comprises of absorber, generator driven by heat and a solution heat exchanger. Electric energy consumed by this type of system is used only to drive solution pumps inside the cycle. Nevertheless, to minimize the energy use by final consumers, passive architecture is becoming more and more popular and attractive. Those buildings are characterised by good insulating properties, installed systems of ventilation heat recuperation, use of internal gains and passive use of solar energy. Passive buildings are also equipped with cooling structures like ground heat exchanger or evaporative cooling. A system that is expected to have the potential of covering the cooling demand of an inhabitant is a device using the phenomenon of heat exchange with a radiating nocturnal sky. The idea proposed in this study is a theoretical investigation of possibilities of radiative cooling system application into a residential building in Nowy Sącz, Poland.

Radiative cooling phenomenon

Radiative cooling belongs to one of the heat dissipation techniques, where heat is transferred to a lower temperature sink. Radiative cooling exploits sky as the sink and the heat loss is conducted by long-wave radiation to the sky [1]. On every exposed surface, beyond the convection mechanism, a radiative heat exchange with the sky takes place. This phenomenon is most effective during night-time, when no solar gains appear and the nocturnal sky temperature as low as even -50°C . The efficiency of radiative cooling system is affected by cloud cover, wind and humidity of the air. That is the reason why those systems are most commonly installed in the desert climates, while the intensive ambient temperature drop in the night is additionally advantageous [2]. A scheme of heat exchange between a surface, ambient and nocturnal sky is presented in Fig. 1.

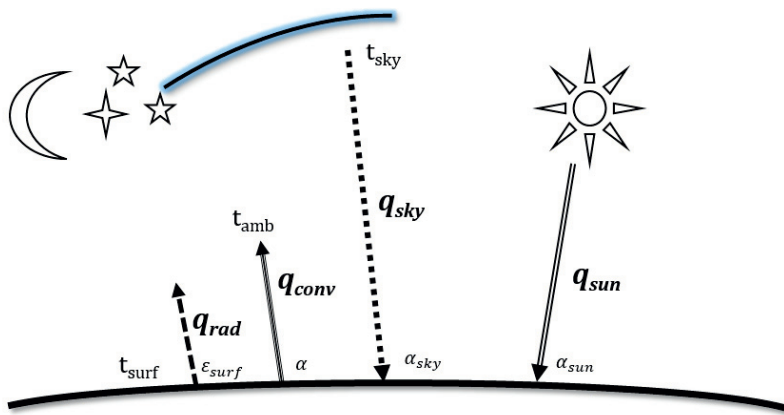


Fig. 1. Heat fluxes for a surface exposed to the sky; t_{surf} [$^{\circ}\text{C}$] – surface temperature, q_{rad} [W/m^2] – surface radiative heat flux, ϵ_{surf} – surface’s emissivity, q_{conv} [W/m^2] – convective heat flux, α [$\text{W}/(\text{m}^2\text{K})$] – convective heat transfer coefficient, q_{sky} [W/m^2] – sky radiative heat flux, α_{sky} – sky-absorptivity factor, t_{sky} [$^{\circ}\text{C}$] – radiative sky temperature, q_{sun} [W/m^2] – absorbed solar radiation heat flux rate, α_{sun} – solar-absorptivity factor

A heat loss from a surface that has been heated during the day will be higher, if the ambient temperature in the night is low. However, unlike the desert climate, the night-time temperature drop in the moderate climate locations does not occur in the hot few-days periods, with cooling demand. In the opposite, if the day is hot, it is highly probable, that the night will be warm as well. If the surface temperature of a radiator drops below the ambient temperature under those conditions, convection gains partially neutralize the radiant heat loss. This tendency is amplified with increasing wind speed. A parameter at which convective heat gains equal radiant heat loss is known as radiator's stagnation temperature [3]. To prevent the heat gains by a forced convection different types of wind screens have already been investigated. Predominantly discussed are: glazings transparent in the infra-red range or some open coverings (eg honeycomb-shaped) that limit the wind speed and general motion of the air above the radiator [3].

It is evidential in the available literature that the issues of radiative cooling were discussed already in 1980s [3]. Various types of radiators have been investigated since then. Erell and Etzion [4] analysed the prospects of using an unglazed flat plate solar collector for purposes of radiative cooling, while Dimoudi [5] performed an experimental study of performance on a roof component comprised of white painted pipes. Bagiorgas and Mihalakakou [1] proposed an experimental model of a roof radiator made of white painted folded aluminium tube used for space cooling in Greece. Farmahini-Farahani and Heidarinejad [6] used flat-plate radiators to pre-cool the air that was subsequently cooled in an evaporative cooling device. They assumed the presence of a water storage tank in the circuit, but Zhang and Niu [7] were to analyse the cooling performance of nocturnal radiative cooling combined with microencapsulated phase change material slurry storage. Al-Obaidi et al [8] reviewed the effect of using different paints and materials on radiative roof's operation.

The idea here proposed considers a performance analysis of a radiator in form of a flat plate collector with white painted pipes that is covering whole roof area of a residential building in moderate climate conditions.

Building under consideration

The radiative cooling system is expected to meet the cooling needs of a one-family detached house with four inhabitants. Construction of the building is assumed to be light-weight with insulated walls made of hollow brick. The building has two levels: ground floor and first floor. No basement or attic are considered. Ground floor is divided into 5 separate spaces: kitchen, bathroom, living room, office and hall. A staircase leads to the first floor, where 5 rooms are located: main bedroom, 2 children bedrooms, a bathroom and a wardrobe. Only the wardrobe is excluded from the group of cooled spaces. A scheme of house under consideration is presented in Fig. 2. Dimensions of every floor are 10×7 m. It is ideally assumed, that whole flat roof is covered with an unglazed flat plate collector playing the role of a passive radiator. The system is combined with a 3 m^3 storage tank.

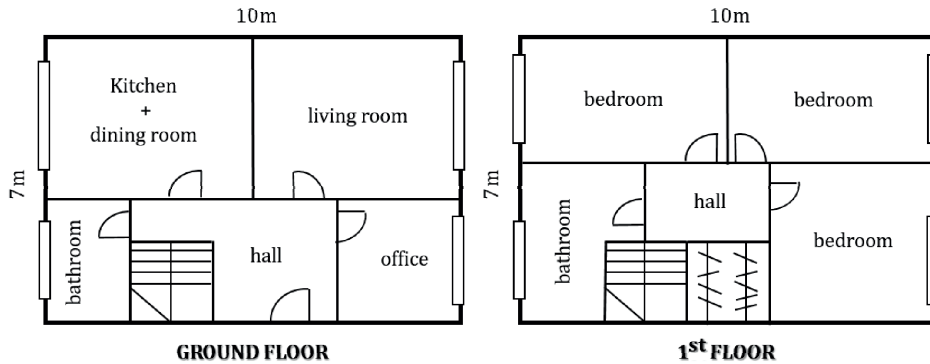


Fig. 2. A simplified scheme of rooms projection inside the project house

The project-building is situated in Nowy Sącz. It is a town located in southern Poland, in Lesser Poland Voivodship, and its coordinates are: $49^{\circ}37'26''\text{N } 20^{\circ}41'50''\text{E}$. Poland represents moderate climate conditions. However, being under eastern continental influences, summers tend to be hot. Consequently, more and more electric energy consumption in the summer results from installing the air conditioning systems. Nevertheless, it has to be emphasized that despite the occurrence of high daily temperatures, night temperature drop is not intense, cloud cover and air pollution appears regularly, which are the factors hindering an effective use of passive radiators.

Cooling demand calculation

For the purpose of this study, cooling demand was declared basing on a German standard VDI 2078, described in [9]. According to this norm cooling demand is amount of heat created by external and internal gains that should be removed from the space, to obtain steady state indoor temperature (26°C). To define the cooling demand, an energy balance has to be made. In Poland, residential buildings are air-conditioned only during summer, so the energy balance has been conducted for five typical cases of the months: May, June, July, August, and September. Each case reflects a simulation of an hour with the highest ambient temperature in the month. Meteorological data used for the calculations consider a typical meteorological year for station in Nowy Sącz [10].

Two types of heat gains are to be considered: external heat through walls, windows, doors etc., as well as internal heat gains from people, machines, lighting, and rooms' walls.

Before any kind of heat balance can be made, the partition properties have to be stated. All of partitions are projected to fulfil obligatory standards in terms of heat transfer coefficient. Table 1 presents types of partitions existing in project house.

Table 1

Heat transfer coefficients of the analyzed partitions

No.	Type of partition	Heat transfer coefficient [W/(m ² K)]
1	Outer wall	0.25
2	Inner wall	1
3	Floor on the ground	0.3
4	Ceiling	1
5	Roof	0.2
6	Window	1.3
7	Outer door	1.7
8	Inner door	5

While simulating a building with walls made of hollow brick, it is also ideally set, that it has a negligible thermal inertia. It means that heat transfer to the inner part of the room is not delayed by accumulative properties of the wall and enables to conduct calculations for real time ambient temperature.

Heat flux through walls and other opaque barriers depends on temperature difference and solar radiation – these phenomena have to be considered together, as solar radiation increases ambient temperature. It requires determination of an equivalent temperature difference $\Delta\vartheta_{eqv}$, taking into account the solar ambient temperature. Values of $\Delta\vartheta_{eqv}$ depends on hour of the day, wall’s orientation and building’s construction class. The values have been empirically determined and tabulated [9] for location ~50°N, ambient temperature $t_{amb} = 24.5^{\circ}\text{C}$ and inner temperature $t_{in} = 22^{\circ}\text{C}$. It imposes a need of a correction, if the conditions differ and is given as $\Delta\vartheta'_{eqv}$:

$$\Delta\vartheta'_{eqv} = \Delta\vartheta_{eqv} + (t_{amb} - 24.5) + (22 - t_{in}) \tag{1}$$

Heat gains through outer walls can be calculated then from equation (2):

$$\dot{Q}_w = k \cdot A \cdot \Delta\vartheta'_{eqv} \tag{2}$$

where k is the heat transfer coefficient [W/(m²K)], while A is the surface area of the wall [m²].

Convective heat gains through windows are determined by the following equation:

$$\dot{Q}_T = k \cdot A \cdot (t_{amb} - t_{in}) \tag{3}$$

Solar radiation heat gains through windows have to be defined separately by equation:

$$\dot{Q}_S = A \cdot I \cdot b \cdot S_a \tag{4}$$

where I is total irradiation on a given surface [W/m²], b is a window transmission coefficient assumed as $b = 0.75$.

S_a is a solar heat-accumulation coefficient which was empirically defined for a specific type of construction, wall's orientation and specific hour of the day [9].

Internal heat gains are a sum of human heat gain, lighting heat gain and electric devices heat gain. Human heat gains are calculated accordingly to determination of occupants residing in one room. It is specified that sensible heat gain from one person equals 70 W. Heat gains from electric lighting may be defined with the help of equation:

$$\dot{Q}_B = N \cdot A_{room} \cdot \varphi \cdot S_i \quad (5)$$

where N stands for the power of installed lighting [W/m^2], A_{room} is the surface area of one room [m^2], φ is the lighting's coincidence factor assumed as 0.7, while S_i is a lamp heat-accumulation coefficient. According to literature [9] S_i may be introduced as 0.63. Depending on the amount of working electric devices in the room, heat gains are calculated from the equation:

$$\dot{Q}_B = \sum_i N_{mach_i} \cdot \varphi_i \quad (6)$$

where N_{mach_i} is heat gain of every device [W] and φ_i is a device's coincidence factor. Values of these factors are taken from Table 2. According to the standard it is simplified and assumed that the heat gains from domestic devices occurs all the time with a constant coincidence factor.

Table 2
Heat gains and coincidence factor of domestic electric devices

Electric device	N_{mach_i} [W]	φ_i [-]
Computer	90	0.5
Screen	50	0.5
Printer	10	0.2
Oven	1500	0.2
Fridge	300	1
Electric kettle	250	0.2
Washing machine	1500	0.2

In order to choose a representative day, cooling demand was calculated for 5 cases: May 18th at 15:00, June 7th at 12:00, July 5th at 12:00, August 8th at 15:00 and September 6th at 12:00.

These hours were not selected randomly, as each represents the warmest hour of every month according to meteorological data. Calculated cooling demand fits within the range 4–6 kW. It is visible on a chart presented in Fig. 3.

Although July 5th at 12:00 is the warmest hour in the analysed group, cooling demand for this point is slightly lower than for June 7th, August 5th and September 6th. It may be clarified with the chart presented in Fig. 4.

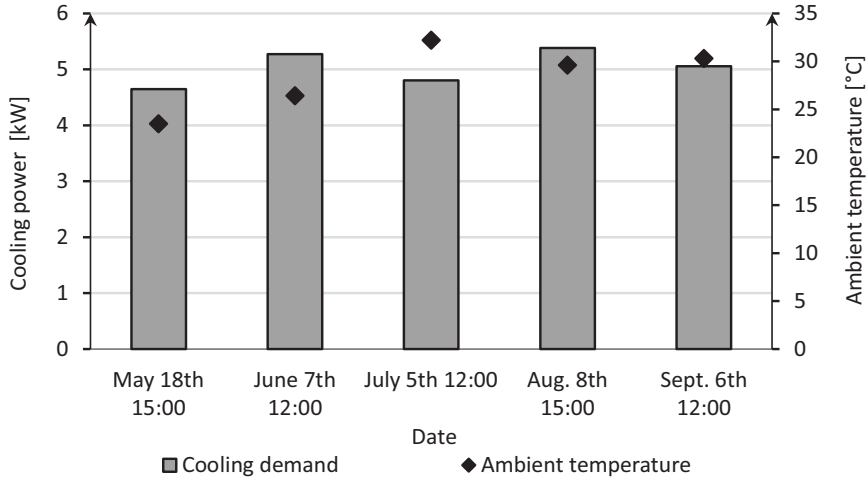


Fig. 3. Calculated cooling demand for each representative hour versus ambient temperature

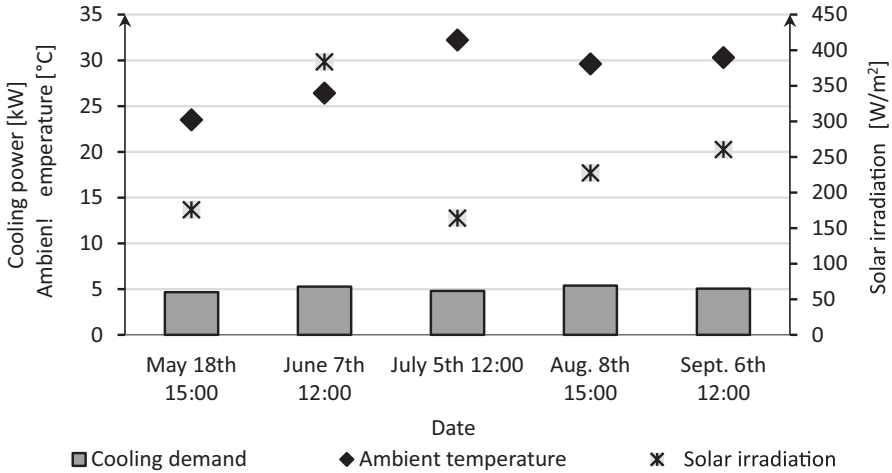


Fig. 4. Calculated cooling demand for each representative hour versus ambient temperature and solar irradiation on northern oriented vertical wall

It is evident that the solar irradiation on northern oriented walls, which represents a large part of the building’s gains is the lowest for the warmest hour, so the cooling demand may be smaller. However, value of northern solar irradiation on August 8th is lower than on June 7th and the cooling demands are higher. It arises from the difference of solar heat-accumulative coefficient for western walls at 15:00 and 12:00. On June 7th

at 12:00 $S_a = 0.17$, while already on August 8th at 15:00 $S_a = 0.53$. Even if the solar radiation on western walls is lower on August 8th at 15:00 (310.8 W/m^2) than on June 7th at 12:00 (436.48 W/m^2), the multiplication factor of accumulative coefficient is decisive. To omit any further ambiguity of this kind, it has been decided that the representative day will be July 5th as the hottest day of the year. Cooling power demand on July 5th at 12:00 equals 4.8 kW. Outdoor temperature is given as 32.2°C , while desired indoor temperature should be 26°C . It allows to calculate an indicator saying how much cooling power has to be delivered to chill one cubic meter of space by one Celsius degree. This indicator equals in the project case $2.11 \text{ W}/(\text{m}^3\text{K})$. Subsequently, cooling demand was determined for each hour between 7:00 and 19:00 on July 5th. This time range should correspond to the period when air-conditioning system is used. It was made, so that the amount of cooling energy needed for a whole day would be known. Following the VDI 2078 standard, the sum of cooling energy needed on July 5th equals 61.8 kWh. For an independent operation of passive cooling system, the value of daily cooling demand should be equal to the amount of cooling energy accumulated during the night activity. This study rests on evaluation of a night-radiator cooling possibilities to meet a daily cooling demand.

Application of radiative cooling system

To determine the possibilities of cooling power generation by heat transfer between passive radiator and radiating nocturnal sky, a heat balance has to be made. Meteorological data needed for the evaluation of the balance (ambient temperature – t_{amb} [$^\circ\text{C}$]; relative humidity – φ [%]; total solar irradiation – G [W/m^2], wind speed – w [m/s]; and wind direction) have been retrieved from meteorological data set for Nowy Sacz [10] for the night (21:00–6:00) preceding July 5th. Simulation was performed for various theoretical cloud cover conditions: for a clear sky and for 25%, 50%, 75%, and 100% of cloud cover. Passive radiator is an unglazed flat-plate collector having dimensions of the roof: $(10 \cdot 7) \text{ m}^2$. Collector is insulated from the roof and in a distance from other objects, no temperature drop according to the height of the roof has been considered. Collector's pipes are made of copper and covered with white paint of a low solar absorptivity factor. To calculate the convective heat transfer coefficient (α [$\text{W}/(\text{m}^2\text{K})$]), the collector is simulated as a flat surface. The night heat balance was conducted in a time step mode, assuming an hourly change of collector's surface temperature.

A heat flux from the surface of collector (\dot{q}_{loss} [W/m^2]) is described by equation:

$$\dot{q}_{loss} = \dot{q}_{conv} + \dot{q}_{sky_{rad}} - \dot{q}_{sun} \quad (7)$$

It takes into consideration convective loss (\dot{q}_{conv}), radiative loss from the surface (\dot{q}_{rad}), nocturnal sky radiative heat gains ($\dot{q}_{sky_{rad}}$), and solar radiation heat gains after sunrise (\dot{q}_{sun}).

Convective heat flux can be calculated from:

$$\dot{q}_{conv} = \alpha (t_{surf} - t_{amb}) \quad (8)$$

where t_{surf} [$^\circ\text{C}$] stands for surface temperature.

To simplify the calculations, during the simulation each hour represents a separate steady state. Surface temperature in the first hour of the calculation is equal to ambient temperature (21.4°C). An independent discussion could consider the evaluation of convective heat transfer coefficient. Various empirically obtained function for α are available in the literature, while the most common is the approach of Clark and Berdahl [5], where α depends only on the wind speed (w), and is equal to 3.5 W/m²K if $w < 1$ m/s, while if $w = 1-5$ m/s then $\alpha = 2.8 + 0.76 w$. Since in this study radiator is simplified to a flat surface of given dimension, convective heat transfer coefficient was calculated basing on determination of criterial numbers: Nusselt, Rayleigh or Reynolds for a parallel flow over flat plates, according to functions available in [11]. Coefficient α depends then on ambient temperature, surface temperature, wind speed and collector's dimensions.

Radiative heat flux from collector's surface is given by equation:

$$\dot{q}_{rad} = \varepsilon_{surf} \cdot \sigma \cdot T_{surf}^4 \quad (9)$$

where ε_{surf} is the surface emissivity and for a white paint equals 0.93 [12], while

$$\sigma = 5.67 \cdot 10^{-8} \frac{\text{W}}{\text{m}^2 \text{K}^4}$$

is the Stefan-Boltzmann constant.

The amount of sky radiation absorbed by the surface can be calculated using equation:

$$\dot{q}_{skyrad} = \alpha_{sky} \cdot \sigma \cdot T_{sky}^4 \quad (10)$$

Since the temperature of the source-sky is of the same order as surface temperature, it is assumed that sky radiation absorptivity equals surface emissivity. Sky temperature T_{sky} [K] can be found in the meteorological data set, but since the cloud cover conditions are not stated, it was calculated basing on an empirical function available in [4], presented in equation:

$$T_{sky} = \varepsilon_{sky}^{0.25} \cdot T_{amb} \quad (11)$$

It allowed to perform an individual investigation of cloud effect on passive system performance.

Sky emissivity (ε_{sky}) was a subject of many researches [13] and is an empirical function depending on air humidity. It was calculated from equation [4]:

$$\varepsilon_{sky} = 0.006 \cdot t_{dp} + 0.74 \quad (12)$$

Dew point temperature, t_{dp} , is a saturation temperature for vapour partial pressure.

Sky radiation heat gains may be increased by a cloudiness factor C , being an empirical function of cloudiness indicator, where $n = 0$ stands for a cloudless sky, and $n = 10$ for overcast sky [5]. Heat gains can be then obtained from following equation:

$$\dot{q}_{sky,rad} = C \cdot \varepsilon_{surf} \cdot \sigma \cdot \varepsilon_{sky} \cdot T_{amb}^4 \quad (13)$$

$$C = 1 + 0.0224 \cdot n - 0.0035 \cdot n^2 + 0.00028 \cdot n^3 \quad (14)$$

It is possible that around morning hours the surface of the collector will be heated by incoming solar radiation. Heat absorbed by the collector is evaluated with the use of equation (15). Solar absorptivity of the white paint equals $\alpha_{sun} = 0.2$:

$$\dot{q}_{sun} = \alpha_{sun} \cdot G \quad (15)$$

It is assumed that under hourly change of ambient conditions, the surface temperature of the collector is changing through heat transfer between collector's surface and nocturnal sky. More accurate calculations would need applying CFD calculations which are not a part of this paper. Therefore, some assumption had to be made connecting the surface temperature and storage tank installed. It is ideally assumed, that the heat lost from the surface during one hour at its initial temperature is equal to the change of internal energy (ΔE_u) of the storage tank, as shown in the equations below. It affects the change of the fluid at outlet of the tank. Since it is also assumed, that the heat transfer fluid flows very quickly in the radiator pipes, surface temperature after one hour of heat exchange equals the storage tank outlet temperature. It can be then an initial value for next hour of heat balance:

$$E_1 = \Delta E_u + E_2 \quad (16)$$

$$E_1 = Q_{loss} + E_2 \quad (17)$$

$$\rho \cdot V \cdot C_p \cdot t_1 = A_{surf} \cdot \dot{q}_{loss} \cdot \tau + \rho \cdot V \cdot C_p \cdot t_2 \quad (18)$$

where: ρ – density [kg/m^3]; V – tank volume [m^3]; C_p – specific heat of storage fluid [$\text{J}/(\text{kgK})$]; t_1 and t_2 fluid temperatures at the inlet and outlet of the tank, respectively.

If the project building was equipped with a solar absorption chiller, the installed storage tank capacity could be chosen according to the ratios available in [14], equal to 40 dm^3 per 1 m^2 of solar collector. It has been decided, that the radiative passive system will be connected with a 3 m^3 storage tank with cold water as a storage fluid.

Results of the radiative cooling simulation

The simulation proposed in this study enabled to define heat loss rate from the passive collector for every hour of the night. According to the foregoing calculation path and taking into account above-mentioned assumptions, a group of results has been obtained. Fig. 5 shows how the hourly heat loss profile could look like, if the sky was clear. The chart present a unit heat loss rate for 1 m^2 of radiator.

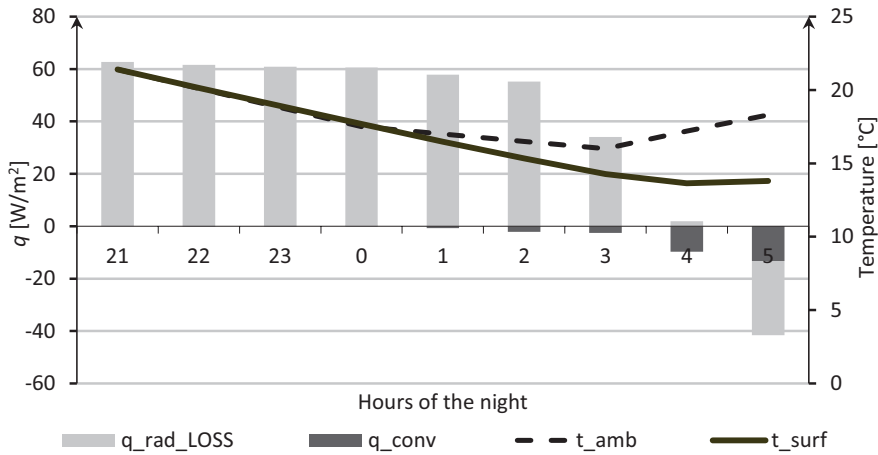


Fig. 5. A chart presenting the heat loss rate from the collector's surface in comparison with its temperature and ambient temperature

The value of presented q_{rad_LOSS} equals radiative heat loss from the surface of collector after subtraction of nocturnal sky radiative gains and solar heat gains occurring at dawn. It is evident that by losing around $60 W/m^2$ of heat, the surface temperature may fall well below the ambient temperature. If the night temperature drop was bigger, the heat loss rate could be much higher, what speaks against application of radiative cooling system in moderate climate. Together with the decrease below outdoor temperature, convective heat gains have to increase. The heat loss from the surface drops dynamically at 3:00. If not for the solar heat gains, the heat loss rate would decrease much slower. At 3:00 solar heat gain rate equals $19.1 W/m^2$, while at 4:00 and at 5:00 already $42.1 W/m^2$ and $67.92 W/m^2$, respectively. Cooling power for every hour of the passive radiator operation can be obtained by multiplication of unit heat loss rate \dot{q}_{loss} and surface of collector ($A_{surf} = 70 m^2$), results are presented in Table 3.

Table 3

Heat loss rates from the total surface of the passive collector

Hour	21:00	22:00	23:00	00:00	1:00	2:00	3:00	4:00	5:00
Heat loss rate [kW]	4.390	4.311	4.264	4.242	3.995	3.715	2.210	-0.540	-2.908

Calculated heat loss implies temperature drop inside the ideally assumed chilled water storage tank. If the cooling power generated by the passive radiator could be accumulated in a form of chilled water inside the ideally insulated storage tank, the sum of accumulated cooling energy, by losing heat from collector's surface, would equal 23.68 kWh. To compare the values, the afore-mentioned cooling energy demand of the project building should equal 61.8 kWh. By the assumption of an average cooling power demand of 5 kW, the storage tank would be unloaded already after 4 hours and

44 minutes. Main conclusions coming from this comparison is that passive cooling is not sufficient for covering cooling demands in whole extent and system should be assisted for instance by compression chiller.

Second analysis concerns the impact of cloud cover on the performance of a radiative cooling system. According to equation (13) and (14), 4 stages of cloudiness have been analysed: 25%, 50%, 75% and 100%. A chart presented in Fig. 6. shows, how the heat loss rate changes with the increase of cloud cover indicator.

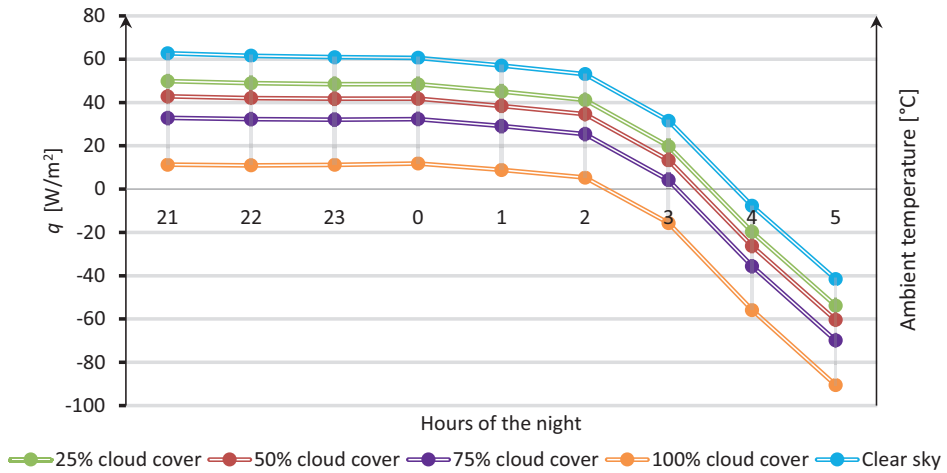


Fig. 6. Chart of a unit heat loss rate's profile during the night (July 4th/5th) under different cloud cover conditions

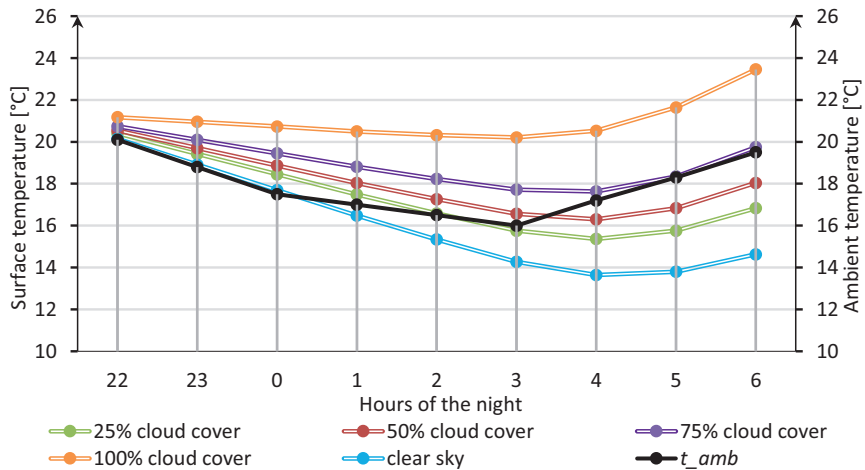


Fig. 7. Chart of the surface temperature change profile during the night (July 4th/5th) under different cloud cover conditions versus ambient temperature

It is visible that clouds are a factor which increases the sky radiation heat gains leading to the decrease of total unit heat loss rate from the surface. Additionally, theoretical change of surface temperature under the same cloud cover variation is shown in Fig. 7.

If the sky is overcast, or covered with clouds in 75%, the surface temperature would never fall below the ambient temperature. It is clear, that operating a radiative system under those conditions can be only efficient if ambient temperature at night is low (eg 10°C), while the following day is expected to be hot (eg 30°C). However, as mentioned before, this tendency is more typical for tropical and subtropical climates rather than for moderate climate locations.

It is valuable to compare the daily cooling energy demand and nightly passive cooling energy supply for the above discussed dates. Those values are presented in Fig. 8.

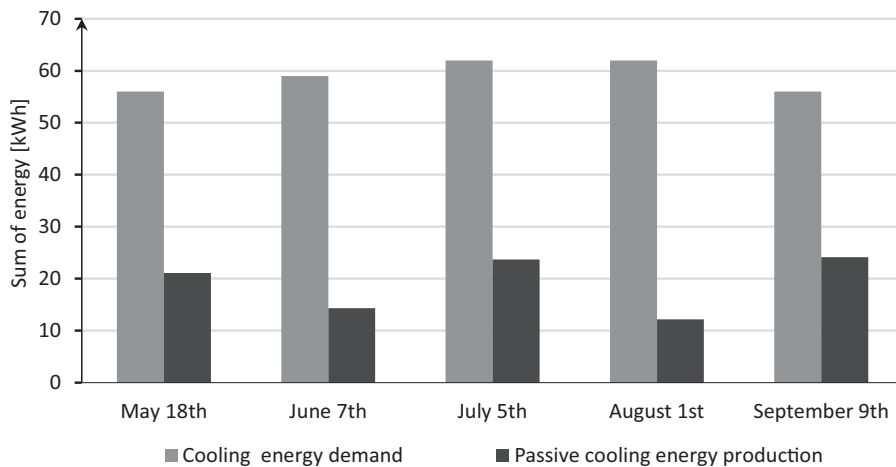


Fig. 8. Daily cooling energy demand and nightly cooling energy supply for given days

The chosen five days are the hottest of each month. Consequently, it influences the cooling energy demand and causes its value similar. However, solar heat gain is the highest for July and August, what results in the supreme cooling energy demand for these days. It could be suspected that the increment of average night temperature has a direct impact on the decrease of heat loss from surface. It is evident while comparing the cooling energy supply on colder nights of May and September with the cooling energy production on slightly warmer nights of June and August, as the nocturnal sky temperature is the lowest in this case in May and September. However, the example of night in July shows, that summer nights may have higher cooling energy supply under specific conditions. It is strictly bound with the surface initial temperature. For the night of July 4th/5th, according to the meteorological data, initial temperature was relatively high (21.4°C) resulting in high radiative heat loss from the surface, while nocturnal sky heat gain was comparable to other nights'. The gradual decrease of surface temperature shown in Fig. 5. enables to maintain a positive value of convective heat loss till

midnight. The initial surface temperatures at 21:00 on June 6th and August 1st are 15.5°C and 16.5°C, respectively. Already after one hour of radiator's operation, surface temperature falls below ambient temperature and the convective heat gains begin to increase, leading to stagnation. It proves the positive effects of desert climate. Surfaces warmed during the day accumulate part of heat and are able to lose more heat through radiation on a cold night. Therefore, the initial temperature of surface in simulation should take into account the fact of being heated during the day. Even more reasonable could be a 24-hours-simulation of change of surface temperature. Moreover, from a thermo-economic point of view, the investigation should be supplemented by the analysis of the cooling quality of temperature level at which heat is lost from the surface.

Conclusions

A theoretical analysis of possibilities, that installing a radiative cooling system into a residential building under moderate climate may bring, has been conducted. Cooling power demand of a project house on July 5th at 12:00 was defined as 4.8 kW, while total cooling energy foreseen for this day equaled 61.8 kWh. A passive flat plate collector installed on the 70 m² flat roof can generate a heat loss rate close to 60 W/m² during the night, if no clouds on the sky appear, and almost no wind occurs. It means a 4.2 kW heat loss from the whole surface of the radiator. Whole night of exploitation may bring a theoretical value of 23 kWh of cold accumulated in chilled water. If the storage tank had to be unloaded, it would be sufficient for 4.5 hours of utilization. Furthermore, if the sky was partially covered with clouds or overcast, the heat loss rate would gradually decrease, preventing the use of nocturnal radiator. It is visible, that even under idealised conditions, a radiative nocturnal cooling system is not sufficient to fulfil a daily cooling demand rate under moderate climate conditions for the project building. Nevertheless, it might be considered as an attractive, eco-friendly supplement to a conventional air-conditioner, what could require further investigation. It is worth mentioning, that in systems, where domestic hot water is generated by solar collectors, installation of a passive radiator would not be an obstacle, as it can be located on the northern roof slope. Application of nocturnal radiative cooling systems is believed to be more sensible in spaces, where the cooling power could be consumed simultaneously, like server rooms. Moreover, it could support food preservation processes, or the operation of cold stores leading to limitation of non-renewable energy consumption in the agricultural industry.

Acknowledgements

This research has been supported by the statutory research funds of the Faculty of Power and Environmental Engineering of the Silesian University of Technology.

References

- [1] Bagiorgas HS, Mihalakakou G. Experimental and theoretical investigation of a nocturnal radiator for space cooling. *Renew Energy*. 2008;33:1220-1227. DOI:10.1016/j.renene.2007.04.015.

- [2] Al-Nimr M, Tahat M, Al-Rashdan M. Night cold storage system enhanced by radiative cooling – a modified Australian cooling system. *Appl Therm Eng.* 1999;19:1013-1026. DOI:10.1016/S1359-4311(98)00103-3.
- [3] Santamouris M. *Advances in Passive Cooling.* New York: Earthscan publishing; 2007.
- [4] Erell E, Etzion Y. Radiative cooling of buildings with flat-plate solar collectors. *Build Environ.* 2000;35:297-305. DOI:10.1016/S0360-1323(99)00019-0.
- [5] Dimoudi A, Androutsopoulos A. The cooling performance of a radiator based roof component. *Sol Energy.* 2006;80:1039-1047. DOI:10.1016/j.solener.2005.06.017.
- [6] Farmahini-Farahani M, Heidarinejad G. Increasing effectiveness of evaporative cooling by pre-cooling using nocturnally stored water, *Appl Therm Eng.* 2012;38:117-123. DOI:10.1016/j.applthermaleng.2012.01.023.
- [7] Zhang S, Niu J. Cooling performance of nocturnal radiative cooling combined with microencapsulated phase change material (MPCM) slurry storage. *Energ Buildings.* 2012;54:122-130. DOI:10.1016/j.enbuild.2012.07.041.
- [8] Al-Obaidi K, Ismail M, Abdul Rahman A. M. Passive cooling techniques through reflective and radiative roofs in tropical houses in Southeast Asia: A literature review. *Frontiers Architectural Res.* 2014;3:283-297. DOI:10.1016/j.foar.2014.06.002.
- [9] Recknagel H. *Handbook for Heating and Air Conditioning Technology.* Wroclaw. Omni Scala publishing. 2008.
- [10] Meteorological data file for Nowy Sącz, available at: http://www.mir.gov.pl/budownictwo/rynek_budowlany_i_technika/Efektywnosc_energetyczna_budynkow/typowe_lata_meteorologiczne/ Strony/start.aspx.
- [11] Cengel YA. *Heat Transfer: A Practical Approach.* New York: McGraw-Hill publishing; 2002;373:468.
- [12] Solar absorptivity data tables. [Http://www.solarmirror.com/fom/fom-serve/cache/43.html](http://www.solarmirror.com/fom/fom-serve/cache/43.html).
- [13] Chen B, Kasher J, Maloney J, Girgis G. A, Clark D. Determination of the clear sky emissivity for use in cool storage roof and roof pond applications. *Proc ASES Annual Meeting.* 1991;1-5. http://www.ceen.unomaha.edu/solar/documents/SOL_26.pdf [accessed 05.03.2015].
- [14] Molero-Villar N, Cejudo-Lopez JM, Dominguez-Munoz F, Carrillo-Andres A. A comparison of solar absorption system configurations. *Sol Energy.* 2012;86:242-252. DOI:10.1016/j.solener.2011.09.

OCENA MOŻLIWOŚCI STOSOWANIA PASYWNEGO CHŁODZENIA DO CELÓW DOMOWYCH W KLIMACIE UMIARKOWANYM

Instytut Techniki Ciepłej, Wydział Inżynierii Środowiska i Energetyki Politechniki Śląskiej
Politechnika Śląska, Gliwice

Abstrakt: Wobec wymagań środowiskowych systemy wykorzystujące odnawialne źródła energii są coraz częściej stosowane i wdrażane również do rozwiązań budownictwa pasywnego. Celem pracy jest analiza efektów energetycznych wykorzystania pasywnego chłodzenia w budynku mieszkalnym. Podmiotem pracy jest system opierający swoje działanie na promienistej wymianie ciepła z nocnym nieboskłonem. Na powierzchni każdego ciała wyeksponowanej ku niebu, oprócz konwekcyjnej wymiany ciepła, odbywa się również radiacyjna wymiana ciepła z nieboskłonem. Analiza ukazuje potencjał chłodzenia pasywnego tego typu w produkcji chłodu, jednakże wskazuje na silną zależność systemu od warunków otoczenia oraz na fakt, że podaż chłodu jest odwrotnie proporcjonalna do zapotrzebowania. Niskie wartości strumieni strat ciepła z pasywnego radiatora sprawiają, że system nie może stanowić samodzielnego źródła produkcji chłodu, jednak może stać się atrakcyjnym, przyjaznym środowisku dodatkiem do konwencjonalnego układu klimatyzacyjnego.

Słowa kluczowe: chłodzenie pasywne, nocny nieboskłon, kolektor słoneczny, chłodzenie radiacyjne

Karolina PETELA^{1*} and Andrzej SZŁĘK¹

ASSESSMENT OF PASSIVE COOLING IN RESIDENTIAL APPLICATION UNDER MODERATE CLIMATE CONDITIONS

OCENA MOŻLIWOŚCI STOSOWANIA PASYWNEGO CHŁODZENIA DO CELÓW DOMOWYCH W KLIMACIE UMIARKOWANYM

Abstract: In the face of environmental regulations, renewable energy systems are anticipated to become more attractive. Passive buildings may appear promising in terms of energy saving. The aim of the work is an investigation of energy effects of using radiative passive cooling. System analysed here bases on the radiative heat exchange with nocturnal sky. On every exposed surface, beyond the convection mechanism, a radiative heat exchange with the sky takes place. Analysis shows that passive cooling has a potential in cold production, however is sensitive to ambient conditions and that cold supply is inversely proportional to demands. Small value of average heat loss from the radiator makes the system independently unable to fulfil cooling demand, however may become an attractive, eco-friendly supplement to a conventional air-conditioner.

Keywords: passive cooling, nocturnal sky, solar collector, residential cooling

Introduction

The subject of limiting the use of non-renewable energy sources is still important, considering the continuous worldwide growth of electric energy usage and demand. One has to be aware of the tendency, that the use of electric energy increases in summer as well, which results from increasing use of air conditioning systems. Most commonly applied are compression chillers. However, in order to decrease the use of non-renewable energy, alternatives are needed. One of the possibilities is the application of commercially-spread sorption chillers. Their mode of operation is analogical to that of compression chiller, but the electric compressor is substituted by a colloquially named

¹ Faculty of Energy and Environmental Engineering, Institute of Thermal Technology, Silesian University of Technology, ul. Konarskiego 22, 44-100 Gliwice, Poland, phone: +48 32 237 10 31, +48 32 237 10 41, fax: +48 32 237 28 72, email: karolina.petela@polsl.pl, andrzej.szlek@polsl.pl

* Corresponding author: karolina.petela@polsl.pl

sorption compressor which comprises of absorber, generator driven by heat and a solution heat exchanger. Electric energy consumed by this type of system is used only to drive solution pumps inside the cycle. Nevertheless, to minimize the energy use by final consumers, passive architecture is becoming more and more popular and attractive. Those buildings are characterised by good insulating properties, installed systems of ventilation heat recuperation, use of internal gains and passive use of solar energy. Passive buildings are also equipped with cooling structures like ground heat exchanger or evaporative cooling. A system that is expected to have the potential of covering the cooling demand of an inhabitant is a device using the phenomenon of heat exchange with a radiating nocturnal sky. The idea proposed in this study is a theoretical investigation of possibilities of radiative cooling system application into a residential building in Nowy Sacz, Poland.

Radiative cooling phenomenon

Radiative cooling belongs to one of the heat dissipation techniques, where heat is transferred to a lower temperature sink. Radiative cooling exploits sky as the sink and the heat loss is conducted by long-wave radiation to the sky [1]. On every exposed surface, beyond the convection mechanism, a radiative heat exchange with the sky takes place. This phenomenon is most effective during night-time, when no solar gains appear and the nocturnal sky temperature as low as even -50°C . The efficiency of radiative cooling system is affected by cloud cover, wind and humidity of the air. That is the reason why those systems are most commonly installed in the desert climates, while the intensive ambient temperature drop in the night is additionally advantageous [2]. A scheme of heat exchange between a surface, ambient and nocturnal sky is presented in Fig. 1.

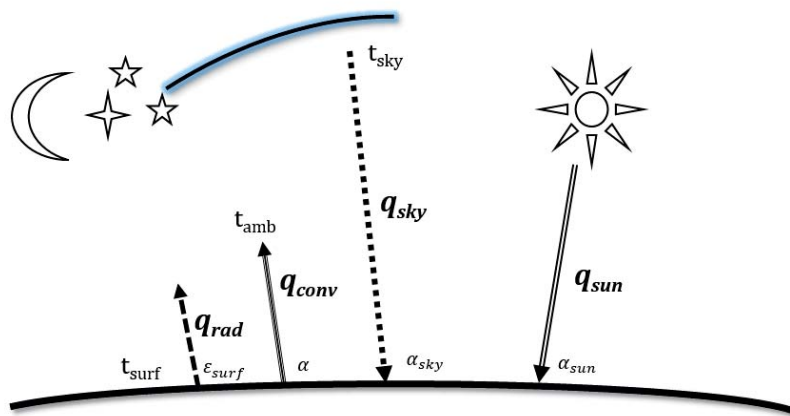


Fig. 1. Heat fluxes for a surface exposed to the sky; t_{surf} [$^{\circ}\text{C}$] – surface temperature, q_{rad} [W/m^2] – surface radiative heat flux, ε_{surf} – surface's emissivity, q_{conv} [W/m^2] – convective heat flux, α [$\text{W}/(\text{m}^2\text{K})$] – convective heat transfer coefficient, q_{sky} [W/m^2] – sky radiative heat flux, α_{sky} – sky-absorptivity factor, t_{sky} [$^{\circ}\text{C}$] – radiative sky temperature, q_{sun} [W/m^2] – absorbed solar radiation heat flux rate, α_{sun} – solar-absorptivity factor

A heat loss from a surface that has been heated during the day will be higher, if the ambient temperature in the night is low. However, unlike the desert climate, the night-time temperature drop in the moderate climate locations does not occur in the hot few-days periods, with cooling demand. In the opposite, if the day is hot, it is highly probable, that the night will be warm as well. If the surface temperature of a radiator drops below the ambient temperature under those conditions, convection gains partially neutralize the radiant heat loss. This tendency is amplified with increasing wind speed. A parameter at which convective heat gains equal radiant heat loss is known as radiator's stagnation temperature [3]. To prevent the heat gains by a forced convection different types of wind screens have already been investigated. Predominantly discussed are: glazings transparent in the infra-red range or some open coverings (eg honeycomb-shaped) that limit the wind speed and general motion of the air above the radiator [3].

It is evidential in the available literature that the issues of radiative cooling were discussed already in 1980s [3]. Various types of radiators have been investigated since then. Erell and Etzion [4] analysed the prospects of using an unglazed flat plate solar collector for purposes of radiative cooling, while Dimoudi [5] performed an experimental study of performance on a roof component comprised of white painted pipes. Bagiorgas and Mihalakakou [1] proposed an experimental model of a roof radiator made of white painted folded aluminium tube used for space cooling in Greece. Farmahini-Farahani and Heidarinejad [6] used flat-plate radiators to pre-cool the air that was subsequently cooled in an evaporative cooling device. They assumed the presence of a water storage tank in the circuit, but Zhang and Niu [7] were to analyse the cooling performance of nocturnal radiative cooling combined with microencapsulated phase change material slurry storage. Al-Obaidi et al [8] reviewed the effect of using different paints and materials on radiative roof's operation.

The idea here proposed considers a performance analysis of a radiator in form of a flat plate collector with white painted pipes that is covering whole roof area of a residential building in moderate climate conditions.

Building under consideration

The radiative cooling system is expected to meet the cooling needs of a one-family detached house with four inhabitants. Construction of the building is assumed to be light-weight with insulated walls made of hollow brick. The building has two levels: ground floor and first floor. No basement or attic are considered. Ground floor is divided into 5 separate spaces: kitchen, bathroom, living room, office and hall. A staircase leads to the first floor, where 5 rooms are located: main bedroom, 2 children bedrooms, a bathroom and a wardrobe. Only the wardrobe is excluded from the group of cooled spaces. A scheme of house under consideration is presented in Fig. 2. Dimensions of every floor are 10×7 m. It is ideally assumed, that whole flat roof is covered with an unglazed flat plate collector playing the role of a passive radiator. The system is combined with a 3 m^3 storage tank.

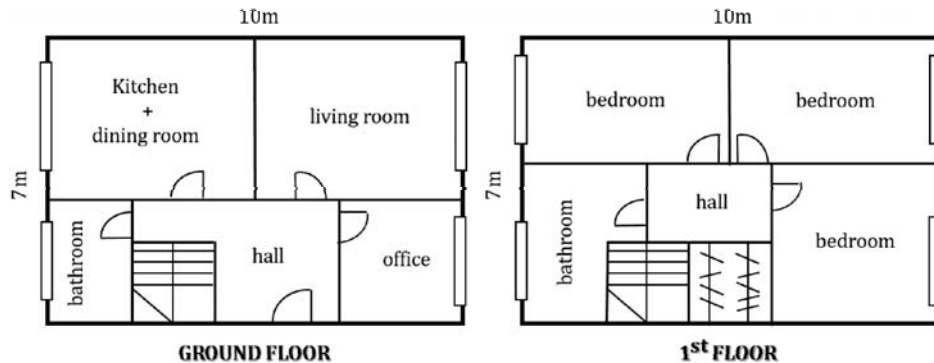


Fig. 2. A simplified scheme of rooms projection inside the project house

The project-building is situated in Nowy Sącz. It is a town located in southern Poland, in Lesser Poland Voivodship, and its coordinates are: 49°37'26"N 20°41'50"E. Poland represents moderate climate conditions. However, being under eastern continental influences, summers tend to be hot. Consequently, more and more electric energy consumption in the summer results from installing the air conditioning systems. Nevertheless, it has to be emphasized that despite the occurrence of high daily temperatures, night temperature drop is not intense, cloud cover and air pollution appears regularly, which are the factors hindering an effective use of passive radiators.

Cooling demand calculation

For the purpose of this study, cooling demand was declared basing on a German standard VDI 2078, described in [9]. According to this norm cooling demand is amount of heat created by external and internal gains that should be removed from the space, to obtain steady state indoor temperature (26°C). To define the cooling demand, an energy balance has to be made. In Poland, residential buildings are air-conditioned only during summer, so the energy balance has been conducted for five typical cases of the months: May, June, July, August, and September. Each case reflects a simulation of an hour with the highest ambient temperature in the month. Meteorological data used for the calculations consider a typical meteorological year for station in Nowy Sącz [10].

Two types of heat gains are to be considered: external heat through walls, windows, doors etc., as well as internal heat gains from people, machines, lighting, and rooms' walls.

Before any kind of heat balance can be made, the partition properties have to be stated. All of partitions are projected to fulfil obligatory standards in terms of heat transfer coefficient. Table 1 presents types of partitions existing in project house.

Table 1

Heat transfer coefficients of the analyzed partitions

No.	Type of partition	Heat transfer coefficient [W/(m ² K)]
1	Outer wall	0.25
2	Inner wall	1
3	Floor on the ground	0.3
4	Ceiling	1
5	Roof	0.2
6	Window	1.3
7	Outer door	1.7
8	Inner door	5

While simulating a building with walls made of hollow brick, it is also ideally set, that it has a negligible thermal inertia. It means that heat transfer to the inner part of the room is not delayed by accumulative properties of the wall and enables to conduct calculations for real time ambient temperature.

Heat flux through walls and other opaque barriers depends on temperature difference and solar radiation – these phenomena have to be considered together, as solar radiation increases ambient temperature. It requires determination of an equivalent temperature difference $\Delta\vartheta_{eqv}$, taking into account the solar ambient temperature. Values of $\Delta\vartheta_{eqv}$ depends on hour of the day, wall's orientation and building's construction class. The values have been empirically determined and tabulated [9] for location $\sim 50^{\circ}\text{N}$, ambient temperature $t_{amb} = 24.5^{\circ}\text{C}$ and inner temperature $t_{in} = 22^{\circ}\text{C}$. It imposes a need of a correction, if the conditions differ and is given as $\Delta\vartheta'_{eqv}$:

$$\Delta\vartheta'_{eqv} = \Delta\vartheta_{eqv} + (t_{amb} - 24.5) + (22 - t_{in}) \quad (1)$$

Heat gains through outer walls can be calculated then from equation (2):

$$\dot{Q}_w = k \cdot A \cdot \Delta\vartheta'_{eqv} \quad (2)$$

where k is the heat transfer coefficient [W/(m²K)], while A is the surface area of the wall [m²].

Convective heat gains through windows are determined by the following equation:

$$\dot{Q}_T = k \cdot A \cdot (t_{amb} - t_{in}) \quad (3)$$

Solar radiation heat gains through windows have to be defined separately by equation:

$$\dot{Q}_S = A \cdot I \cdot b \cdot S_a \quad (4)$$

where I is total irradiation on a given surface [W/m²], b is a window transmission coefficient assumed as $b = 0.75$.

S_a is a solar heat-accumulation coefficient which was empirically defined for a specific type of construction, wall's orientation and specific hour of the day [9].

Internal heat gains are a sum of human heat gain, lighting heat gain and electric devices heat gain. Human heat gains are calculated accordingly to determination of occupants residing in one room. It is specified that sensible heat gain from one person equals 70 W. Heat gains from electric lighting may be defined with the help of equation:

$$\dot{Q}_B = N \cdot A_{room} \cdot \varphi \cdot S_i \quad (5)$$

where N stands for the power of installed lighting [W/m^2], A_{room} is the surface area of one room [m^2], φ is the lighting's coincidence factor assumed as 0.7, while S_i is a lamp heat-accumulation coefficient. According to literature [9] S_i may be introduced as 0.63. Depending on the amount of working electric devices in the room, heat gains are calculated from the equation:

$$\dot{Q}_B = \sum_i N_{mach_i} \cdot \varphi_i \quad (6)$$

where N_{mach_i} is heat gain of every device [W] and φ_i is a device's coincidence factor. Values of these factors are taken from Table 2. According to the standard it is simplified and assumed that the heat gains from domestic devices occurs all the time with a constant coincidence factor.

Table 2
Heat gains and coincidence factor of domestic electric devices

Electric device	N_{mach_i} [W]	φ_i [-]
Computer	90	0.5
Screen	50	0.5
Printer	10	0.2
Oven	1500	0.2
Fridge	300	1
Electric kettle	250	0.2
Washing machine	1500	0.2

In order to choose a representative day, cooling demand was calculated for 5 cases: May 18th at 15:00, June 7th at 12:00, July 5th at 12:00, August 8th at 15:00 and September 6th at 12:00.

These hours were not selected randomly, as each represents the warmest hour of every month according to meteorological data. Calculated cooling demand fits within the range 4–6 kW. It is visible on a chart presented in Fig. 3.

Although July 5th at 12:00 is the warmest hour in the analysed group, cooling demand for this point is slightly lower than for June 7th, August 5th and September 6th. It may be clarified with the chart presented in Fig. 4.

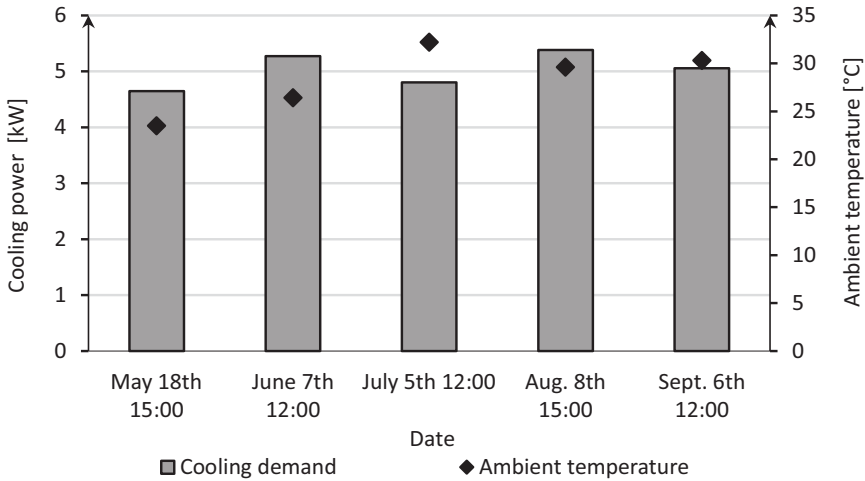


Fig. 3. Calculated cooling demand for each representative hour versus ambient temperature

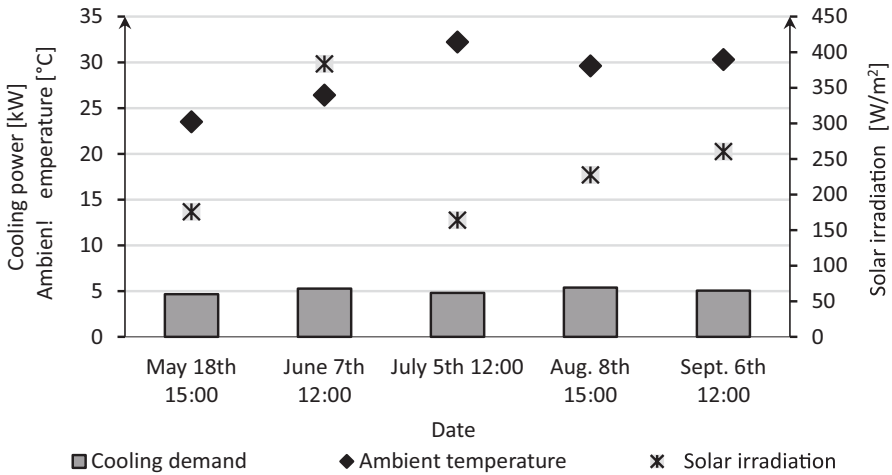


Fig. 4. Calculated cooling demand for each representative hour versus ambient temperature and solar irradiation on northern oriented vertical wall

It is evident that the solar irradiation on northern oriented walls, which represents a large part of the building’s gains is the lowest for the warmest hour, so the cooling demand may be smaller. However, value of northern solar irradiation on August 8th is lower than on June 7th and the cooling demands are higher. It arises from the difference of solar heat-accumulative coefficient for western walls at 15:00 and 12:00. On June 7th

at 12:00 $S_a = 0.17$, while already on August 8th at 15:00 $S_a = 0.53$. Even if the solar radiation on western walls is lower on August 8th at 15:00 (310.8 W/m^2) than on June 7th at 12:00 (436.48 W/m^2), the multiplication factor of accumulative coefficient is decisive. To omit any further ambiguity of this kind, it has been decided that the representative day will be July 5th as the hottest day of the year. Cooling power demand on July 5th at 12:00 equals 4.8 kW. Outdoor temperature is given as 32.2°C , while desired indoor temperature should be 26°C . It allows to calculate an indicator saying how much cooling power has to be delivered to chill one cubic meter of space by one Celsius degree. This indicator equals in the project case $2.11 \text{ W}/(\text{m}^3\text{K})$. Subsequently, cooling demand was determined for each hour between 7:00 and 19:00 on July 5th. This time range should correspond to the period when air-conditioning system is used. It was made, so that the amount of cooling energy needed for a whole day would be known. Following the VDI 2078 standard, the sum of cooling energy needed on July 5th equals 61.8 kWh. For an independent operation of passive cooling system, the value of daily cooling demand should be equal to the amount of cooling energy accumulated during the night activity. This study rests on evaluation of a night-radiator cooling possibilities to meet a daily cooling demand.

Application of radiative cooling system

To determine the possibilities of cooling power generation by heat transfer between passive radiator and radiating nocturnal sky, a heat balance has to be made. Meteorological data needed for the evaluation of the balance (ambient temperature – t_{amb} [$^\circ\text{C}$]; relative humidity – φ [%]; total solar irradiation – G [W/m^2], wind speed – w [m/s]; and wind direction) have been retrieved from meteorological data set for Nowy Sacz [10] for the night (21:00–6:00) preceding July 5th. Simulation was performed for various theoretical cloud cover conditions: for a clear sky and for 25%, 50%, 75%, and 100% of cloud cover. Passive radiator is an unglazed flat-plate collector having dimensions of the roof: $(10 \cdot 7) \text{ m}^2$. Collector is insulated from the roof and in a distance from other objects, no temperature drop according to the height of the roof has been considered. Collector's pipes are made of copper and covered with white paint of a low solar absorptivity factor. To calculate the convective heat transfer coefficient (α [$\text{W}/(\text{m}^2\text{K})$]), the collector is simulated as a flat surface. The night heat balance was conducted in a time step mode, assuming an hourly change of collector's surface temperature.

A heat flux from the surface of collector (\dot{q}_{loss} [W/m^2]) is described by equation:

$$\dot{q}_{loss} = \dot{q}_{conv} + \dot{q}_{sky_{rad}} - \dot{q}_{sun} \quad (7)$$

It takes into consideration convective loss (\dot{q}_{conv}), radiative loss from the surface (\dot{q}_{rad}), nocturnal sky radiative heat gains ($\dot{q}_{sky_{rad}}$), and solar radiation heat gains after sunrise (\dot{q}_{sun}).

Convective heat flux can be calculated from:

$$\dot{q}_{conv} = \alpha (t_{surf} - t_{amb}) \quad (8)$$

where t_{surf} [$^\circ\text{C}$] stands for surface temperature.

To simplify the calculations, during the simulation each hour represents a separate steady state. Surface temperature in the first hour of the calculation is equal to ambient temperature (21.4°C). An independent discussion could consider the evaluation of convective heat transfer coefficient. Various empirically obtained function for α are available in the literature, while the most common is the approach of Clark and Berdahl [5], where α depends only on the wind speed (w), and is equal to 3.5 W/m²K if $w < 1$ m/s, while if $w = 1-5$ m/s then $\alpha = 2.8 + 0.76 w$. Since in this study radiator is simplified to a flat surface of given dimension, convective heat transfer coefficient was calculated basing on determination of criterial numbers: Nusselt, Rayleigh or Reynolds for a parallel flow over flat plates, according to functions available in [11]. Coefficient α depends then on ambient temperature, surface temperature, wind speed and collector's dimensions.

Radiative heat flux from collector's surface is given by equation:

$$\dot{q}_{rad} = \varepsilon_{surf} \cdot \sigma \cdot T_{surf}^4 \quad (9)$$

where ε_{surf} is the surface emissivity and for a white paint equals 0.93 [12], while

$$\sigma = 5.67 \cdot 10^{-8} \frac{\text{W}}{\text{m}^2 \text{K}^4}$$

is the Stefan-Boltzmann constant.

The amount of sky radiation absorbed by the surface can be calculated using equation:

$$\dot{q}_{skyrad} = \alpha_{sky} \cdot \sigma \cdot T_{sky}^4 \quad (10)$$

Since the temperature of the source-sky is of the same order as surface temperature, it is assumed that sky radiation absorptivity equals surface emissivity. Sky temperature T_{sky} [K] can be found in the meteorological data set, but since the cloud cover conditions are not stated, it was calculated basing on an empirical function available in [4], presented in equation:

$$T_{sky} = \varepsilon_{sky}^{0.25} \cdot T_{amb} \quad (11)$$

It allowed to perform an individual investigation of cloud effect on passive system performance.

Sky emissivity (ε_{sky}) was a subject of many researches [13] and is an empirical function depending on air humidity. It was calculated from equation [4]:

$$\varepsilon_{sky} = 0.006 \cdot t_{dp} + 0.74 \quad (12)$$

Dew point temperature, t_{dp} , is a saturation temperature for vapour partial pressure.

Sky radiation heat gains may be increased by a cloudiness factor C , being an empirical function of cloudiness indicator, where $n = 0$ stands for a cloudless sky, and $n = 10$ for overcast sky [5]. Heat gains can be then obtained from following equation:

$$\dot{q}_{sky,rad} = C \cdot \varepsilon_{surf} \cdot \sigma \cdot \varepsilon_{sky} \cdot T_{amb}^4 \quad (13)$$

$$C = 1 + 0.0224 \cdot n - 0.0035 \cdot n^2 + 0.00028 \cdot n^3 \quad (14)$$

It is possible that around morning hours the surface of the collector will be heated by incoming solar radiation. Heat absorbed by the collector is evaluated with the use of equation (15). Solar absorptivity of the white paint equals $\alpha_{sun} = 0.2$:

$$\dot{q}_{sun} = \alpha_{sun} \cdot G \quad (15)$$

It is assumed that under hourly change of ambient conditions, the surface temperature of the collector is changing through heat transfer between collector's surface and nocturnal sky. More accurate calculations would need applying CFD calculations which are not a part of this paper. Therefore, some assumption had to be made connecting the surface temperature and storage tank installed. It is ideally assumed, that the heat lost from the surface during one hour at its initial temperature is equal to the change of internal energy (ΔE_u) of the storage tank, as shown in the equations below. It affects the change of the fluid at outlet of the tank. Since it is also assumed, that the heat transfer fluid flows very quickly in the radiator pipes, surface temperature after one hour of heat exchange equals the storage tank outlet temperature. It can be then an initial value for next hour of heat balance:

$$E_1 = \Delta E_u + E_2 \quad (16)$$

$$E_1 = Q_{loss} + E_2 \quad (17)$$

$$\rho \cdot V \cdot C_p \cdot t_1 = A_{surf} \cdot \dot{q}_{loss} \cdot \tau + \rho \cdot V \cdot C_p \cdot t_2 \quad (18)$$

where: ρ – density [kg/m^3]; V – tank volume [m^3]; C_p – specific heat of storage fluid [$\text{J}/(\text{kgK})$]; t_1 and t_2 fluid temperatures at the inlet and outlet of the tank, respectively.

If the project building was equipped with a solar absorption chiller, the installed storage tank capacity could be chosen according to the ratios available in [14], equal to 40 dm^3 per 1 m^2 of solar collector. It has been decided, that the radiative passive system will be connected with a 3 m^3 storage tank with cold water as a storage fluid.

Results of the radiative cooling simulation

The simulation proposed in this study enabled to define heat loss rate from the passive collector for every hour of the night. According to the foregoing calculation path and taking into account above-mentioned assumptions, a group of results has been obtained. Fig. 5 shows how the hourly heat loss profile could look like, if the sky was clear. The chart present a unit heat loss rate for 1 m^2 of radiator.

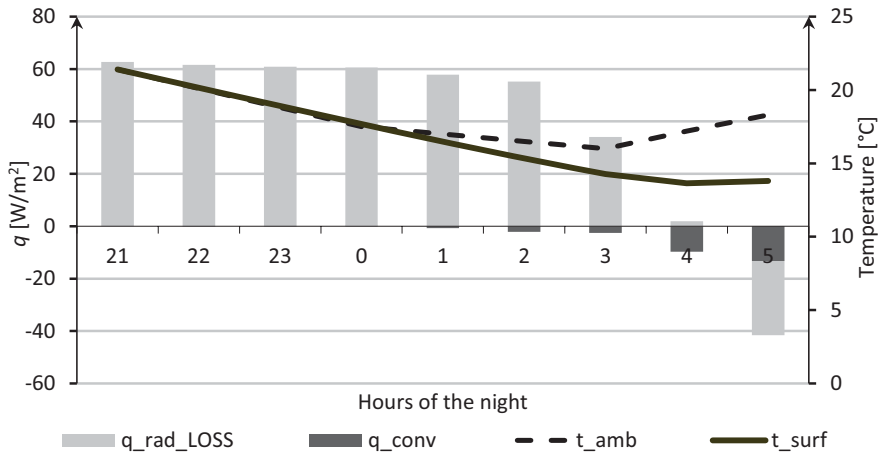


Fig. 5. A chart presenting the heat loss rate from the collector’s surface in comparison with its temperature and ambient temperature

The value of presented q_{rad_LOSS} equals radiative heat loss from the surface of collector after subtraction of nocturnal sky radiative gains and solar heat gains occurring at dawn. It is evident that by losing around 60 W/m^2 of heat, the surface temperature may fall well below the ambient temperature. If the night temperature drop was bigger, the heat loss rate could be much higher, what speaks against application of radiative cooling system in moderate climate. Together with the decrease below outdoor temperature, convective heat gains have to increase. The heat loss from the surface drops dynamically at 3:00. If not for the solar heat gains, the heat loss rate would decrease much slower. At 3:00 solar heat gain rate equals 19.1 W/m^2 , while at 4:00 and at 5:00 already 42.1 W/m^2 and 67.92 W/m^2 , respectively. Cooling power for every hour of the passive radiator operation can be obtained by multiplication of unit heat loss rate \dot{q}_{loss} and surface of collector ($A_{surf} = 70 \text{ m}^2$), results are presented in Table 3.

Table 3

Heat loss rates from the total surface of the passive collector

Hour	21:00	22:00	23:00	00:00	1:00	2:00	3:00	4:00	5:00
Heat loss rate [kW]	4.390	4.311	4.264	4.242	3.995	3.715	2.210	-0.540	-2.908

Calculated heat loss implies temperature drop inside the ideally assumed chilled water storage tank. If the cooling power generated by the passive radiator could be accumulated in a form of chilled water inside the ideally insulated storage tank, the sum of accumulated cooling energy, by losing heat from collector’s surface, would equal 23.68 kWh. To compare the values, the afore-mentioned cooling energy demand of the project building should equal 61.8 kWh. By the assumption of an average cooling power demand of 5 kW, the storage tank would be unloaded already after 4 hours and

44 minutes. Main conclusions coming from this comparison is that passive cooling is not sufficient for covering cooling demands in whole extent and system should be assisted for instance by compression chiller.

Second analysis concerns the impact of cloud cover on the performance of a radiative cooling system. According to equation (13) and (14), 4 stages of cloudiness have been analysed: 25%, 50%, 75% and 100%. A chart presented in Fig. 6. shows, how the heat loss rate changes with the increase of cloud cover indicator.

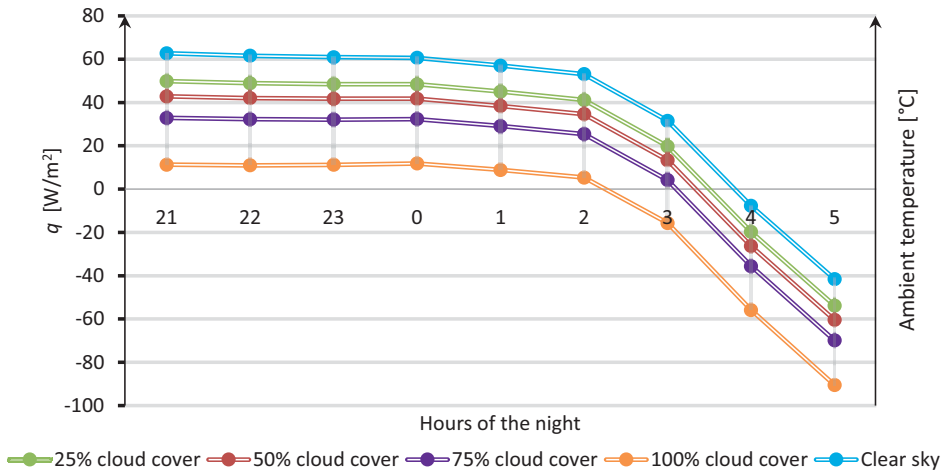


Fig. 6. Chart of a unit heat loss rate's profile during the night (July 4th/5th) under different cloud cover conditions

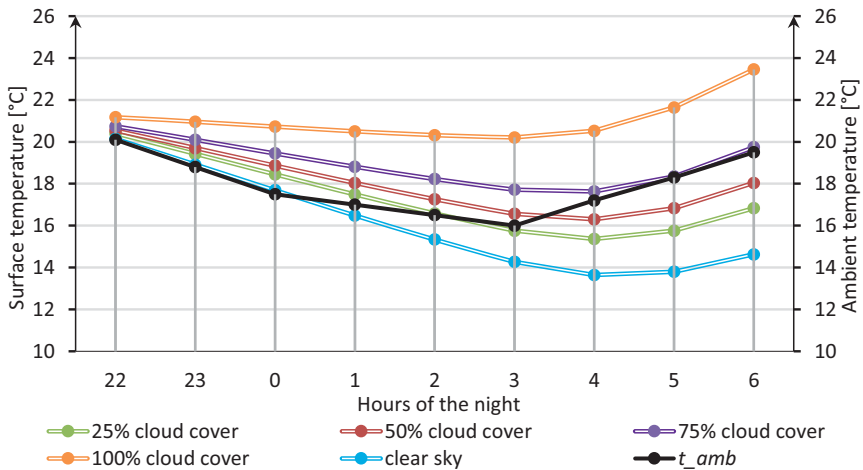


Fig. 7. Chart of the surface temperature change profile during the night (July 4th/5th) under different cloud cover conditions versus ambient temperature

It is visible that clouds are a factor which increases the sky radiation heat gains leading to the decrease of total unit heat loss rate from the surface. Additionally, theoretical change of surface temperature under the same cloud cover variation is shown in Fig. 7.

If the sky is overcast, or covered with clouds in 75%, the surface temperature would never fall below the ambient temperature. It is clear, that operating a radiative system under those conditions can be only efficient if ambient temperature at night is low (eg 10°C), while the following day is expected to be hot (eg 30°C). However, as mentioned before, this tendency is more typical for tropical and subtropical climates rather than for moderate climate locations.

It is valuable to compare the daily cooling energy demand and nightly passive cooling energy supply for the above discussed dates. Those values are presented in Fig. 8.

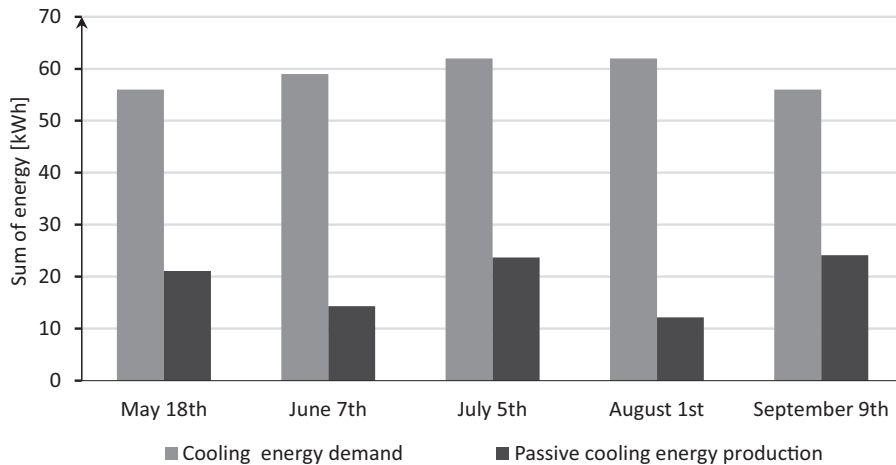


Fig. 8. Daily cooling energy demand and nightly cooling energy supply for given days

The chosen five days are the hottest of each month. Consequently, it influences the cooling energy demand and causes its value similar. However, solar heat gain is the highest for July and August, what results in the supreme cooling energy demand for these days. It could be suspected that the increment of average night temperature has a direct impact on the decrease of heat loss from surface. It is evident while comparing the cooling energy supply on colder nights of May and September with the cooling energy production on slightly warmer nights of June and August, as the nocturnal sky temperature is the lowest in this case in May and September. However, the example of night in July shows, that summer nights may have higher cooling energy supply under specific conditions. It is strictly bound with the surface initial temperature. For the night of July 4th/5th, according to the meteorological data, initial temperature was relatively high (21.4°C) resulting in high radiative heat loss from the surface, while nocturnal sky heat gain was comparable to other nights'. The gradual decrease of surface temperature shown in Fig. 5. enables to maintain a positive value of convective heat loss till

midnight. The initial surface temperatures at 21:00 on June 6th and August 1st are 15.5°C and 16.5°C, respectively. Already after one hour of radiator's operation, surface temperature falls below ambient temperature and the convective heat gains begin to increase, leading to stagnation. It proves the positive effects of desert climate. Surfaces warmed during the day accumulate part of heat and are able to lose more heat through radiation on a cold night. Therefore, the initial temperature of surface in simulation should take into account the fact of being heated during the day. Even more reasonable could be a 24-hours-simulation of change of surface temperature. Moreover, from a thermo-economic point of view, the investigation should be supplemented by the analysis of the cooling quality of temperature level at which heat is lost from the surface.

Conclusions

A theoretical analysis of possibilities, that installing a radiative cooling system into a residential building under moderate climate may bring, has been conducted. Cooling power demand of a project house on July 5th at 12:00 was defined as 4.8 kW, while total cooling energy foreseen for this day equaled 61.8 kWh. A passive flat plate collector installed on the 70 m² flat roof can generate a heat loss rate close to 60 W/m² during the night, if no clouds on the sky appear, and almost no wind occurs. It means a 4.2 kW heat loss from the whole surface of the radiator. Whole night of exploitation may bring a theoretical value of 23 kWh of cold accumulated in chilled water. If the storage tank had to be unloaded, it would be sufficient for 4.5 hours of utilization. Furthermore, if the sky was partially covered with clouds or overcast, the heat loss rate would gradually decrease, preventing the use of nocturnal radiator. It is visible, that even under idealised conditions, a radiative nocturnal cooling system is not sufficient to fulfil a daily cooling demand rate under moderate climate conditions for the project building. Nevertheless, it might be considered as an attractive, eco-friendly supplement to a conventional air-conditioner, what could require further investigation. It is worth mentioning, that in systems, where domestic hot water is generated by solar collectors, installation of a passive radiator would not be an obstacle, as it can be located on the northern roof slope. Application of nocturnal radiative cooling systems is believed to be more sensible in spaces, where the cooling power could be consumed simultaneously, like server rooms. Moreover, it could support food preservation processes, or the operation of cold stores leading to limitation of non-renewable energy consumption in the agricultural industry.

Acknowledgements

This research has been supported by the statutory research funds of the Faculty of Power and Environmental Engineering of the Silesian University of Technology.

References

- [1] Bagiorgas HS, Mihalakakou G. Experimental and theoretical investigation of a nocturnal radiator for space cooling. *Renew Energy*. 2008;33:1220-1227. DOI:10.1016/j.renene.2007.04.015.

- [2] Al-Nimr M, Tahat M, Al-Rashdan M. Night cold storage system enhanced by radiative cooling – a modified Australian cooling system. *Appl Therm Eng.* 1999;19:1013-1026. DOI:10.1016/S1359-4311(98)00103-3.
- [3] Santamouris M. *Advances in Passive Cooling.* New York: Earthscan publishing; 2007.
- [4] Erell E, Etzion Y. Radiative cooling of buildings with flat-plate solar collectors. *Build Environ.* 2000;35:297-305. DOI:10.1016/S0360-1323(99)00019-0.
- [5] Dimoudi A, Androutsopoulos A. The cooling performance of a radiator based roof component. *Sol Energy.* 2006;80:1039-1047. DOI:10.1016/j.solener.2005.06.017.
- [6] Farmahini-Farahani M, Heidarinejad G. Increasing effectiveness of evaporative cooling by pre-cooling using nocturnally stored water, *Appl Therm Eng.* 2012;38:117-123. DOI:10.1016/j.applthermaleng.2012.01.023.
- [7] Zhang S, Niu J. Cooling performance of nocturnal radiative cooling combined with microencapsulated phase change material (MPCM) slurry storage. *Energ Buildings.* 2012;54:122-130. DOI:10.1016/j.enbuild.2012.07.041.
- [8] Al-Obaidi K, Ismail M, Abdul Rahman A. M. Passive cooling techniques through reflective and radiative roofs in tropical houses in Southeast Asia: A literature review. *Frontiers Architectural Res.* 2014;3:283-297. DOI:10.1016/j.foar.2014.06.002.
- [9] Recknagel H. *Handbook for Heating and Air Conditioning Technology.* Wroclaw. Omni Scala publishing. 2008.
- [10] Meteorological data file for Nowy Sącz, available at: http://www.mir.gov.pl/budownictwo/rynek_budowlany_i_technika/Efektywnosc_energetyczna_budynkow/typowe_lata_meteorologiczne/ Strony/start.aspx.
- [11] Cengel YA. *Heat Transfer: A Practical Approach.* New York: McGraw-Hill publishing; 2002;373:468.
- [12] Solar absorptivity data tables. [Http://www.solarmirror.com/fom/fom-serve/cache/43.html](http://www.solarmirror.com/fom/fom-serve/cache/43.html).
- [13] Chen B, Kasher J, Maloney J, Girgis G. A, Clark D. Determination of the clear sky emissivity for use in cool storage roof and roof pond applications. *Proc ASES Annual Meeting.* 1991;1-5. http://www.ceen.unomaha.edu/solar/documents/SOL_26.pdf [accessed 05.03.2015].
- [14] Molero-Villar N, Cejudo-Lopez JM, Dominguez-Munoz F, Carrillo-Andres A. A comparison of solar absorption system configurations. *Sol Energy.* 2012;86:242-252. DOI:10.1016/j.solener.2011.09.

OCENA MOŻLIWOŚCI STOSOWANIA PASYWNEGO CHŁODZENIA DO CELÓW DOMOWYCH W KLIMACIE UMIARKOWANYM

Instytut Techniki Ciepłej, Wydział Inżynierii Środowiska i Energetyki Politechniki Śląskiej
Politechnika Śląska, Gliwice

Abstrakt: Wobec wymagań środowiskowych systemy wykorzystujące odnawialne źródła energii są coraz częściej stosowane i wdrażane również do rozwiązań budownictwa pasywnego. Celem pracy jest analiza efektów energetycznych wykorzystania pasywnego chłodzenia w budynku mieszkalnym. Podmiotem pracy jest system opierający swoje działanie na promienistej wymianie ciepła z nocnym nieboskłonem. Na powierzchni każdego ciała wyeksponowanej ku niebu, oprócz konwekcyjnej wymiany ciepła, odbywa się również radiacyjna wymiana ciepła z nieboskłonem. Analiza ukazuje potencjał chłodzenia pasywnego tego typu w produkcji chłodu, jednakże wskazuje na silną zależność systemu od warunków otoczenia oraz na fakt, że podaż chłodu jest odwrotnie proporcjonalna do zapotrzebowania. Niskie wartości strumieni strat ciepła z pasywnego radiatora sprawiają, że system nie może stanowić samodzielnego źródła produkcji chłodu, jednak może stać się atrakcyjnym, przyjaznym środowisku dodatkiem do konwencjonalnego układu klimatyzacyjnego.

Słowa kluczowe: chłodzenie pasywne, nocny nieboskłon, kolektor słoneczny, chłodzenie radiacyjne

Jakub SIKORA^{1*}, Marcin NIEMIEC²,
Anna SZELAŁG-SIKORA¹, Michał CUIPAŁ¹
and Anna KLIMAS¹

UTILIZATION OF POST-FERMENT FROM CO-FERMENTATION METHANE FOR ENERGY PURPOSES

WYKORZYSTANIE POFERMENTU Z KOFERMENTACJI METANOWEJ NA CELE ENERGETYCZNE

Abstract: The main civilization issue of the 21st century is a rapid increase of the waste and pollution amount which influences the natural environment degradation. As early as in the 20th century, the increase in the amount of municipal waste and waste from agri-food industry was reported. Waste chemical composition gives optimal conditions for the development of microorganisms. Under aerobic and non-aerobic conditions bacteria decompose organic compounds which results in gases emission (CH₄, H₂S, CO₂, NO_x), while nitrogen, phosphorus and potassium compounds remain in the post-ferment. These compounds may be diffused into the environment and create a risk of homeostasis corruption. Biogenic elements are transferred to surface water and corrupt the ecosystem balance causing its eutrophication. Various types of fermentation may be distinguished, but the methane fermentation may play a special role with regard to the sustainable energy sources and waste management. This process converts energy included in the biomass into the utility fuel – a source of clean sustainable energy which does not negatively influence the environment. Biogas may be combusted in the boiler in order to obtain thermal energy used for heating rooms or in a gas engine which drives the current generator. It is worth noticing that the above method is a desired one of transforming waste *ie* organic recycling. The research results of biogas production from the organic fraction of municipal waste in co-fermentation with the agricultural mass as well as the suitability of the post-ferment for energy purposes were presented in the paper. In order to image the calorific value of the post-ferment, the tests were carried out on 6 batch mixes where in each one the organic fraction of municipal waste occurred.

Keywords: biogas, organic recycling, waste disposal, renewable energy

In terms of the energy produced, two Mg of biomass are equal to 1 Mg of hard coal. On account of burdening the environment, biomass combustion gives better results,

¹ Institute of Agricultural Engineering and Informatics, Faculty of Production and Power Engineering, University of Agriculture in Krakow, ul. Balicka 116B, 30–149 Kraków, Poland, phone: +48 12 662 46 18, email: Jakub.Sikora@ur.krakow.pl

² Faculty of Agriculture and Economics, University of Agriculture in Krakow, al. Mickiewicza 21, 31–120 Kraków, Poland, phone/fax: + 48 12 662 43 41.

* Corresponding author: Jakub.Sikora@ur.krakow.pl

which is related to lower SO₂ emission than in the case of coal. Carbon dioxide emission balance is zero since during combustion the same amount of CO₂ as plants previously took is returned to the atmosphere [1–3]. Recently, great hopes are pinned in the use of biogas produced as a result of biomass fermentation, which is a waste itself. Non-aerobic fermentation is a complex biochemical process which takes place under non-aerobic conditions. Organic substances are decomposed by bacteria into simple compounds – mainly methane and carbon dioxide. Up to 60% of organic substance is converted into biogas during the non-aerobic fermentation. A decomposition rate depends mainly on the type and mass of raw material and optimally selected duration of the process. Over the increase of the organic mass load in the fermentation chamber to the border value, the biogas production increases. Upon reaching the maximum, the production decreases, since the system gets overloaded. Therefore, it is necessary to recognize the optimal scope of loading the digester. A correct fermentation temperature is 30–35°C for mesophilic bacteria and 50–60 degrees for thermophilic bacteria. Presently: straw, beetroot leaves, potato haulms, maize stalks, clover, grass and sewage sludge are used as biomass for biogas production. These are installations at agricultural farms or sewage treatment plants [3, 4].

The possibility of using biodegradable waste from the stream of municipal waste has almost been ignored, entirely (biogas is recovered from municipal waste only by degassing of post-landfill areas. Methane is a greenhouse gas and it should be combusted as such and not emitted to the atmosphere) [5].

The possibility of using biodegradable waste from the stream of municipal waste has almost been ignored, entirely (biogas is recovered from municipal waste only by degassing of post-landfill areas. Methane is a greenhouse gas and it should be combusted as such and not emitted to the atmosphere).

Research studies carried out by other authors report a considerable, almost 50% share of municipal waste in the whole stream (plant and animal waste 33%, paper 21%) [1–3]. Moreover, the European Council Directive 99/31/WE of 26th April 1999 on storing waste requires limitation of the biodegradable substances content deposited on landfills up to 75% of the initial mass within 5 years from implementation, up to 50% within 8 years, and up to 35% within 15 years. May, 2004, 1st is regarded as the initial moment of implementation and the reference point is the amount of waste produced in 1995. It means that installation neutralizing these wastes in a way different than storing will have to be created within the next years [6].

Biodegradable fractions which are the most popular in municipal waste include: potato waste, cabbage leaves, vegetable peels, citrus fruit and banana peels and animal waste. These substrates occur in rural and urban-rural areas and may be used for energy purposes. So far, there are no solutions for conducting anaerobic fermentation based on the mixture of these organic masses. The optimal model of biogas supply should obtain biomass energy and the same utilize the waste biomass (municipal waste biomass, liquid manure and manure). The determination of biogas profitability of the accepted substrates and parameters of the conducted biogas fermentation in the laboratory chamber allowed determination of biomass usability for gassing purposes during methane fermentation. Selection of these substrates for research is explained by

searching for the optimal process of obtaining energy and biomass utilization in rural and urban-rural areas. Agricultural mass is a basic batch in the case of conducting fermentation based on these substrates. Its biochemical variability is low, while municipal biomass constitutes additional batch mass utilized on the spot [1, 2].

Calorific value of biogas depends mainly on the methane content. At the average $0.42 \text{ m}^3 \text{ CH}_4$ is produced of 1 kg of carbohydrates, $0.47 \text{ m}^3 \text{ CH}_4$ of 1 kg of apples and $0.75 \text{ m}^3 \text{ CH}_4$ of fats. Calorific value of methane is $35 \text{ MJ} \cdot \text{m}^{-3}$. Average calorific value of biogas obtained from municipal biowaste is approx. $21.54 \text{ MJ} \cdot \text{m}^{-3}$. Energy included in 1 m^3 of such biogas responds to energy included in 0.93 m^3 of natural gas, 1 dm^3 of diesel oil, 1.25 kg of coal and responds to 9.4 kWh of electric energy [7]. However, one should remember that both components of the volatilizing biogas as well as its combustion products get into atmosphere and affect the environment on account of toxics and smell. A lot of them, especially chlorinated carbohydrates show carcinogen activity. Chlorine occurrence in biogas, at disadvantageous conditions of its combustion, may cause emission of dioxines and furans [7].

Material and methods

Renewable energy sources have been amongst the most crucial elements of the European Union policy for a long time. Presently, they have become significant in terms of possibilities of the technology development, which may limit the effects and duration of the economic, energy and climatic crisis. The Directive 2009/28/EC obliges to increase the share of Renewable Energy Sources in the final energy consumption up to 20% (in Poland up to 15%) by 2020.

The program of agricultural biogas plants construction developed by the Ministry of Agriculture and Rural Areas Development assumes that in 2013 the biogas production in Poland will reach the level of 1 billion m^3 annually, and by 2020 this value will have been doubled. The economic situation for biogas plants predicted for the next years [8] forces out development of analytical methods of the biogas composition and parameters assessment [9]. A governmental programme "Biogas plant in each municipality" assumes that by 2020 at least one such an agricultural plant will be operating in each Polish municipality. Each facility will have power of 0.7 to 3.0 MW. According to Gebrezgabher et al [10] profitability of biogas investment is available for the case of the investment of high powers.

Knowledge concerning the biomass use for energy purposes and especially the biogas production is more and more extensive but still inadequate and often inconsistent and inexplicit, both among specialists and advisers as well as farmers. It concerns both batch for fermentation as well as management of the obtained post-fermentation product and the biogas management. Animal waste biogas (from liquid manure and rarely from dung) is in Poland the most frequently produced in agricultural biogas plants. Biogas production especially from the maize silage is the second solution.

The efficient conversion of plant material into biogas is a challenge on account of complex structure of the cell wall of plants. In order to simplify and fasten the efficient hydrolysis of carbohydrates an initial biomass processing is required [11]. The initial

processing of lignocellulose materials may be carried out in a physical way (mechanical refining, pyrolysis), chemical (with diluted acid, with the use of alkaline processing), physical and chemical (vapour burst) and biological (fungus producing hydrolytic enzymes) [12]. However, one should remember that such an approach to the management of biomass surplus in a farm leads to a mono-culture cultivation. It concerns the requirements of the standard production balancing according to the rules of the Code of Good Agricultural Practices (Polish: KDPR) and requirements of a lower degree of agriculture chemicalization.

The objective of the research was to develop an optimal biogas technology so the biogas plant activity would be economically justified and batch to the fermentor could be so varied that it would conform to the good culture in the agricultural production and would use municipal waste biomass that occurs in the area of operation of the biogas plant.

The research was carried out in the biogas laboratory of the University of Agriculture in Krakow placed in the Department of Production Engineering and Energy Power. Material for the research was obtained in 2012 from the individual dairy farm in Golezow municipality. Moreover, the organic fractions of municipal waste were obtained from the area of Krakow municipality. The following fractions were accepted for the research:

- organic plant mass: maize silage, cattle manure,
- organic fraction of municipal waste.

The fractions were fragmented and five samples were collected from each. Samples were weighed in order to determine their weight before drying. The fragmented material was hydrated to approx. 90% moisture forming optimal conditions for development of mesophilic bacteria. Six mixtures of batches of parameters presented in table 1 were accepted for the research. Fermentation was carried out in the digester of 20 dm³ volume with the regulated temperature environment. The following parameters were controlled in the fermentor used: pH, redox potential and the batch temperature. The produced biogas was collected in the container of a variable volume. A schematic representation of the stand with a digester is presented in Fig. 1.

Table 1

Characteristics of batches for Digesters

Name	Fractions		
	Maize silage [%]	Cattle manure [%]	Fine fraction of municipal waste [%]
Batch 1	65	5	30
Batch 2	100	0	0
Batch 3	0	0	100
Batch 4	50	5	45
Batch 5	20	5	75
Batch 6	75	5	20

Batch 1, accepted as control material is proved and introduced to the digester. Batch 1 is placed in the digester (2) in which by means of sondes (5) fermentation parameters, such as temperature, redox and pH are controlled. These parameters are automatically saved with time interval on the hard disc of a computer of the measuring system. In the digester, the batch is mixed with a mechanical mixer (4) to avoid delamination. The mixer may be smoothly regulated within 0 to 400 rot./min. is equipped with three blades of regulated spacing, which enables the change of intensity of mixing zones in the fermentor.

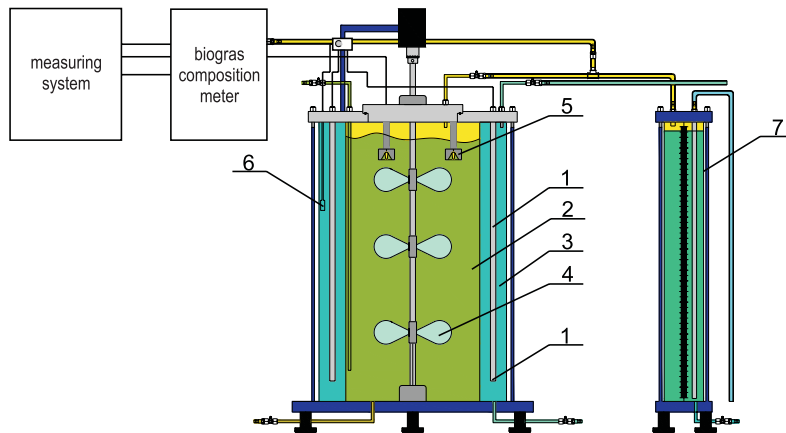


Fig. 1. A schematic representation of the test stand with a 20 litre fermenter: 1 – cartridge heaters, 2 – batch, 3 – water jacket, 4 – mechanical mixer, 5 – sondes, 6 – thermometer, 7 – container

The digester of the fermenter is equipped with a water jacket (3) where three cartridge heaters are placed (1), responsible for heating liquid. The measuring system equipped with a thermometer (6) PT100 is responsible for controlling the process temperature. The produced biogas is collected over the surface of the batch in the fermentor and in the container (7) of variable volume, from which it is sucked in by the biogas composition measuring meter. This meter analyses the following parameters: moisture, temperature, pressure, methane CH_4 , oxygen O_2 , carbon dioxide CO_2 and hydrogen sulphide H_2S . The measured biogas composition parameters are automatically saved on the computer disc of the measuring system.

Determination of the intensity of the biogas production in the remaining batches was carried out according to standard DIN 38414. Batch mixes were fermented under static conditions consisting in a single introduction of fraction to digesters and conducting the process till the end of fermentation.

Fermentation devices were installed in a container with the regulated temperature forming a part of the test stand, which was additionally composed of a switch panel and the measuring system. A schematic representation of the test stand is presented in Fig. 2. Devices for maintaining a constant temperature environment are mounted to a rack (1) located next to the container (2). Controlling takes place by means of the

electronic thermostat ESCO ES-20 (unit switch 16A) with a precision up to $\pm 0.2^{\circ}\text{C}$ resulting from a sensor hysteresis. Temperature decrease by value exceeding 0.1°C causes switching on a heater of 1500 W (3) power with a simultaneous start of the water pump Hanning DPO 25–205 (4) in order to ensure a uniform distribution of temperature in the whole chamber. After heating water to the temperature exceeding the set temperature by 0.1°C the heater switched off with a 30 seconds delay of the pump.

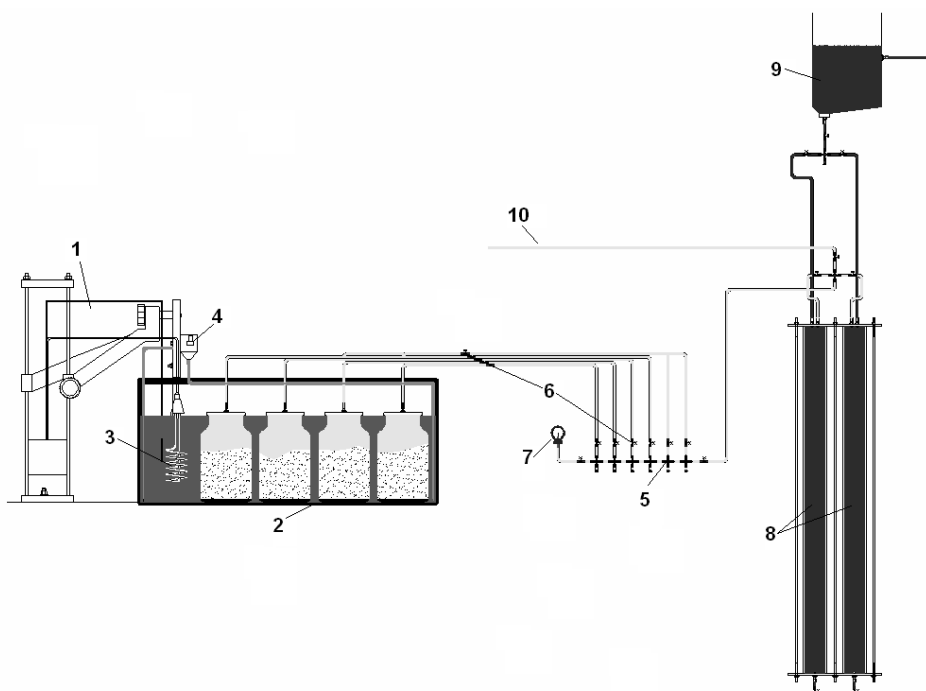


Fig. 2. A schematic representation of the test stand with a 2 litre fermenter: 1 – rack, 2 – container, 3 – heater, 4 – water pump, 5 – switch board, 6 – cut-off valves, 7 – manometer, 8 – system of measuring volume, 9 – columns, 10 – conduit

Separators combined in a row along with cut-off valves (6) and a manometer (7) which measures pressure in particular measuring branches constitute a switch board (5). Due to the use of such system for service of all fermenters, only one measuring system was enough. The system of measuring volume (8) was composed of two columns filled with water with drain valves and a container for filling up the liquid level in columns (9). The measuring system was combined with a switchboard and a biogas composition meter by means of a conduit (10) which was presented in Fig. 1.

A chemical analysis was carried out for all the tested batches before the commencement of fermentation. Dry mass of fraction and reaction were determined. For each batch, fermentation was carried out simultaneously. The amount of the produced gas was read out twice daily at the same time.

Results and a discussion

During planning of the biogas plant construction, standard assumptions of efficiency of the possessed fermentation substrates are accepted for calculation of productivity of installation and determination of economic parameters. Not always, however, these values respond to real biogas yield and its composition; therefore, a detailed research for correct determination of the biogas production value should be carried out in each case. The apparatus presented in Fig. 2 was used in agricultural biogas plants for determination of the biogas yield from an organic fraction of municipal waste as a co-fermentation mass. At the same time, the apparatus with a digester of 20 dm³ volume was used for determination of energy parameters of a post-ferment. The enlargement of the chamber resulted from the need of obtaining a bigger amount of the post-ferment in order to subject it to pelletization or briquetting.

The research on the fermentation process at laboratory conditions allowed comparison of intensity of biogas emission, following fermentation phases and assessment of susceptibility of the tested batch mixes on biochemical processes of the organic mass decomposition. Parameters of the researched fractions are presented in Table 2. Figure 3 and 4 present the total amount of the produced biogas and intensity of biogas emission during fermentation. The amount and intensity of biogas emission are parameters which prove the course of the process.

Table 2

Physical and chemical properties of the analyzed components

Item number	Name of the batch component	pH [-]	Dry mass [%]
1	Maize silage	3.8	26.3
2	Cattle manure	7.5	12.0
3	Organic fraction of municipal waste	5.8	54.0

Parameters of the maize silage or the organic fraction of municipal waste did not diverge from the literature value, whereas manure was characterized with a bigger, than presented in literature, content of dry mass, which was within 12%. Such values result from the animal maintenance system applied on the dairy cows farm.

The results of the biogas yield analysis in relation to dry mass proved directly the highest batch 1 efficiency, which was 223 Ndm³ · kg⁻¹ (Ndm³ – biogas volume at atmospheric pressure) of dry mass. Maize silage batch (batch 2) had a slightly lower efficiency, and the value of this parameter was 184 Ndm³ · kg⁻¹ of dry mass. As seen in Fig. 3, in the course of fermentation of batch 2 made of the maize silage only, a visible delay of the increase of biogas volume was observed, which was caused by the batch reaction. The highest inhibition of the increase and delay of biogas production during fermentation was reported for batch 3 which was made only of the organic fraction of municipal waste. A common course of biogas production efficiency was obtained for batch 6, made of 75% maize silage, 5% manure and 20% organic fraction of municipal waste.

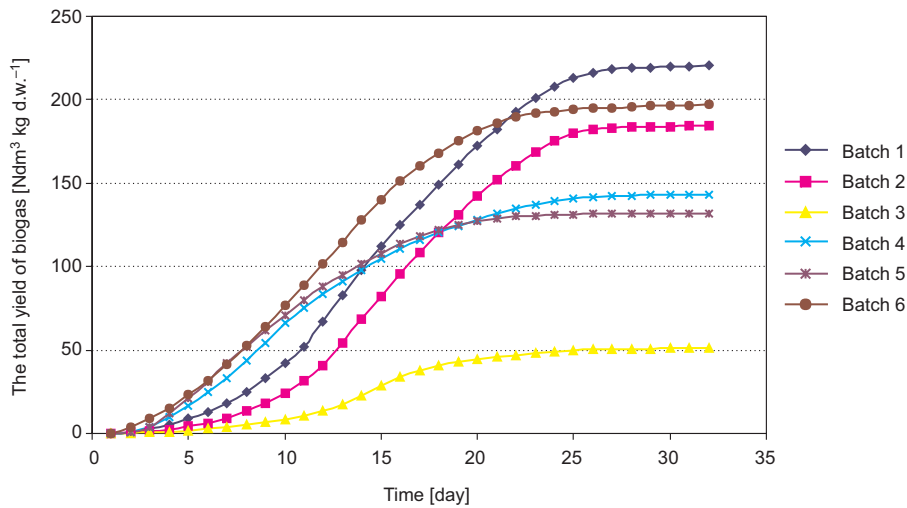


Fig. 3. The total amount of produced biogas

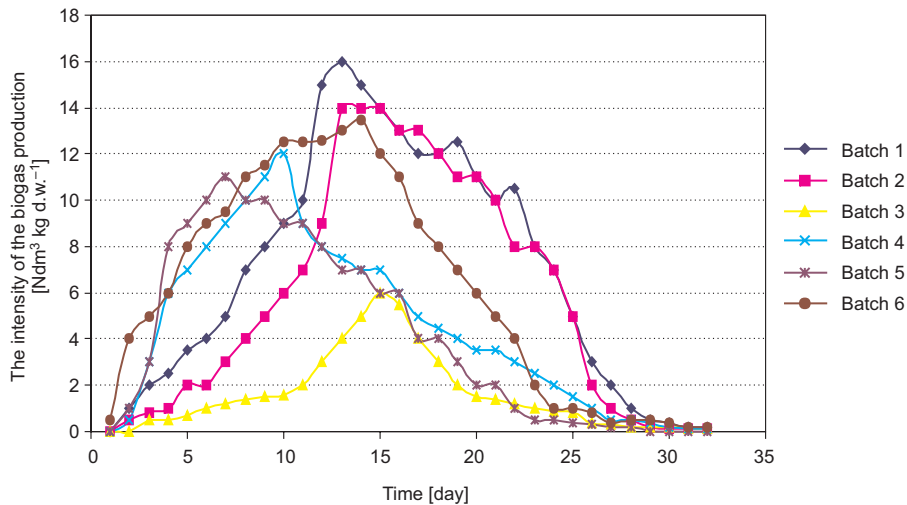


Fig. 4. The intensity of the biogas production

The use of batch made only of the organic fraction of municipal waste for methane fermentation caused a decrease of the biogas yield effect. Such batch may be successfully used for stabilization of waste fractions but not for energy production.

The other apparatus was used for research related to the energy potential of post-fermentation pulp than for batch masses biogas yield. A bioreactor of 20 dm³ volume was used for the production of briquette from the post-fermentation pulp. From this bioreactor, enough amount of post-fermentation waste could be obtained to subject it to centrifugation, drying and briquetting. A batch for fermentation was disintegrated,

therefore the obtained post-ferment was a difficult material for centrifugation. Due to the above reason, during realization of the research, this problem was solved in the following manner: first, the material was compressed on estruders and then subjected to the drying and pellettization process on piston pelleting machines. Then, technological parameters of the material obtained after methane fermentation were determined. Mechanical endurance of briquettes was determined according to the applicable standards [13] in the following way: a prepared sample of briquettes of 1 kg mass was rotated in a drum with rotational speed of 21 rot/min for 5 minutes or for 105 rotations of the drum. Then, a sample remaining on a sieve was weighed and mechanical endurance of briquettes was calculated in percentages depending on:

$$DU = \frac{A}{C} \cdot 100\% \quad (1)$$

where: DU – mechanical endurance of briquettes,

A – mass of sieved briquettes after processing in the drum in grams,

C – total batch applied to the drum in grams.

The experiment was repeated 3 times and the mean value was calculated with a precision to 0.1 percent.

The obtained results of the research on mechanical endurance of briquettes are shown in Table 3.

Table 3

Technical parameters of energy material made of the batch post-ferment masses

Name	C – total batch to the drum [g]	A – mass of sieved briquettes after processing in the drum [g]	DU – mechanical endurance of briquettes [%]
Batch 1	890	81	9.10
Batch 2	910	75	8.24
Batch 3	1170	78	7.29
Batch 4	1100	91	8.27
Batch 5	1050	79	7.52
Batch 6	905	85	9.39

The obtained material in the form of briquette was characterized with mechanical properties comparable to the wood dust.

Calorific value, which depends on the chemical composition and moisture, constitutes the most important thermophysical parameter of various forms of organic masses. The research aimed at indicating the validity of processing the post-ferment from biogas plants which use co-fermentations of organic municipal waste mixed with agricultural waste masses for energy purposes. Post-fermentation mass was dried to the moisture level within 10–20%, and the results of the obtained calorific values are presented in Table 4.

Table 4

The calorific value of the biomass of the post ferment batch masses

Name	Calorific value in a dry state [MJ · kg ⁻¹]
Batch 1	11.36
Batch 2	10.79
Batch 3	9.56
Batch 4	10.86
Batch 5	9.64
Batch 6	11.12

The obtained research results allow assumption that the investigated material may be used as fuel for production of energy at the simultaneous utilization of post-fermentation waste from biogas plants. The obtained material shows properties similar to commonly used briquette and grain straw pellet.

The study proved the improvement of a fermentation ability of batches in co-fermentation. Fraction mixing caused the increase of the intensity of biogas emission during fermentation. In batches based on maize silage in 65% and 75% proportions the highest biogas efficiency was obtained during fermentation. Although there is a possibility of one-component de-fermentation of maize silage, the research proved that de-fermentation of silage as a co-substrate with manure and organic fraction of municipal waste was more efficient. Fermentation using different substrates may significantly increase the efficiency of the process. Fermentation combined with utilization of post-fermentation products for energy purposes seems to be an optimal solution. The replacement of fossil fuels with biogas usually reduces not only emission of greenhouse gases but also nitrogen oxides, hydrocarbons and particles. Due to the high content of nutrients in the waste digestate can be used as a means of improving soil fertility. Use of waste after fermentation as a means to improve the fertility of the soil will reduce the losses of nutrients. Particular importance is the possibility of recycling the elements contained in municipal waste [14].

Conclusions

1. Making batch in proportion 70–30 increases biogas yield; this type of mix may be used for biogas production of energy purposes since the yield from 1 kg of batch was obtained on the level of approx. 200 Ndm³.

2. Post-ferment obtained from the mix made of organic mass and biofraction of municipal waste upon its preparation may be formed and its calorific value is on the level of the used fuels formed of straw materials.

3. Innovativeness of the presented research and consequently the possibility of applying such activities in economy will allow solution of the issue concerning the post-fermentation waste in the future. In the light of the law on fertilizers, the post-fermentation waste from agricultural biogas plant may be used for fertilization of

fields as a natural fertilizer, whereas it may not be a subject of the trade turnover. When investigating biogas plants of great power (over 600 kW) the post-production waste becomes a considerable issue concerning production profitability. The suggested way of utilization of post-ferment seems to be the most efficient, the least problematic on account of social issues and consequently economically and environmentally justified activity.

References

- [1] Sikora J, Szelaż-Sikora A, Cupiał M, Niemiec M, Klimas A. Możliwość wytwarzania biogazu na cele energetyczne w gospodarstwach ekologicznych (Biogas production potential for energy purposes in ecological farms). *Proc ECOpole*. 2014;8(1):279-288. DOI: 10.2429/proc.2014.8(1)037.
- [2] Madlener R, Antunes C, Dias L.C. Assessing the performance of biogas plants with multi-criteria and data envelopment analysis. *Eur J Oper Res*. 2009;197(3):1084-1094. DOI: 10.1016/j.ejor.2007.12.051.
- [3] Kaltschmitt M, Hartmann H. *Energie aus Biomasse – Grundlagen, Techniken und Verfahren*; Springer Verlag Berlin, 2001; <http://link.springer.com/book/10.1007%2F978-3-540-85095-3>.
- [4] Chasnyk, O, Sołowski, G, Shkarupa O. Historical, technical and economic aspects of biogas development: Case of Poland and Ukraine. *Renew Sust Energ Rev*. 2015;52:227-239. DOI:10.1016/j.rser.2015.07.122.
- [5] Chamrádová K, Rusín J. Use of biogas biscuit meal EKPO-EB for agricultural biogas plant for substitution of energy crops utilization with organic waste. *Pol J Chem Technol*. 2015;17(3):40-46. DOI: 10.1515/pjct-2015-0048.
- [6] Council Directive 1999/31/EC of 26 April 1999 on the landfill of waste. *Official J L* 182, 16/07/1999,1-19. http://eur-lex.europa.eu/legal_content/en/ALL/?uri=CELEX:31999_L0031.
- [7] Brzuzi LP, Hites RA. Global mass balance for polychlorinated dibenzo-p-dioxins and dibenzofurans. *Environ Sci Technol*, 1996;30:3646-3648. DOI: 10.1021/es950714n.
- [8] Polish Energy Policy until 2030, Ministerstwo Gospodarki, 2009;14-17. <http://bip.mg.gov.pl/node/24670>.
- [9] Zamorska-Wojdyła D, Gaj K, Hołtra A, Sitariska M. Quality Evaluation of Biogas and Selected Methods of its Analysis. *Ecol Chem Eng S*. 2012;19(1):77-87. DOI: 10.2478/v10216-011-0008-9.
- [10] Gebrezgabher AS, Meuwissen PMM, Prins AMB, Oude Lansink GJMA. Economic analysis of anaerobic digestion-A case of Green power biogas plant in the Netherlands. *NJAS – Wag J Life Sci*. 2010;57(2):109-115. DOI.org/10.1016/j.njas.2009.07.006.
- [11] Hong-Wei Y, David EB. Anaerobic co-digestion of algal sludge and waste paper to produce methane. *Biores Technol*. 2007;98(1):130-134. DOI: 10.1016/j.biortech.2005.11.010.
- [12] Bobleter O. Hydrothermal degradation of polymers derived from plants. *Prog Polym Sci*. 1994;19(5):797-841. DOI: 10.1016/0079-6700(94)90033-7.
- [13] PN-G-04650:1997 Formed fuels – Determination of mechanical strength by drumming method ICS: 75.160.10 <http://m.freestd.us/soft4/3861352.htm>.
- [14] Börjesson P, Berglund M. Environmental systems analysis of biogas systems – Part I: Fuel-cycle emissions. *Biomass Bioenerg*. 2006;30(5):469-485. DOI 10.1016/j.biombioe.2005.11.014.

WYKORZYSTANIE POFERMENTU Z KOFERMENTACJI METANOWEJ NA CELE ENERGETYCZNE

¹ Instytut Inżynierii Rolniczej i Informatyki, Wydział Inżynierii Produkcji i Energetyki

² Katedra Chemii Rolnej i Środowiskowej, Wydział Rolniczo-Ekonomiczny
Uniwersytet Rolniczy im. Hugona Kołłątaja, Kraków

Abstrakt: Głównym problemem cywilizacyjnym XXI wieku jest gwałtowny wzrost ilości odpadów i zanieczyszczeń przyczyniających się do degradacji środowiska naturalnego. Już w XX wieku dał się zauważyć wzrost ilości odpadów komunalnych i pochodzących z przemysłu rolno-spożywczego. Ich skład chemiczny stwarza optymalne warunki do rozwoju mikroorganizmów. Bakterie w warunkach tlenowych i beztlenowych

rozkładają związki organiczne w procesie fermentacji. W wyniku tej przemiany następuje emisja gazów (CH_4 , H_2S , CO_2 , NO_x) i związków azotowych, fosforowych i potasowych. Związki te przedostają się do atmosfery i wód powierzchniowych, gdzie naruszają równowagę ekosystemu, powodując jego eutrofizację. Wyróżniamy różnego rodzaju fermentacje, jednak to fermentacja metanowa może odgrywać szczególną rolę w kontekście pozyskiwania odnawialnych źródeł energii i gospodarki odpadami. Proces ten przekształca energię zawartą w biomacie w użyteczne paliwo będące źródłem czystej energii odnawialnej, niewpływającej negatywnie na środowisko. Biogaz może być spalany w kotle w celu uzyskania energii cieplnej wykorzystanej do ogrzewania pomieszczeń, lub w silniku gazowym napędzającym generator prądu. Warto zauważyć, że metoda wykorzystująca fermentację metanową należy do pożądaných sposobów przekształcania odpadów, tj. recyklingu organicznego.

W pracy przedstawiono wyniki badań wytwarzania biogazu z organicznej frakcji odpadów komunalnych w kofermentacji z masą pochodzenia rolniczego oraz wykazano przydatność pofermentu na cele energetyczne. Do zobrazowania wartości opałowej pofermentu badania przeprowadzono na sześciu mieszkankach wsadowych, gdzie w każdym występowała frakcja organiczna odpadów komunalnych.

Słowa kluczowe: biogaz, recykling organiczny, utylizacja odpadów komunalnych, energia odnawialna

Krzysztof SORNEK*

THE IMPACT OF MICRO SCALE COMBUSTION OF BIOMASS FUELS ON ENVIRONMENT

WPLYW SPALANIA BIOMASY W UKŁADACH MIKROSKALOWYCH NA ŚRODOWISKO

Abstract: This paper shows the results of works aimed to determine the impact of biomass combustion in micro scale devices on the environment. The impact of burning conditions on the level of CO, CO₂, SO₂ and NO_x emissions were determined using the stove-fireplace with accumulation. Based on the analysis of its typical operation (when incomplete combustion of CO has occurred), the air distribution system was modified and new control system, based on the PLC controller, was introduced. These modifications allowed to obtain a level of CO emission required by the Ecodesign Directive.

Keywords: clean combustion, stove-fireplace with accumulation, biomass, micro scale systems

Introduction

One of the most popular heat sources in residential sector are biomass-fired devices, such as central heating boilers and room heaters (fireplaces, stoves and stove-fireplaces with accumulation). These devices are assessed due to the emission of different pollutants to the atmosphere. Boilers are classified using EN 303-5:2012 standard. The highest class units emit no more than 700 ppm of carbon monoxide (in the case of manually feeding system) or 500 ppm (in the case of automatic feeding system). The EN 303-5:2012 standard includes also requirements for boilers' efficiency and limits of the dust and volatile organic compounds (VOC) emission. Determination of the concentration of nitrogen oxides in flue gas is not obligatory, but is indicated if possible. On the other hand, the room heaters are validated by the EN 13229:2001, Ecodesign and BImSchV 2 standards. The first one standard limits the CO emission at the level of 3345 mg/m³. Much more restrictive are the other two documents. Due to the European Directive 2009/125/WE (Ecodesign) the CO concentration in the flue gas

¹ AGH University of Science and Technology, Faculty of Energy and Fuels, Department of Sustainable Energy Development, al. A. Mickiewicza 30, 30-059 Kraków, Poland, phone: +48 12 617 50 94, fax: +48 12 617 45 47, email: krzysztof.sornek@agh.edu.pl

must not exceed 1500 mg/m^3 , when the Austrian BImSchV 2 standard indicates the maximum CO concentration at a level of 1250 mg/m^3 . In both cases, the CO emission is calculated to the 13% of O_2 concentration.

The analysis of the operation of the existing devices shows the strong dependence of the CO emission with their construction and a level of their automation. The formation of pollutants during the combustion process (eg CO) results mainly from incomplete combustion of fuels and is generally correlated with a local lack of O_2 . Incomplete combustion occurs mainly in a simple, manually controlled furnaces. It may also occur also in automatically controlled units in the starting phase of combustion process or in the case of wrong operation of the automation system. In the case of good mixing of flue gas with air, properly low emission may be achieved.

State of the art

The literature sources consist interesting results of studies carried out in the area of clean combustion in the fireplaces and stoves (but actually not in the case of the stove-fireplaces). The main physical characteristics and operating conditions of commonly used in the domestic heating fireplace and stove were determined during works described in [1]. The combustion of softwood (from pine) and hardwood (from eucalyptus) was divided into three main periods, differing by specific flue gas composition. These results were confirmed by other experimental studies, where the CO emission during the ignition phase was about 3–4 times higher than in the combustion phase [2]. Also in the case of investigations performed in terms of number of particles and the size distribution, the number emissions were in strict relationship with the combustion conditions in the fireplace [3]. The results of other studies carried out in order to evaluate non-steady phase contribution to the total emissions of a pellet stove, once again shown that the ignition phase, even though it lasts only 10–20 min, can contribute to pollutant emission. In this investigation, CO and NO emission factors in ignition phase were differ from other operating conditions: NO emission factor was lower, while CO was much higher (it was a product of incomplete combustion) [4].

To avoid a problem with high CO emission caused by incomplete biomass combustion, the modifications of the furnace construction were proposed in [5]. Proposal was based on the results obtained in a way of mathematical modeling. Two-dimensional turbulent flow model with homogeneous chemical reactions has been developed. Accuracy of the model has been previously confirmed with experimental data obtained on the existing furnace [6]. Also other mathematical models have been developed. The models reflect all relevant parts of the furnace and may be subsequently used for the design of the control unit [7].

Taking into account all of mentioned above aspects, a new general strategy for automatic control of the primary and secondary air streams for firewood combustion was applied in [8]. The design consists in two in situ gas sensors (oxygen and CO/HC) and gives consideration to the combustion temperature. Such configuration of the controller enabled to reduce the CO/HC-emissions to the level of about 50% (central

heater) and 15% (tiled stove) in comparison to the use of the typical controller, provided by manufacturer.

The significant impact on the carbon monoxide and other pollutants emission has also the proper choice of the wood species. During tests carried out to determine the effect of ignition technique, biomass load and cleavage on carbon monoxide, total hydrocarbon, particulate matter (PM10) and particle number emissions from a wood-stove, the pine and beech wood were burned. The highest CO and total hydrocarbon emission factors were observed, respectively, for pine and beech, for high and low fuel loads [9]. Another seven fuels (four types of wood pellets and three agro-fuels) were tested in an automatic pellet stove. Particulate matter emission factors and the corresponding chemical compositions for each fuel were also obtained. The CO emission factors ranged from 90.9 ± 19.3 (pellets type IV) to 1480 ± 125 mg/MJ (olive pit) [10].

Presented above studies may be only in some part related to the stove-fireplace with accumulation. Therefore, the impact of the burning conditions on the level of CO, CO₂, SO₂ and NO_x emissions were determined using the stove-fireplace with accumulation equipped with a 550 kg accumulative furnace and a 1050 kg accumulative exchanger located next to the furnace. Basis on the results of previously studies [11], the improvements in the air distribution system and combustion process control system were applied.

Experimental set-up

The experimental set-up with the stove-fireplace with accumulation is equipped with modular PLC controller combined with the set of measurement elements and actuators:

- temperature sensors placed inside the furnace, accumulative mass and chimney as well as on the external side of accumulative exchanger;
- thermoanemometers to measure the flow rate of the air blown into the furnace area;
- platform scale equipped with 4 strain gauges with the resolution of 0.1 kg to measure the weight loss of fuel during the combustion process;
- flue gas analyser to measure the concentration of O₂ (using the electrochemical method) and the concentrations of CO, CO₂, NO, NO₂ and SO₂ (using NDIR method);
- servo-mechanisms to control the air throttles positions.

The monitoring and process data acquisition system was performed in the CoDeSys environment. It allows to observe the real time variations of the measured values, archive measurement data and control the system operation [12].

The main elements of control and measurement system, used during described studies, are presented in Fig. 1.

The proposed control system is different from originally used combustion optimizer, which operation rule is very simple – the system controls the combustion process and keeps the ember phase using the air damper. Due to lowering the combustion curve in the phase of temperature raise and raising the combustion curve upon decrease in temperature, the optimizer prolongs the process of burning.

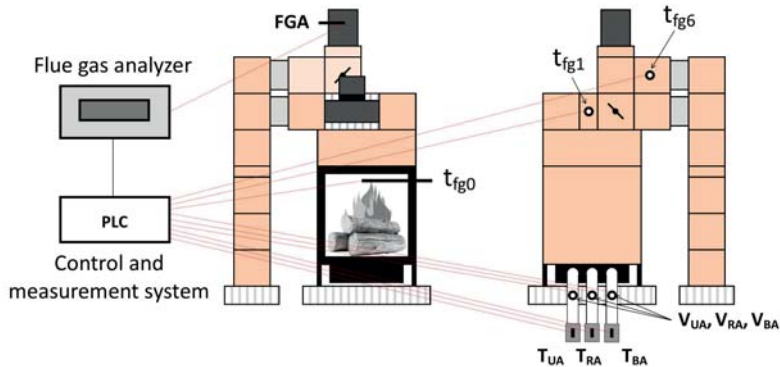


Fig. 1. The main elements of control and measurement system (FGA – flue gas analyser, t_{fg0} , t_{fg1} and t_{fg6} – temperature sensors, T_{UA} , T_{RA} and T_{BA} – respectively upper, rear and bottom air throttle, V_{UA} , V_{RA} and V_{BA} – respectively upper, rear and bottom air speed sensors)

The combustion optimizer controls the level of damper opening based on temperature measurement and an internal control algorithm. The algorithm divides the process of combustion into several phases. The sample combustion curve has been presented in Fig. 2.

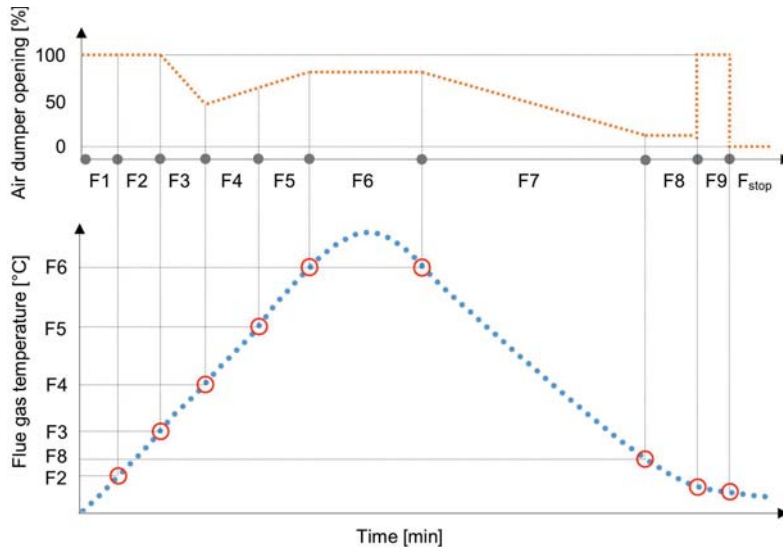


Fig. 2. Theoretical combustion curve with combustion phases marked

The proposed control system is based on the use of PLC controller which allows to control the operation of three air dumpers basis on the CO and O₂ measurements. The introduction of an additional air streams blown to the furnace area from the bottom and rear sides is a follow-up solution in relation to the basic control system of the considered devices. Providing an additional air streams may be really beneficial

to the combustion process, causing better burning-out of fuel and decreased emission of carbon monoxide to the atmosphere (this is especially significant in the first and the last phase of the combustion process, in which the peaks of carbon monoxide emissions occur). The control of the operation of a system of three dampers should be performed by means of a specially developed control algorithm which is capable of controlling three devices.

Experimental results

The first part of presented studies was performed using typical optimizer connected with an upper air throttle. In this case, the air was blown into the furnace using a gap

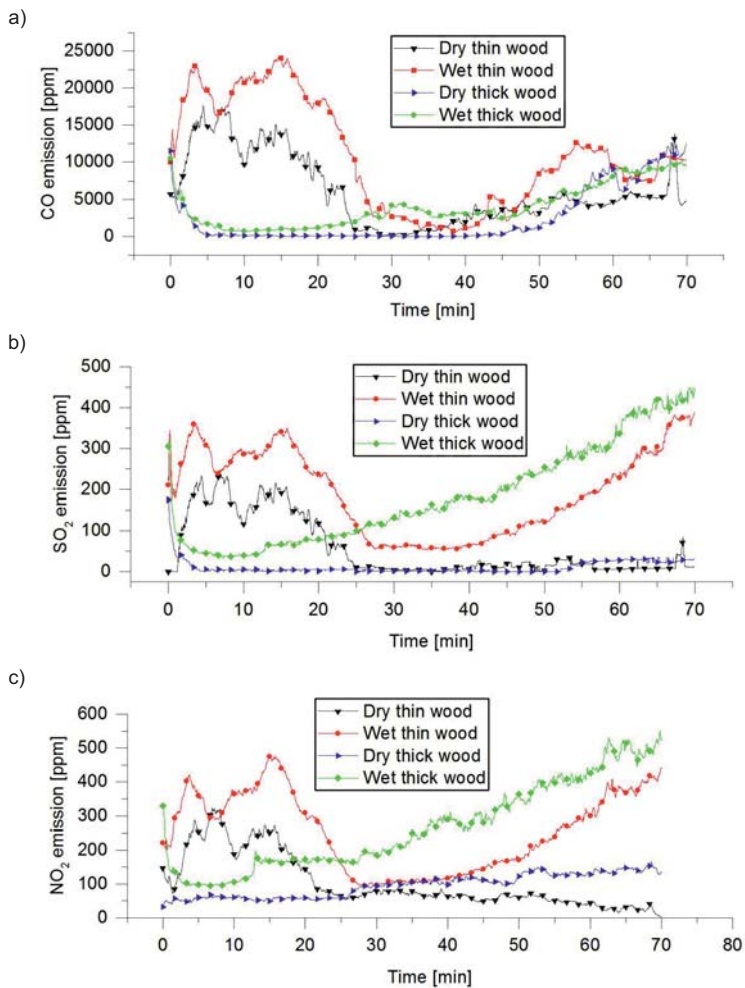


Fig. 3. The variations of the concentration of a) CO, b) SO₂ and c) NO_x in flue gas

located over the door (the air inlet was directed towards the pane to keep it clean). The level of the throttle opening was dependent from the predefined heating curve and the current flue gas temperature (measured at the outlet from the furnace).

During this part of studies, as a fuel was used a hardwood (mixed beech and oak wood). In each from four combustion processes, divided into two series, a wood characterized by different parameters was burned. It was respectively: i) dry thin wood, ii) wet thin wood, iii) dry thick wood and iv) wet thick wood. The variations of the emissions of CO, SO₂ and NO_x were shown in Fig. 3a–3c.

As we can see in Fig. 3, the size of the wood pieces has a significantly greater impact on the clean combustion, than their humidity. The lowest emissions were obtained during combustion of dry thick wood, when the average concentration of the carbon monoxide was less than 1800 ppm. Comparing this value to other measured concentrations of CO, we have 2 times less emission than in the case of burning wet thick wood, 3 times less emission than in the case of burning dry thin wood and 5 time less emission than in the case of burning wet thin wood. In general, the trends for SO₂ and NO_x emission were the same, but the measured values and differences between them were visibly lower.

Detailed analysis of data presented in Fig. 3 shows, that the highest emissions occurred in the ignition phase. One of the reasons was limited access of the air to the wood bed. Significantly lower values were measured in the combustion phase. The average CO emission in this phase was lower than 500 ppm in the case of burning dry thick wood. On the other hand, the CO emission in the case of burning wet thin wood was more than 20 times higher. The values obtained in the afterburning phase (starting between 40 and 50 minute) show the increasing trends, but there are not representative (the high amount of the oxygen is connected mainly with the fact, that the fire has died out).

The improvements in the stove-fireplace construction

Based on above results, two ways to improve efficiency of the starting phase of combustion process and reduce the average emission of CO were proposed: i) introduce additional air inlets and ii) develop new control system. Additional air inlets (allow to delivery air in the periods of a time, when the carbon monoxide burning is incomplete), were located under the pane and on the rear wall of the furnace. In opposite to upper air inlet, there were directed towards the fuel bed. The impact of their application on the CO emission has been shown in Fig. 4. As before, 12 kg of thick wood with was burnt during combustion process. The furnace was preheated and therefore fuel was ignited from the ignition layer.

The analysis of the CO emission during combustion process shows, that air supplied from inlet located under the pane limited the carbon monoxide emission in its ignition phase. In this phase, the opening of upper-air throttle was insufficient, while the supply of air from the rear inlet had any impact on the CO emission. On the other hand, the use of rear air inlet had a really positive impact in the combustion phase.

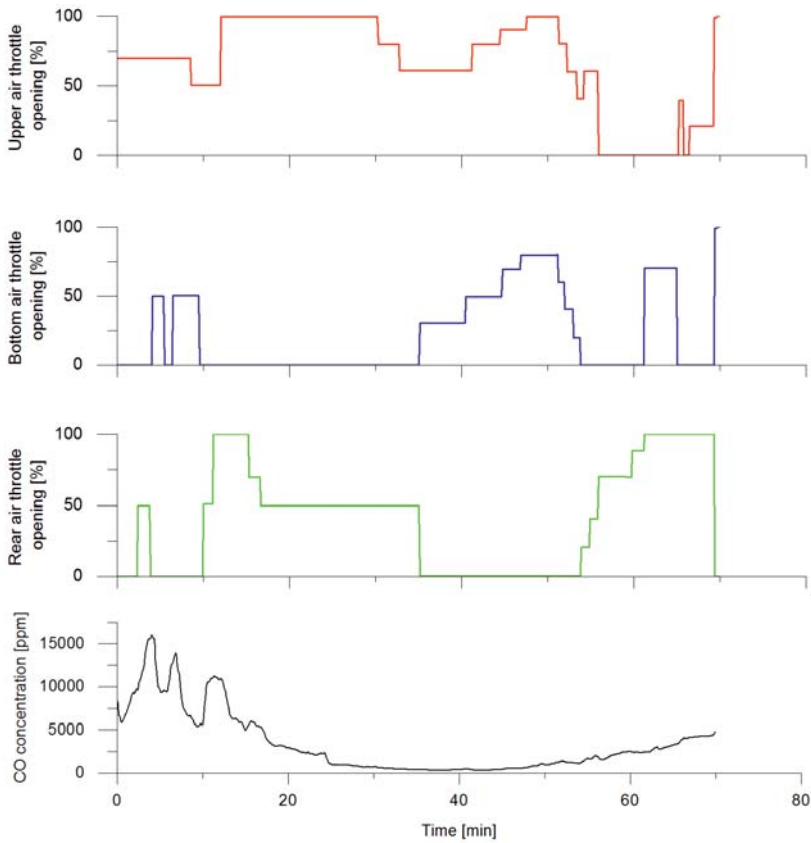


Fig. 4. The variations of the concentration of CO in the case of using three air inlets

If we compare a level of CO emission from the typical stove-fireplace with only one air throttle and a level of CO emission from modified unit with three air throttles, we can see that the new device is more environmental friendly. The improvements in its operation is connected with better air distribution allows to limit incomplete combustion of the wood. On the other hand, construction changes were complemented by develop new regulator replacing non-efficient optimizer provided by manufacturer.

Introduction of the new regulator

The new regulator was developed in the CoDeSys software using such programming languages as CFC (Continous Function Chart) and ST (Structured Text). The signals from temperature sensors (t_{fg0} , t_{fg1} and t_{fg6}) and flue gas analyzer (CO and O₂) have been connected to the analog input modules of the PLC controller and used to control the level of the air throttles opening (T_{UA} , T_{RA} and T_{BA}). The volume of O₂ and volume of CO emissions have been coupled respectively with upper and rear air throttles

opening control. Bottom air throttle was controlled separately and it was used in the ignition phase.

The throttles were opening and closing depending on actual values of the O_2 and CO concentrations and boundary conditions (minimum set content of oxygen in the flue gas and the maximum set content of carbon monoxide). The emission of CO in the case of using new developed regulator was shown in Fig. 5.

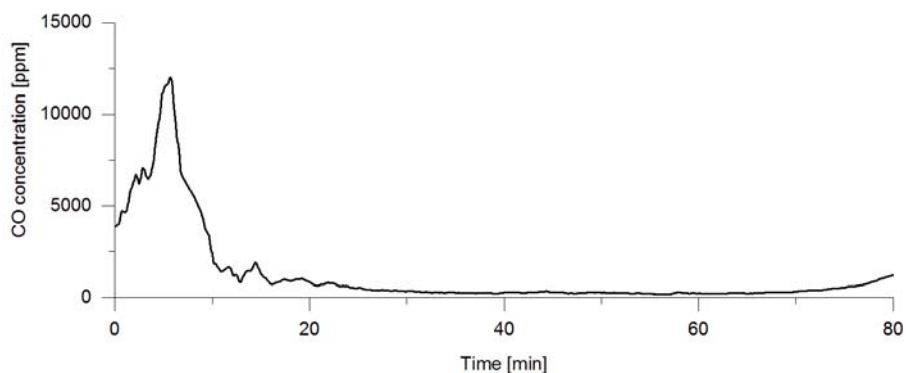


Fig. 5. The variations of the concentration of CO in the case of using new regulator

The use of additional air inlets and developed regulator limited CO emission in the ignition phase. As a result, the average CO emission during whole combustion process was lower than 1200 ppm. Expressing this value in the milligrams per cubic meter it is about $1\,450\text{ mg/m}^3$ (in comparison to the level of $2\,156\text{ mg/m}^3$ in the case of the typical unit). Of course, proposed solution is still developing in order to further reduce CO emission (mainly in the ignition phase).

The amount of NO_x and SO_2 emissions, measured during this part of study, were also on the acceptable level. The variations of NO_x and SO_2 emissions were shown in Fig. 6.

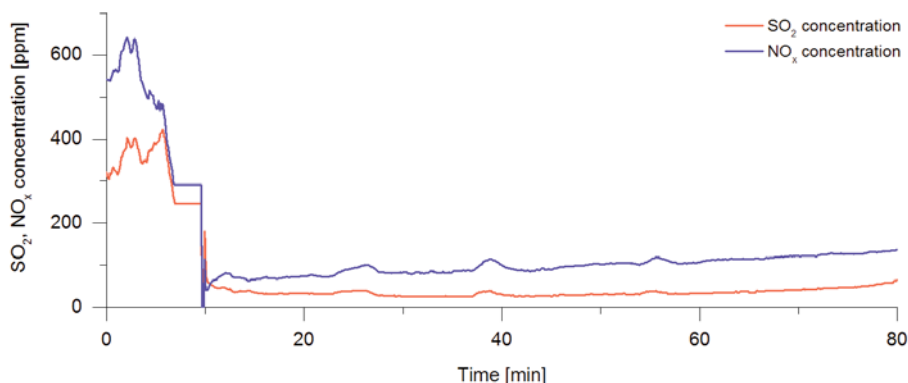


Fig. 6. The variations of the concentration of NO_x and SO_2 in the case of using new regulator

Analyzing histogram presented in Fig. 6 we can conclude that concentrations of NO_x and SO_2 were quite high only in the ignition phase. In the combustion phase emissions were significantly lower – respectively lower than 100 ppm (NO_x) and lower than 200 ppm (SO_2).

Conclusions

The introduction of the a new air distribution system and regulator allowed significantly reduce CO emission to the atmosphere and preserve NO_x and SO_2 emissions at satisfactory level. The average concentration of CO in the flue gas during whole combustion process meets the restrictive requirements of Ecodesign standard.

On the other hand, if we take into account the fact, that combustion process took about 80 minutes and heat accumulated in the heat exchanger was transferred to the room for the next 6–8 hours after fire died out, the average value of CO emission calculated for this time is lower than 200 mg/m^3 . Such a low value definitely meets the BImSchV 2 requirements.

Further development of the proposed air distribution system and regulator will allow to achieve even better results (further decrease of the CO and other pollutants emission to the atmosphere). However, in order to productize the developed solution, it is necessary to apply cheap CO sensors or to change the CO signal with another signal (due to high costs of the circuits for the measurement of carbon monoxide concentration in flue gas). The further research should thus address the possibility of applying only a lambda probe (or another sensor measuring the indicated value) as the element sufficient for the proper control of the operation of the stove-fireplace with accumulation.

Acknowledgements

The work has been completed as part of the statutory activities of the Faculty of Energy and Fuels at the AGH UST in Krakow “Studies concerning the conditions of sustainable energy development”.

Supervisor: Ph.D. Mariusz Filipowicz, associate professor.

References

- [1] Calvo AI, Tarelho LAC, Alves CA, Duarte M, Nunes T. Characterization of operating conditions of two residential wood combustion appliances. *Fuel Processing Technol.* 2014;126:222-232. DOI: 10.1016/j.fuproc.2014.05.001.
- [2] Obaidullah M, Dyakov IV, Thomassin JD, Duquesne T, Bram S, Contino F, De Ruyck J. CO Emission Measurements and Performance Analysis of 10 kW and 20 kW Wood Stoves. *Energy Procedia.* 2014; 61:2301-2306. DOI: 10.1016/j.egypro.2014.12.443.
- [3] Ozgen S, Cernuschi S, Giugliano M. Experimental evaluation of particle number emissions from wood combustion in a closed fireplace. *Biomass Bioenergy.* 2013;50:65-74. DOI: 10.1016/j.biombioe.2013.01.015
- [4] Bäfver LS, Leckner B, Tullin C. Particle emissions from pellets stoves and modern and old-type wood stoves. *Biomass Bioenergy.* 2011;35:3648-3655 DOI: 10.1016/j.biombioe.2011.05.027
- [5] Venturini E, Vassura A, Zanetti C, Pizzic A, Toscano G, Passarini F. Evaluation of non-steady state condition contribution to the total emissions of residential wood pellet stove. *Energy.* 2015;88:650-657. DOI: 10.1016/j.energy.2015.05.105.

- [6] Djurović D, Nemoda S, Repić B, Dakić D, Adžić M. Influence of biomass furnace volume change on flue gases burn out process. *Renew Energy*. 2015;76:1-6. DOI: 10.1016/j.renene.2014.11.007.
- [7] Göllés M, Reiter S, Brunner T, Dourdoumas N, Obemberger I. Model based control of a small-scale biomass boiler. *Control Eng Practice* 2014;22:94-102. DOI: 10.1016/j.conengprac.2013.09.012.
- [8] Butschbach, P.; Hammer F, Kohler H, Potreck A, Trautmann T. Extensive reduction of toxic gas emissions of firewood-fueled low power fireplaces by improved in situ gas sensorics and catalytic treatment of exhaust gas. *Sensors Actuators B: Chemical* 2009; 137:32-41. DOI: 10.1016/j.snb.2008.12.007.
- [9] Vicente ED, Duarte MA, Calvo AI, Nunes TF, Tarelho L, Alves CA. Emission of carbon monoxide, total hydrocarbons and particulate matter during wood combustion in a stove operating under distinct conditions. *Fuel Processing Technol.* 2015;131:182-192. DOI: 10.1016/j.fuproc.2014.11.021.
- [10] Vicente ED, Duarte MA, Tarelho L, Nunes TF, Amato F, Querol X, et al. Particulate and gaseous emissions from the combustion of different biofuels in a pellet stove. *Atmosph Environ.* 2015;120:15-27. DOI: 10.1016/j.atmosenv.2015.08.067.
- [11] Sornek K, Filipowicz M, Rzepka K. Study of clean combustion of wood in a stove-fireplace with accumulation. *Journal of the Energy Institute*, In Press, DOI: 10.1016/j.joei.2016.05.001
- [12] Sornek K, Filipowicz M, Rzepka K. The development of a thermoelectric power generator dedicated to stove-fireplaces with heat accumulation systems. *Energy Convers Manage*, In Press. DOI: 10.1016/j.enconman.2016.05.091

WPLYW SPALANIA BIOMASY W UKŁADACH MIKROSKALOWYCH NA ŚRODOWISKO

AGH Akademia Górniczo-Hutnicza, Kraków
Wydział Energetyki i Paliw, Katedra Zrównoważonego Rozwoju Energetycznego

Abstrakt: W artykule przedstawione zostały wyniki badań, których celem było określenie wpływu spalania biomasy (drewna) w jednostkach mikroskalowych na środowisko naturalne. Badania przeprowadzone zostały na stanowisku badawczym wyposażonym w piec ceramiczny z wymiennikiem akumulacyjnym – urządzenie stanowiące połączenie typowego kominka z tradycyjnym piecem akumulacyjnym. Bazując na analizie typowej pracy piecokominka, podczas której następowało niezupełne spalanie węgla zawartego w biomase i powstawanie tlenku węgla, opracowany został dodatkowy układ doprowadzania powietrza, który zlokalizowano na tylnej ścianie paleniska. W kolejnym kroku opracowano system kontrolno-pomiarowy, oparty na zastosowaniu sterownika PLC oraz własnego algorytmu sterującego, który rozwija możliwości standardowych regulatorów procesu spalania. Otrzymane wyniki obejmujące emisję CO, CO₂, O₂, SO₂ i NO_x pokazują, że wprowadzenie opisanych zmian pozwala na znaczącą redukcję wpływu spalania biomasy na środowisko naturalne (szczególnie w aspekcie emisji tlenku węgla).

Słowa kluczowe: czyste spalanie, piecokominiek, biomasa, systemy mikroskalowe

Varia

INVITATION FOR ECOpole '16 CONFERENCE



CHEMICAL SUBSTANCES IN ENVIRONMENT

We have the honour to invite you to take part in the 25th annual Central European Conference ECOpole '16, which will be held in 5–8.10.2016 (Wednesday–Saturday) in Hotel Antalowka in Zakopane, PL.

The Conference Programme includes oral presentations and posters and will be divided into four sections:

- SI Chemical Pollution of Natural Environment and Its Monitoring
- SII Environment Friendly Production and Use of Energy
- SIII Forum of Young Scientists and Environmental Education in Chemistry
- SIV Impact of Environment Pollution on Food and Human Health

The Conference language is English.

Contributions to the Conference will be published as:

- abstracts on the CD-ROM (0.5 page of A4 paper sheet format),
- extended Abstracts (6–8 pages) in the semi-annual journal *Proceedings of ECOpole*,
- full papers will be published in successive issues of the *Ecological Chemistry and Engineering/Chemia i Inżynieria Ekologiczna* (Ecol. Chem. Eng.) ser. A or S.

Additional information one could find on Conference website:

ecopole.uni.opole.pl

The deadline for sending the Abstracts is **15th July 2016** and for the Extended Abstracts: **1st October 2016**. The actualized list (and the Abstracts) of the Conference contributions accepted for presentation by the Scientific Board, one can find (starting from **31st July 2016**) on the Conference website.

The papers must be prepared according to the Guide for Authors on Submission of Manuscripts to the Journals.

At the Reception Desk each participant will obtain abstracts of the Conference contributions as well as the Conference Programme recorded on electronic media (the Programme will be also published on the ECOpole '16 website).

After the ECOpole '16 Conference **it will be possible to publish electronic version of presented contributions** (oral presentations as well as posters) on this site.

Further information is available from:

Prof. dr hab. inż. Maria Waclawek
Chairperson of the Organising Committee
of ECOpole '16 Conference
University of Opole
email: Maria.Waclawek@o2.pl
and mrajfur@o2.pl
phone: +48 77 401 60 42
fax +48 77 401 60 51

Conference series

1. 1992 Monitoring '92 Opole
2. 1993 Monitoring '93 Turawa
3. 1994 Monitoring '94 Pokrzywna
4. 1995 EKO-Opole '95 Turawa
5. 1996 EKO-Opole '96 Kędzierzyn Koźle
6. 1997 EKO-Opole '97 Duszniki Zdrój
7. 1998 CEC ECOpole '98 Kędzierzyn-Koźle
8. 1999 CEC ECOpole '99 Duszniki Zdrój
9. 2000 CEC ECOpole 2000 Duszniki Zdrój
10. 2001 CEC ECOpole '01 Duszniki Zdrój
11. 2002 CEC ECOpole '02 Duszniki Zdrój
12. 2003 CEC ECOpole '03 Duszniki Zdrój
13. 2004 CEC ECOpole '04 Duszniki Zdrój
14. 2005 CEC ECOpole '05 Duszniki Zdrój
15. 2006 CEC ECOpole '06 Duszniki Zdrój
16. 2007 CEC ECOpole '07 Duszniki Zdrój
17. 2008 CEC ECOpole '08 Piechowice
18. 2009 CEC ECOpole '09 Piechowice
19. 2010 CEC ECOpole '10 Piechowice
20. 2011 CEC ECOpole '11 Zakopane
21. 2012 CEC ECOpole '12 Zakopane
22. 2013 CEC ECOpole '13 Jarnołtówek
23. 2014 CEC ECOpole '14 Jarnołtówek
24. 2015 CEC ECOpole '15 Jarnołtówek

ZAPRASZAMY DO UDZIAŁU W ŚRODKOWOEUROPEJSKIEJ KONFERENCJI ECOpole '16



SUBSTANCJE CHEMICZNE W ŚRODOWISKU PRZYRODNICZYM w dniach 5–8 X 2016 r. w hotelu Antałówka w Zakopanem

Będzie to **dwudziesta piąta z rzędu** konferencja poświęcona badaniom podstawowym oraz działaniom praktycznym dotyczącym różnych aspektów ochrony środowiska przyrodniczego.

Doroczne konferencje ECOpole mają charakter międzynarodowy i za takie są uznane przez Ministerstwo Nauki i Szkolnictwa Wyższego. Obrady konferencji ECOpole '16 będą zgrupowane w czterech Sekcjach:

- SI Chemiczne substancje w środowisku przyrodniczym oraz ich monitoring
- SII Odnawialne źródła energii i jej oszczędne pozyskiwanie oraz użytkowanie
- SIII Forum Młodych (FM) i Edukacja prośrodowiskowa
- SIV Wpływ zanieczyszczeń środowiska oraz żywności na zdrowie ludzi

Materiały konferencyjne będą opublikowane w postaci:

- abstraktów (0,5 strony formatu A4) na CD-ROM-ie,
- rozszerzonych streszczeń o objętości 6–8 stron w półroczniku *Proceedings of ECOpole*,
- artykułów: w abstraktowanych czasopismach: *Ecological Chemistry and Engineering/Chemia i Inżynieria Ekologiczna (Ecol. Chem. Eng.)* ser. A i S oraz w półroczniku *Chemistry – Didactics – Ecology – Metrology (Chemia – Dydaktyka – Ekologia – Metrologia)*.

Termin nadsyłania angielskiego i polskiego streszczenia o objętości 0,5–1,0 strony (wersja cyfrowa) planowanych wystąpień upływa w dniu 15 lipca 2016 r., a rozszerzonych streszczeń – **1 października 2016 r.** Lista prac zakwalifikowanych przez Radę Naukową Konferencji do prezentacji będzie sukcesywnie publikowana od 31 lipca 2016 r. na stronie internetowej konferencji. Aby praca (dotyczy to także streszczenia, które powinno mieć tytuł w języku polskim i angielskim, słowa kluczowe w obydwu językach) przedstawiona w czasie konferencji mogła być opublikowana, jej tekst winien być przygotowany zgodnie z wymaganiami stawianymi artykułom drukowanym w czaso-

pismach *Ecological Chemistry and Engineering* ser. A oraz S, które są dostępne w wielu bibliotekach naukowych w Polsce i za granicą. Zalecenia te są również umieszczone na stronie internetowej Towarzystwa Chemii i Inżynierii Ekologicznej:

tchie.uni.opole.pl

Wszystkie nadsyłane prace podlegają zwykłej procedurze recenzyjnej.

Wszystkie streszczenia oraz program konferencji zostaną wydane na CD-ROM-ie, który otrzyma każdy z uczestników podczas rejestracji. Program będzie także umieszczony na stronie internetowej konferencji

ecopole.uni.opole.pl

Po konferencji będzie możliwość opublikowania elektronicznej wersji prezentowanego wystąpienia (wykładu, a także posteru) na tej stronie.

Prof. dr hab. inż. Maria Waclawek
Przewodnicząca Komitetu Organizacyjnego
Konferencji ECOpole '16

Wszelkie uwagi i zapytania można kierować na adres:
maria.waclawek@o2.pl lub mrajfur@o2.pl
tel. 77 401 60 42 lub fax 77 401 60 51

GUIDE FOR AUTHORS

A digital version of the manuscript should be sent to:

Prof dr hab. Witold Waclawek,
Editor-in-Chief of Ecological Chemistry and Engineering A
Uniwersytet Opolski
ul. kard. B. Kominka 6
45-032 Opole
Poland
phone +48 77 401 60 42, +48 77 455 91 49
fax +48 77 401 60 51
email: maria.waclawek@o2.pl
mrajfur@o2.pl

The Editor assumes, that an Author submitting a paper for publication has been authorised to do that. It is understood the paper submitted to be original and unpublished work, and is not being considered for publication by another journal. After printing, the copyright of the paper is transferred to *Towarzystwo Chemii i Inżynierii Ekologicznej (Society for Ecological Chemistry and Engineering)*.

“Ghostwriting” and “guest authorship” are a sign of scientific misconduct. To counteract them, please provide information, for the Editor, on the percentage contribution of individual Authors in the creation of publications (including the information, who is the author of concepts, principles, methods, etc.). Editorial Board believes that the main responsibility for those statements bears the Author sending the manuscript.

In preparation of the manuscript please follow the general outline of papers published in *Ecological Chemistry and Engineering A*, available on the website:

tchie.uni.opole.pl

a sample copy can be sent, if requested.

Papers submitted are supposed to be written in English language and should include a summary and keywords, if possible also in Polish language.

Generally, a standard scientific paper is divided into:

- Introduction: you present the subject of your paper clearly, indicate the scope of the subject, present state of knowledge on the paper subject and the goals of your paper;
- Main text (usually divided into: Experimental – you describe methods used; Results and Discussion);
- Conclusions: you summarize your paper;
- References.

The first page should include the author's (authors') given name(s) without titles or scientific degrees like Prof., Ph.D., etc., their affiliations, phone and fax numbers and their email addresses however, with the corresponding author marked by an asterisk.

It is urged to follow the units recommended by the *Système Internationale d'Unités* (SI). Graph axis labels and table captions must include the quantity units.

Symbols recommended by the International Union of Pure and Applied Chemistry (Pure and Appl Chem. 1979;51:1-41) are to be followed. Graphics (drawings, plots) should be supplied in the form of digital vector-type files, eg CorelDraw v.9, Excel, Inkscape or at least in a bitmap format (TIF, JPG) 600 DPI. In the case of any query please feel free to contact with the Editorial Office. Footnotes, tables and graphs should be prepared as separate files. References cited chronologically should follow the examples given below:

- [1] Lowe DF, Oubre CL, Ward CH. Surfactants and cosolvents for NAPL remediation. A technology practices manual. Boca Raton: Lewis Publishers; 1999.
- [2] Fasino CR, Carino M, Bombelli F. Oxidant profile of soy standardized extract. In: Rubin R, Stryger CS, editors. Joint Meeting 2001 – Book Abstracts '2001 Year of Natural Products Research'. New York: Harper and Row; 2001.
- [3] Wosiński S. Effect of composition and processing conditions of ceramic and polymer composites on the electric field shielding ability [PhD Thesis]. Poznań: Poznan University of Technology; 2010.
- [4] Trapido M, Kulik N, Veressinina Y, Munter R. Water Sci Technol. 2009;60:1795-1801. DOI: 10.2166/wst.2009.585.
- [5] Cañizares P, Lobato J, Paz R, Rodrigo MA, Sáez C. Chemosphere. 2007;67:832-838. DOI: 10.1016/j.chemosphere.2006.10.064.
- [6] Hakala M, Nygård K, Manninen S, Huitari S, Buslaps T, Nilsson A, et al. J Chem Phys. 2006;125:084504-1-7. DOI: 10.1063/1.2273627.
- [7] Kowalski P. Statistical calibration of model solution of analytes. Ecol Chem Eng A. Forthcoming 2016.

Please remember that every sign in the references counts.

Journal titles should preferably follow the Chem. Abst. Service recommended abbreviations.

Each publication is evaluated by at least two independent Reviewers from outside of the unit. In the case of paper written in a foreign language, at least one of Reviewers is affiliated to a foreign institution other than the Author's work.

As a rule double-blind review process is used (the Author(s) and Reviewers do not know their identities). In any case Editor must be sure that no conflict of interest (direct personal relationships, professional relationships, or direct scientific cooperation in the past two years) occurs between the Reviewer and the Author. Reviewer has to fill in the Reviewers report. On its end must be an explicit request to the approval of the article for publication or its rejection.

Receipt of a paper submitted for publication will be acknowledged by email. If no acknowledgement has been received, please check it with the Editorial Office by email, fax, letter or phone.

In the case of any query please feel free to contact with the Editorial Office.

Editors

TECHNICAL EDITOR
Halina Szczegot

LAYOUT
Jolanta Brodziak

COVER DESIGN
Jolanta Brodziak

